SNAP-21 PROGRAM, PHASE II

DEEP SEA RADIOISOTOPE-FUELED THERMOELECTRIC GENERATOR POWER SUPPLY SYSTEM

QUARTERLY REPORT NO. 7

Space and Defense Products
ELECTRICAL PRODUCTS GROUP
3-M CENTER, ST. PAUL, MINN. 55101, PH 633-9400
3M COMPANY

DISCLAIMER

Report No. MMM 3691-30

AEC RESEARCH AND DEVELOPMENT REPORT

This report has been prepared under Contract AT(30-1)3691
with the U.S. Atomic Energy Commission

SNAP-21 PROGRAM, PHASE II

DEEP SEA RADIOISOTOPE-FUELED THERMOELECTRIC GENERATOR POWER SUPPLY SYSTEM

QUARTERLY REPORT NO. 7

APRIL 1968

Period Covered
January 1, 1968 to March 31, 1968

Prepared by:

F. Fox
R. Herrlich

Approved by:

J. Brandt
Program Manager
SNAP-21 Program

Issued by

Space and Defense Products

MINNESOTA MINING AND MANUFACTURING COMPANY

ST. PAUL, MINNESOTA 55101

page blank

LEGAL NOTICE

DISTRIBUTION

Distribution of this document is in accordance with TID-4500 (50th Edition) category UC33.

page blank

TABLE OF CONTENTS

TABLE OF CONTENTS (Continued)

TABLE OF CONTENTS (Continued)

page blank

LIST OF FIGURES

LIST OF FIGURES (Continued)

LIST OF TABLES

LIST OF TABLES (Continued)

1.0 SUMMARY

The following items represent the significant accomplishments on the SNAP-21 Program during the past quarter:

- Completed fuel capsule weld development
- Insulation system 10D1 was dynamically tested to specification and the thermal characteristics retested
- Completed thermal testing of insulation system 10D2
- Completed insulation wrapping, closure and thermal testing of system 10D3
- Completed insulation wrapping, closure and thermal testing of system 10D4
- Completed forging, radiographic inspection, machining and final inspection of first three pressure vessels
- Finalized the thermoelectric generator design
- Completed test fixture for long term evaluation of insulation system
- Completed two test cabinets for long term testing of power conditioners
- Completed assembly of in-line generator A10D7
- Completed assembly and testing of power conditioners H10D2, H10D3, and H10D4
- Completed dynamic testing on insulation system 10D3

- Completed hydrostatic testing of pressure vessel D10D1
- Completed short-term testing and dynamic testing of ball and socket generators A10D1, A10D2, and A10D4
- Completed specification level dynamic testing of in-line generators A10D5, A10D6, and A10D7
- Completed system test and test data analysis of Phase I System B-1 and Phase II System S10D1
- Completed system test of Early Fueled System, S10D1A
- External radiation level measurements of System S10D1A were made at Oak Ridge National Laboratory
- Four electrically heated fuel capsules were implanted in the ocean off San Clemente Island
- Completed semi-annual updating of the SNAP-21 Program Plan

2.0 TASK I – 10-WATT SYSTEM

2.1 INTEGRATED SYSTEM DESIGN AND ANALYSIS

2.1.1 SYSTEM PERFORMANCE

As an integral part of establishing the final thermoelectric generator design during this report period, the system heat transfer program was used to determine the system temperature profile and heat balance. Details of this analysis will be presented in a forthcoming topical report that presents the final generator design; consequently, only a summary of the results and the final system heat balance will be included in this report.

A summary of the predicted system temperature profile at EOL, BOL and shipping conditions is shown in Table 2-1. Figure 2-1 is a schematic of the system defining calculated temperature locations.

It should be noted that the computer predicted temperature for the hot and cold junctions of the thermoelectric legs is different than the design temperatures (see paragraph 2.2.6). After considering this difference, it was decided that it did not warrant another generator design iteration. The difference is within the accuracy of the analysis and permits building with a slightly conservative design.

The final heat balance for the system is shown in Table 2-2. This heat balance was calculated using typical material properties and conditions; consequently, the fuel loading shown is representative of that required. Oak Ridge National Laboratory (ORNL) states that fuel loading in this range can be controlled to within 5 percent of the total, or approximately 10 watts total tolerance. In view of this and the fuel capsule capacity, the final fuel loading has been established as 209-219 thermal watts.

Table 2-1. Calculated Temperature Distribution for 10-Watt System in Sea Water and Air with Heat Transfer Fins Attached

Identification Number (5)	Location within the System	Environment		
		Sea Water (40°F)		Air-Fins Attached (130°F)
		BOL (1)	EOL (1)	BOL (1)
1	Pressure Vessel Cover - Upper Hemisphere	47	47	141
2	Pressure Vessel Body - Flange	49	48	143
3	Segmented Retaining Ring - Generator Mounting Plate	60	58	155
4	Segmented Retaining Ring - Interface with Pressure Vessel Wall	48	47	144
5	Cold Frame - Interface with Mounting Plate	64	62	158
6	Neck Tube - Top	166	152	253
7	Emitter Plate	1215	1112	1270
	Generator Hot Frame (External)	1080 (2) est	967 (2) est	1090 (2) est
	Generator Hot Frame (Internal)	1036 (2) est	927 (2) est	1050 (2) est
8	Hot Button	1010	912	1020 (3) 1080 (4)
9	Cold Cap	100	93	204 (3) 194 (4)
10	Cold Frame (Internal)	77	72	169
11	Fuel	1325	1175	1375

Notes:

1) All temperatures in °F.

2) Analysis does not include nodal points at these positions. Temperatures are estimates based on emperical temperature drop from emitter plate to hot frame.

3) These temperatures are based on the thermopile operating at near short circuit conditions.

4) These temperatures are based on the thermopile operating at normal load voltage.

5) Refer to Figure 2-1 for further definition of temperature locations.

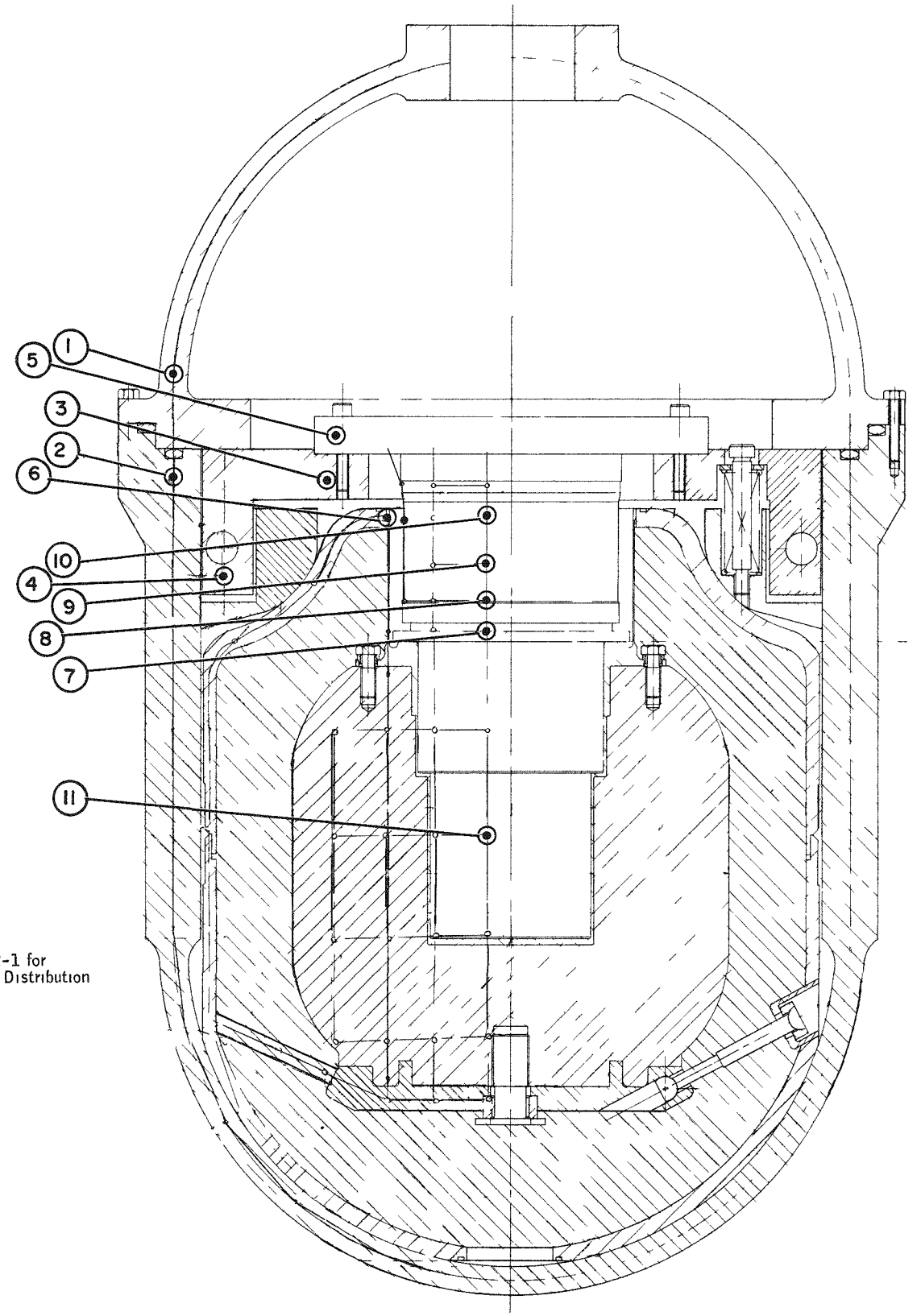

NOTE:
See Table 2-1 for Temperature Distribution

Figure 2-1. System Schematic Showing Calculated Temperature Locations

Table 2-2. SNAP-21 System Heat Balance

Component	BOL	EOL
Generator		
Legs	139	119
Insulation	9	8
Outer Case	13	12
Insulation System		
Neck Tube	20	18
Tie Rods	14	13
Foils	12	11
Other		
Generator Case to Insulation System Neck Tube	8	8
Total Fuel Loading - Thermal Watts	215	189

2.1.2 SYSTEM COOLING DURING SHIPMENT

The SNAP-21 system shipping container is being designed to allow shipment of the system without any form of auxiliary cooling to dissipate the system heat. Consequently, a means of rejecting this system heat to the air environment which serves as the heat sink during handling, shipping and storage must be found. Since the ambient air may reach temperatures of up to +130°F, it is obvious that the heat rejection surfaces of the system must operate at temperatures in excess of +130°F.

To prevent overheating of internal system components during shipment and yet have hot junction temperatures during ocean operation as high as possible, it is necessary to keep the system temperature rise during shipment as low as possible. This is achieved by adding temporary heat rejection fins to the outside of the pressure vessel during shipment. These clamp-on fins serve to increase the heat

rejection surface and thus allow the pressure vessel to operate at a lower temperature for a given total heat flow.

To determine the quantity and size of fins required, an ASME design paper (62-HT-7, "Predicting the Performance of Free-Convection Air Heat Exchangers" by J.G. Bartas and J.N. Shinn) was used. This paper consists of a series of formulas and parametric design curves that can be used to design fin-type heat transfer surfaces. The authors verified the theoretical method presented in the paper by comparing actual test data with theoretical predictions. The data agreed to within 5 percent.

Using the method presented in this paper, it was determined that a total of 180 aluminum fins, 13 inches in height by 4 inches in length by 0.025 inch thick, could dissipate the system heat at a maximum pressure vessel temperature of 150°F. A drop of 10°F was assumed from the pressure vessel surface to the base of the fins.

Details of this analysis are shown in Appendix A.

2.2 COMPONENT DESIGN AND DEVELOPMENT

2.2.1 FUEL CAPSULE

Weld development has been completed on the fuel capsule. Modification of weld parameters has resulted in a deep narrow beam penetration with only a minimum of surface bead (Figure 2-2). The inner liner design has been changed to provide slightly greater clearances between the liner and the Hastelloy capsule. The fuel loading for the prototype systems has been specified at 209-219 watts. Fuel pellet preparation will be completed during the next quarter.

2.2.2 BIOLOGICAL SHIELD AND SPIDER

There was no design or development effort on this component during the period covered by this report.

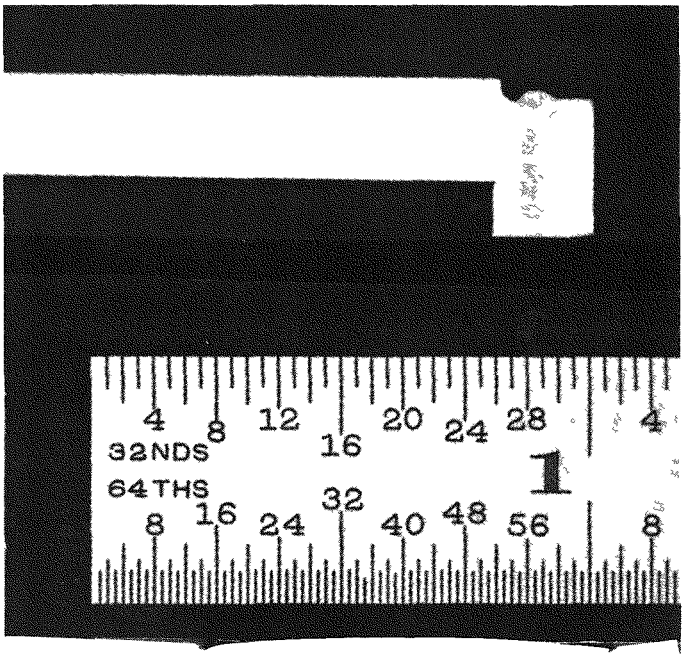

Figure 2-2. Electron Beam Fuel Capsule weldment (Current = 140 ma; voltage = 30 KV, speed = 60 in/min with preheat to 560°F)

2.2.3 INSULATION SYSTEM

A thermal retest of insulation system 10D1 was accomplished after the dynamic test to specification. The thermal test of system 10D2 was also completed. The unit insulation, closure and thermal test were completed on system 10D3. Assembly insulation, closure and thermal testing was completed on system 10D4.

2.2.3.1 Thermal Retest of System 10D1

Following the dynamic vibration and shock tests to specification level on system 10D1, a thermal retest was performed to determine if there was any change in insulation system performance.

The copper heat transfer rod used during the dynamic tests to increase the unit heat loss was removed and the cavity occupied by the rod was filled with tightly packed powdered Min-K 2000 insulation. During the removal of the copper rod it was necessary to cool the unit to 250°F as the copper rod broke off at the cover plate. It was necessary to remove the cover plate and the first layer of Min-K

insulation to remove the copper rod. During removal, the threaded end of the rod twisted off even with the emitter plate into which it was threaded. The inner liner Min-K insulation was reassembled and the unit was heated to 1285°F for the thermal test.

The thermal performance test was conducted using Ogden Laboratories calibrated wattmeter, voltmeter, and ammeter. At a steady hot end inner liner temperature of 1285°F, the unit required 26.3 volts and 2.84 amps, or an input of 74.69 watts. Following the test, the power lead wiring from the instrumentation to the unit was returned to Linde. At Linde it was determined that the power leads exhibited a resistance of 0.622 ohm. The I^2R loss in the power lead wire is, therefore, 5.02 watts. Subtracting the power lead loss results in a corrected input power of 69.67 watts. The corrected power to the unit before the dynamic test was 61.1 watts. For evaluation of the thermal performance of the unit, see paragraph 2.2.3.6.

2.2.3.2 Unit Thermal Performance Test of Insulation System 10D2

Following the closure, the unit was instrumented for conditioning at 1550°F and a thermal performance test at 1285°F. This unit was instrumented for the thermal test using the inner liner Min-K design as was used for the unit 10D1 dynamic test. This design was used so that the system could assume its backup function and be dynamically tested in the event of premature failure of unit 10D1. A schematic of the Min-K insulation system design is shown in Figure 2-3.

All four heaters were connected in parallel and wired through a wattmeter, recording ammeter, variac, constant voltage power supply, and insulation transformer to the line power. Chromel-alumel thermocouples were installed in the following locations on the unit: cover plate (1), upper unit heat (1), cylindrical portion of unit near girth weld (2), near flat on bottom heat (1). All thermocouples were connected to a temperature recorder. The unit was continuously evacuated throughout the heatup, conditioning, and thermal test period. Power was supplied to the heaters initially at 50 watts for 16.75 hours. At this time the unit temperature was 295°F. The power input was then increased to 80 watts and continued at that level until the total accumulated time was 24 hours and the unit temperature was 425°F. The power was then increased to 100 watts where it

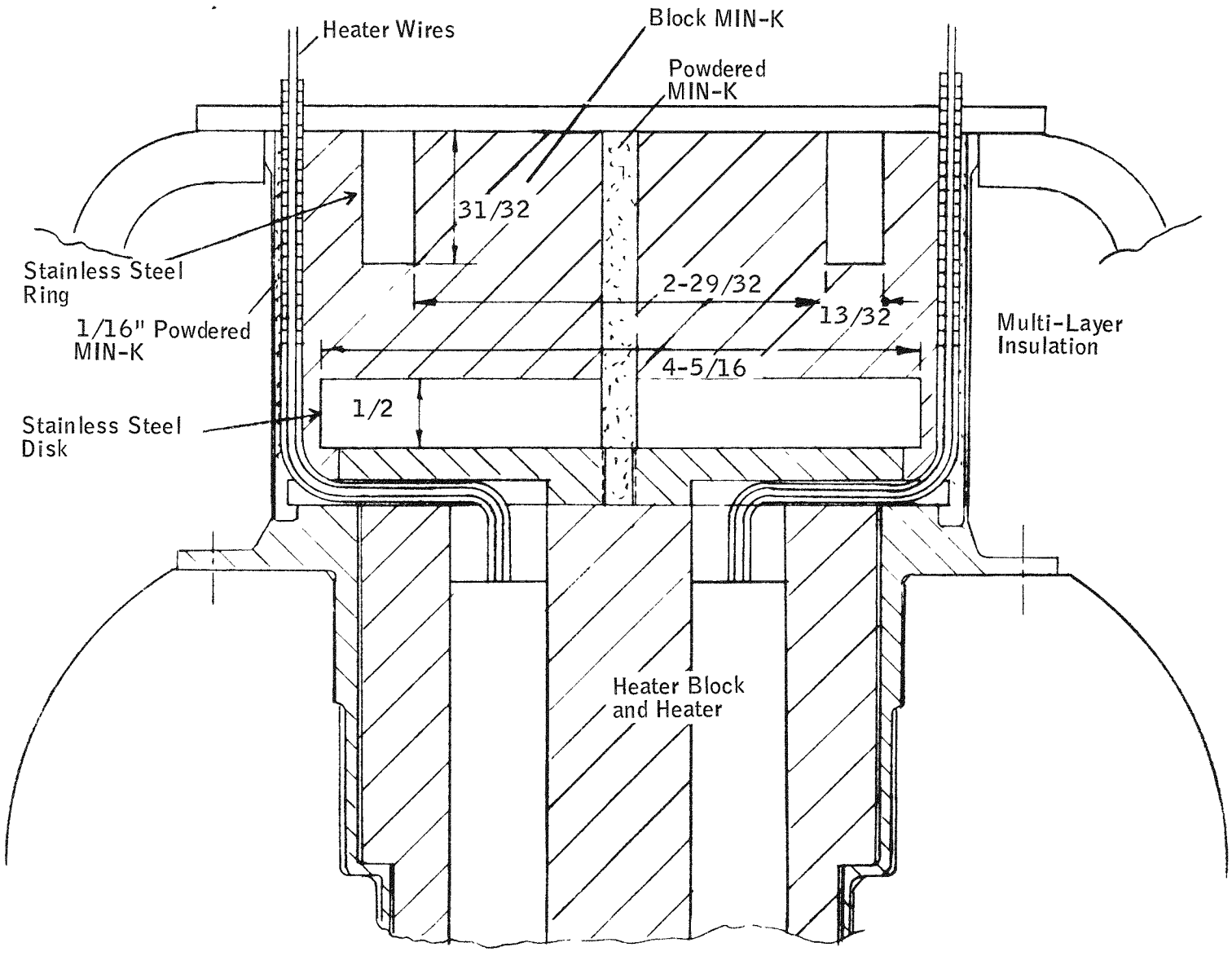

Figure 2-3. Schematic of Inner Liner Insulation – Arrangement for System 10D1 Dynamic Test and 10D2, 10D3, and 10D4 Thermal Test

remained until the total accumulated time of 43.8 hours and a unit temperature of 790°F was reached. The power was then increased to 150 watts where it remained until the unit reached the conditioning temperature of 1550°F. A total of 94 hours had elapsed since the start of the test. At this time the power was reduced to approximately 100 watts (adjustments were made when required) to maintain the 1550°F temperature until 140 hours had elapsed. After 140 hours the power was turned off. At 153 hours the unit had cooled to 1300°F and the power was resumed at 65 watts. As the unit slowly cooled, the power was adjusted to maintain a steady 1285°F. The insulation pressure during the thermal performance test was 1.5 microns and the corrected total power to the unit was 71.82 watts (corrected for meter calibration and I^2R loss in power lead wire). For an evaluation of the thermal performance of the unit, see paragraph 2.2.3.6.

During the conditioning of the unit, the evacuation device was accidently separated from the unit causing the unit to be backfilled with air at atmospheric pressure. Evacuation was restarted with less than two minutes of air exposure. Calculations performed considering the limited air exposure show that this loss of vacuum should not change the insulation thermal performance to any significant extent.

Following the thermal performance test when the unit was cooling, a helium leak check of the unit was performed and a slow rise on the leak detector indicator scale was noted. In an attempt to locate the leak, the helium filled bag was removed and the unit components, including the inner liner and top edge weld, vacuum gauge, and outer enclosure heads, the girth weld and receptacle seal-off plugs, were bagged in helium. No leakage was apparent.

From this test, the conclusion may be drawn that the initial leakage was in the rubber "O"-ring that seals the evacuation device to the bottom enclosure head.

At the conclusion of the leak check, 13.25 grams of regular getter was installed in the unit. It was intended to install 15.0 grams, however, 1.75 grams of getter remained in the glass feed tube and did not enter the unit. During subsequent unit getter fills, the unit will be rotated to ensure that the unit will receive all the getter. Offgassing calculations show that the unit only needs 6.4 grams of getter for a five-year life, therefore, the 13.25 grams put in this unit is entirely adequate.

The male getter seal-off device with the gold 'O"-ring was threaded into the female seal-off device and torqued to 75 ft-lb to make the temporary unit seal-off. Following the temporary seal-off, the final seal-off was made, using the following parameters: 50-54 amps, 9.0-10.5 watts, 6 ipm, 25 cfh argon, no filler wire used. Prior to completing the seal-off weld, the volume between the weld and the gold "O'-ring was purged with dry nitrogen gas to reduce the argon concentration that would remain between the two seals when the weld was completed. The unit vacuum gauge readout indicated a unit pressure of less than 0.1 micron after seal-off.

The Min-K insulation and heater block were removed from the inner liner and the unit was installed in a shipping container for 3M pick-up and transport to Oak Ridge National Laboratory where it was integrate into the early fueled system, S10D1A.

2.2.3.3 Development Insulation System 10D3

a) Unit Insulation

The insulation of unit 10D3 was completed using the Linde proprietary insulation technique. A total of 165 insulation layers was applied to the unit. The layer composition, thickness, and layer density is presented in Table 2-3.

Table 2-3. Insulation Composition, Unit 10D3

Number of Layers	Layer Composition	Total Thickness (inch)	Layers per inch
2	Quartz Cloth		
45	Nickel Foil Quartz Paper	0.422	107
60	Copper Foil Quartz Paper	0.539	111
60	Aluminum Foil 106 Paper	0.534	112

Upon completion of the insulation application two layers of nickel foil were applied over the insulation to provide protection during unit closure.

b) Unit Closure

The closure for unit 10D3 was essentially the same as presented in Quarterly Report No. 6 for unit 10D2. The procedure is repeated below to show variations in weld parameters and assembly methods.

The unit enclosure heads were dimensionally inspected and leak checked upon receipt at Linde. The leak rate of each of the heads was determined to be acceptable.

The top head was cleaned and installed over the unit shaft to mate with the top edge of the inner liner. The head was aligned and tack welded to the inner liner using the Tension Rod Alignment Fixture. Following the tacking, the fixture was removed and the semiautomatic edge type weld was performed. The weld parameters recorded for this weld were as follows: 78-80 amps, 12.5 volts, 10 ipm, 25 cfh argon, no filler wire used.

The bottom enclosure head was prepared for assembly on the top head by welding on the following components: enclosure support rod receptacle (3), getter seal-off device female end (1), hydrocarbon getter enclosure assembly (1), and getter retainer assembly (1).

The receptacles were aligned in the bottom head using the receptacle welding fixture. Each receptacle was tack welded in three places and manually welded using 0.045-inch 308L filler wire and 25 cfh argon. Weld parameters were: No. 1 – 76-80 amps, 9.0-10.5 volts; No. 2 – 74-80 amps, 9.0-10.5 volts; No. 3 – 74-80 amps, 9.0-11.0 volts.

The getter seal-off device, female end, was aligned in the bottom head to be flush with the flat on the head. Four tack welds were made 90° apart. The edge weld was manually performed with the following parameters recorded: 48-50 amps, 9.0-10.0 volts, 25 cfh argon, 5-1/2 ipm torch travel, no filler wire added.

The hydrocarbon getter enclosure, which contained 1.006 grams of getter, was centered on the female end of the seal-off device and the attachment lugs were welded to the head using 60-64 amps, 9-10 volts, 25 cfh argon and 0.045-inch 308L filler wire.

The getter retainer assembly was aligned in the bottom head and tack welded in eight places around the circumference. The seal weld was manually performed using 72-80 amps, 8.5-10.5 volts, 2-3 ipm, 0.045-inch 308L filler wire and 25 cfh argon. This weld was not continuous. Approximately two inches were welded at one time before skipping across the diameter to weld the next two inches. This procedure was employed to keep the shrinkage to a minimum.

The bottom head, with all components welded, was cleaned and again leak checked. It was found to have an acceptable leak rate. The head was then mated with the top enclosure head and the angular alignment of the tension rod receptacles was set using the tension rod alignment fixture. The weld joint was closed until there was no gap and the top head was then tack welded to the bottom head with 9 tacks, equally spaced on the circumference. The automatic girth weld was performed in two passes. The following parameters were recorded:

Pass	Amps	Volts	Wire Feed (ipm)	Travel (ipm)	Shield Gas (cfh)
1	288-292	12.5-13.0	80	15	25 argon
2	288-295	15.0-15.5	100	15	75 helium

The filler wire was 0,045 inch diameter 308ELC.

The female tension rods with a 0.355 inch thick spherical washer were threaded on to the respective numbered male rods and sequentially torqued to 40 in-lb to ensure complete seating of the washers. Measurements were then taken to determine the required washer thickness to provide a 2.939 inch long tension rod assembly. It was determined that the following spherical washer thicknesses were required: Rod No. 1 = 0.290 inch, Rod No. 2 = 0.336 inch, Rod No. 3 = 0.267 inch. These spherical washers were ground and installed. The adjusting pins were then installed between the spherical washer and tack welded to the receptacle.

Following the tack welding of the spherical washers, the tension rods were loosened and then sequentially torqued in increments of 5 in-lb to 23 in-lb. The bore of each of the female support rods was then insulated using disks of copper opacified insulation material. The rod anti-rotation devices were then installed and tack

welded to the spherical washers to prevent loosening of the tension rods. The receptacle seal-off plugs were tack welded to the receptacles and then manually welded using 46-50 amps, 8.5-10.5 volts, 2 ipm, 25 cfh argon with 0.030-inch diameter 308L filler wire.

After closure, the unit was evacuated and leak checked with a Veeco MS-9 leak detector. With the unit enclosed in a helium filled bag, leak check showed the unit to have a leak rate of 5.5×10^{-10} atm-cc/sec-air which is acceptable.

Measurements of the completed unit showed that the length from the top flange flat to the imaginary point on the spherical radius on the bottom head was 15.052 inches.

The unit diameter at the top head was 12.417 inches and the diameter at the bottom head was 12.414 inches. The length and diameters, as measured, are within tolerance.

c) Unit Thermal Performance

Following the closure, the unit was instrumented for conditioning at 1550°F and a thermal performance test at 1285°F. This unit was instrumented for the thermal test using the inner liner Min-K design, as shown in Figure 2-3. This Min-K insulation system design is essentially the same as was used during the testing of unit 10D2, except that the disk bolted to the emitter plate was fabricated from copper rather than stainless steel. This was to provide a better thermal path when using the 1/2-inch diameter copper heat transfer rod during the dynamic test, providing a 200-watt heat loss to simulate an operating unit. The test instrumentation was the same as for system 10D2. Power was supplied to the heaters the same as with system 10D2. The conditioning temperature of 1550°F was reached after 96 hours of total elapsed heat up time. At this time the power was reduced to approximately 100 watts (adjustments were made when required) to maintain the 1550°F temperature until 117 hours of total accumulated time. The power was then turned off. While cooling, the unit was leak checked with a helium leak detector. The leak rate was found to be 2×10^{-9} std-cc-air/sec. At 130 hours of total elapsed time the unit had cooled to 1303°F and the power was resumed at 72 watts, uncorrected. As the unit slowly cooled the power was adjusted to maintain a steady 1285°F. The insulation pressure during the thermal

performance test was 1.4 to 2.0 microns and the corrected total power to the unit was 71.3 watts (corrected for meter calibration and I^2R loss in power lead wires).

The calculation of the subtractables to determine the unit thermal performance is summarized in paragraph 2.2.3.6 of this report.

At the conclusion of the thermal test, 15 grams of regular getter were installed in the unit and the male getter seal-off device with the gold "O"-ring was threaded into the female seal-off device and torqued to 75 ft-lb to make the temporary seal-off. Following the temporary seal-off the final seal-off weld was made using the following parameters: 50-54 amps, 8.5-10.0 volts, 5-6 ipm, 25 cfh argon, no filler wire used.

2.2.3.4 Development Insulation System 10D4

a) Unit Insulation

The insulation of unit 10D4 was completed using the Linde proprietary insulation technique. A total of 165 insulation layers was applied to the unit. The layer composition, thickness, and layer density are presented in Table 2-4.

Table 2-4. Insulation Composition, Unit 10D4

Number of Layers	Layer Composition	Total Thickness (inch)	Layers per inch
2	Quartz Cloth		
105	Copper Foil Quartz Paper	0.945	111
60	Aluminum Foil 106 Paper	0.453	132

Upon completion of the insulation application two layers of nickel foil were applied over the insulation to provide protection during unit closure.

b) Unit Closure

The closure for unit 10D4 was essentially the same as for unit 10D3. The procedure is repeated below to show variations in weld parameters and assembly methods.

The unit enclosure heads were dimensionally inspected and leak checked upon receipt at Linde. The leak rate of each of the heads was determined to be acceptable.

The top head was cleaned and installed over the unit shaft to mate with the top edge of the inner liner. The head was aligned and tack welded to the inner liner using the tension rod alignment fixture (E-664061). Following the tacking, the fixture was removed and the semiautomatic edge type weld was performed. The weld parameters recorded for this weld were as follows: 68-72 amps, 10.5-11.5 volts, 10 ipm, 25 cfh argon, no filler wire used.

The bottom enclosure head was prepared for assembly on the top head by welding on the following components: enclosure support rod receptacle (3), getter seal-off device female end (1), hydrocarbon getter enclosure assembly (1), and getter retainer assembly (1).

The receptacles were aligned in the bottom head using the receptacle welding fixture. Each receptacle was tack welded in three places and manually welded using 0.045-inch 308ELC filler wire and 25 cfh argon. Weld parameters were: No 1. — 74-80 amps, 9.0-10.5 volts; No. 2 — 72-78 amps, 9.0-10.5 volts; No. 3 — 74-80 amps, 9.0-11.0 volts.

The getter seal-off device, female end, was aligned in the bottom head to be flush with the flat on the head. Four tack welds were made 90° apart. The edge weld was manually performed with the following parameters recorded: 48-52 amps, 9.5-11.0 volts, 25 cfh argon, 6 ipm torch travel, no filler wire added.

The hydrocarbon getter enclosure which contained 1.004 grams was centered on the seal-off device, female end, and the attachment lugs were welded to the head using 60-64 amps, 9-10 volts, 25 cfh argon, 0.045-inch 308ELC filler wire.

The getter retainer assembly was aligned in the bottom head and tack welded in eight places around the circumference. The seal weld was manually performed using 72-80 amps, 8.0-10.0 volts, 2-3 ipm, 0.045-inch 308ELC filler wire, 25 cfh argon. This weld was not continuous. Approximately two inches were welded at a time, before skipping across the diameter to weld the next two inches. This procedure was employed to keep the shrinkage to a minimum.

The bottom head, with all components welded, was cleaned and again leak checked. It was found to have an acceptable leak rate. The head was then mated with the top enclosure head and the angular alignment of the tension rod receptacles was set using the tension rod alignment fixture. The weld joint was closed until there was no gap and the top head was then tack welded to the bottom head with 9 tacks, equally spaced on the circumference. The automatic girth weld was performed in two passes with the following parameters recorded.

Pass	Amps	Volts	Wire Feed ipm	Travel ipm	Shield Gas cfh
1	286-295	12.5-14.0	80	15	25 argon
2	286-295	15.0-16.0	100	15	75 helium

The filler wire was 0.045-inch diameter 308ELC.

The female tension rods with a 0.355-inch thick spherical washer were threaded on to the respective numbered male rods and sequentially torqued to 23 in-lb to ensure complete seating of the washers. Measurements were then taken to determine the required washer thicknesses to provide a 2.939-inch long tension rod assembly. It was determined that the following spherical washer thicknesses were required: Rod No. 1 = 0.276 inch, Rod No. 2 = 0.276 inch, Rod No. 3 = 0.284 inch. These spherical washers were ground and installed. The spherical washer seat and ball were coated with Molykote Type Z powder to prevent any cold welding.

To be on the high side of the angle tolerance to ensure rod tightness, it was necessary to recalculate the required tension rod angle. Using the assembly fixture, the tension rods were located at 28° 16' for Rod No. 1, 28° 18' for Rod No. 2, and 28° 19' for Rod No. 3 and torqued to 40 in-lb to temporarily secure the spherical washer in the receptacle. The adjusting pins were then installed between the spherical washer and tack welded to the receptacle.

After tack welding the spherical washers, the tension rods were loosened and then sequentially torqued in increments of 5 in-lb to 23 in-lb. The bore of each of the female support rods was then insulated with disks of copper opacified insulation material. The rod anti-rotation devices were then installed and tack welded to the spherical washers to prevent the tension rods from loosening.

The receptacle seal-off plugs were tack welded to the receptacles and then manually welded using 48-52 amps, 8.5-10.0 volts, 2 ipm, 25 cfh argon, 0.030-inch diameter 308L filler wire.

After closure, the unit was evacuated and leak checked using a Veeco MS-9 leak detector. With the unit enclosed in a helium filled bag, a leak check showed the unit to have a leak rate of 9.7×10^{-10} atm-cc-air/sec, which is acceptable.

Measurements of the completed unit showed that the length from the top flange flat to the imaginary point on the spherical radius on the bottom head was 15.061 inches.

The unit diameter at the top head was 12.415 inches and the diameter at the bottom head was 12.410 inches. The length and diameters, as measured, are within tolerance.

c) Unit Thermal Performance

The unit was instrumented for the thermal test in the same manner as for unit 10D3 discussed in paragraph 2.2.3.2 of this report. The conditioning temperature of 1550°F was reached after a total elapsed heat-up time of 88.7 hours. At this time, the power was reduced to approximately 100 watts to maintain the 1550°F temperature until 121.5 hours of total accumulated time when the power was turned off. While cooling, the unit was leak checked with a helium leak detector. The leak rate was found to be 4.4×10^{-9} std-cc-air/sec.

At 137.5 hours, total accumulated time, the unit had cooled to 1289°F and the power was resumed at 50 watts, uncorrected. As the unit cooled the power was adjusted to maintain a steady 1285°F. The insulation pressure during the thermal performance test was 3.8 microns and the corrected total power to the unit was 67.8 watts (corrected for meter calibration and I^2R loss in power lead wires).

The calculation of the subtractables to determine the unit thermal performance is summarized in paragraph 2.2.3.6 of this report.

During this thermal performance test, one of the electric heaters failed while the power supplied was 150 watts as evidenced by a drop in system current and an increase in system voltage. After the unit was conditioned and the power turned off, the heater resistances were checked and it was found that one heater had a resistance of 85K ohms while the other three heaters had individual resistances of approximately 27 ohms.

At the conclusion of the thermal test, 15 grams of regular getter were installed in the unit and the male getter seal-off device with the gold "O"-ring was threaded into the female seal-off device and torqued to 75 ft-lb to make the temporary unit seal-off. Following the temporary seal-off the final seal-off weld was made using the following parameters: 52-56 amps, 8.5-10.0 volts, 5-6 ipm, 25 cfh argon, no filler wire used.

2.2.3.5 Final Design Review

The Final Design Review of the insulation system for the SNAP-21 10-watt system was held at 3M Company on March 13, 1968. The Linde Quality Control Plan was presented to 3M and reviewed by the 3M Quality Supervisor to ensure that 3M comments which had been previously agreed upon had been incorporated. The Quality Control Plan was accepted with the stipulation that all documents referenced in the plan are a part of the plan.

Linde presented the changes which have been made in the insulation system design since the Preliminary Design Review. These changes are as follows:

1. The spider material was changed from molybdenum to Hastelloy-X.

2. Inconel-625 in the cold end of the tension rods was changed to Inconel-718 to reduce heat loss.

3. The method of supporting the biological shield was changed to the "hot interference - cold friction" method.

4. The spherical washer is now cut to the exact length at assembly.

5. The method of applying insulation material has been changed: (a) copper foils have replaced the nickel foils near the shield; (b) the assembly time has been reduced from three months to one month; (c) the pilot portion of the male half of the tension tie rod was removed; (d) the inside diameter of the female rod (cold end) is being insulated.

The following development activities performed on this contract were then discussed:

- Offgassing evaluation
- Getter tests
- Getter retainer tests
- Seal-off device development
- Compatibility tests
- Weld development
- Dynamic testing

The conclusions which can be drawn from the development units are as follows:

1. Structural integrity of the units has been demonstrated.

2. The specified unit weight of 60 pounds maximum can be achieved. Unit 10D4 weighed 60.3 pounds.

3. The heat loss of the units will be approximately 46 watts.

4. Vacuum integrity of the units has been demonstrated.

The method of determining the thermal performance of a unit was presented. This is shown in paragraph 2.2.3.6 of this report.

The Linde manufacturing procedures which are called out on the face of the drawings were accepted by the 3M contingent upon approval of the drawings. These drawings have been subsequently approved.

The acceptance test procedure was submitted to the 3M Company. These procedures delineate the following requirements:

1. Thermal performance of 45 watts.
2. Leak rate of 6×10^{-8} std-cc/sec-air.
3. Unit weight of 60 pounds.
4. Conformance to envelope and interface requirements.

The following documents were submitted to 3M:

- Acceptance Test Plan
- Drawings
- Quality Control Plan
- Manufacturing Flow Plan
- Analysis of Model "A"

The 3M Company stated that the subcontractor has successfully met the requirements of the Final Design Review and is thereby authorized to proceed with the fabrication and assembly effort to complete the Task I work of the subject contract.

2.2.3.6 Method of Determining Unit Thermal Performance

The subtractable heat losses during a thermal performance test include the heat losses through elements of the test system which are not a part of the insulation system and are therefore not a part of the unit heat loss.

These subtractable losses result from the inner liner Min-K insulation, the heater wire power leads, and the thermocouple wires. In addition to these losses, other subtractable heat losses can be present, depending on the geometry of the Min-K system. For example, if the Min-K temperature adjacent to the neck tube is higher than the neck tube temperature, there will be a lateral heat flow from the Min-K to the inner liner which provides a heat flow to the HTVIS unit. This heat flow can be determined by a two dimensional analysis of the system and must be subtracted from the total heat input. Conversely, if the heat flow is from the neck tube to the Min-K this flow must be added to HTVIS unit heat loss.

To determine the subtractable heat losses a two-dimensional computer analysis was performed on a system consisting of the Min-K insulation, heater wires, neck tube, and multilayer insulation. The thermal conductances of the above components were put in equation form, utilizing the known material properties. A temperature grid was then established in the Min-K, heater wires, neck tube and multilayer insulation and the point temperatures were calculated.

With the use of the point temperatures and the material thermal conductances, vertical and lateral heat flows were computed for the various Min-K insulation geometries used in the development units.

The subtractables calculated by this two-dimensional analysis are presented in Table 2-5 along with the measured total power to the unit. The unit heat loss which results from the total power to the unit minus the subtractables is also shown on the table.

Table 2-5. Development Unit Heat Loss

Unit No.	Corrected Total Power to Unit*	Subtractables		Unit Heat Loss	
		Two Dimen.*	One Dimen.*	Two Dimen.*	One Dimen.*
10D1	61.1	10.94	14.8	50.2	46.3
10D1 Retest after Dynamic Test	69.7	24.03	19.8	45.7	49.9
10D2	71.8	24.15	19.0	47.7	52.8
10D3	71.3	24.33	19.1	47.0	52.2
10D4	67.8	24.90	19.1	42.9	48.7

*Units indicate thermal watts

It should be noted that the subtractables are higher for units 10D1 (retest) through 10D4 than on 10D1 because of the addition of a ring and a disk in the Min-K system to simulate the 3M thermoelectric generator and thus achieve a corresponding temperature profile in the neck tube during the dynamic testing.

The subtractables were also calculated using a one-dimensional analysis (vertical heat flow) to determine the heat loss through the Min-K, heater wires, and thermocouple wires. The subtractables as calculated for the one-dimensional analysis are also presented in Table 2-5.

Because the thermal test conditions are somewhat different than the operating conditions for which the 45-watt heat loss is specified, the allowable heat loss for the test condition is reduced to 42 watts. This reduction is caused by unit outside temperature being 100°F during test and 50°F during operation. Also during operation the bottom of the biological shield will be 1430°F, whereas during the test this temperature is approximately 1285°F. These temperature differences reduce the heat flow through the tension rods and insulation during the thermal test and therefore reduce the allowable heat loss for test condition.

As can be seen from Table 2-5, a significant improvement has been achieved on the thermal performance of unit 10D4 over the other development units. This reduction in heat loss is caused by the fact that the nickel insulation layers were replaced by copper layers on this unit. It should be noted, however, that the heat loss for unit 10D4 is 0.9 watt higher than the allowable 42 watts.

2.2.4 SEGMENTED RETAINING RING

No design or development work was done on this component during this report period.

2.2.5 PRESSURE VESSEL

The first three forgings were completed, radiographically inspected, machined, and given the final inspection during the current reporting period. A historical summary of the processing of these forgings follows.

First Forging

1. Heat treat:

   Solution 1425°F – 1 hour

   Water Quench

   Age 625°F – 3 hours

2. Cut-off test ring

3. Rough machine to long cover dimensions

4. Radiographic inspection

5. Strength test samples from test-ring

6. Final machining to drawing PD-37-4221 dimensions

7. Final inspection including dye penetrant check

8. Shipped to Southwest Research Institute for hydro-test

Second Forging

1. Heat treat:
   Solution 1425°F – 1 hour

   Water Quench

   Age 625°F – 3 hours

2. Cut-off test ring

3. Rough machined to body dimensions

4. Radiographic inspection

5. Re-age 700°F – 3 hours

   Note: Both the test-ring and the rough-machined forging were processed at the same time but were separate pieces.

6. Mechanical properties tests performed on specimens from test ring

7. Final machining to drawing PD-37-4220 dimensions

8. Final inspection including dye penetrant check

9. Shipped to Southwest Research Institute for hydro-test

Third Forging

1. Heat treat:

   Solution 1425°F – 1 hour

   Water Quench

   Age 625°F – 3 hours

2. Cut-off test ring

3. Rough machine to long cover dimensions

4. Radiographic inspection

5. Re-age 700°F – 3 hours

   Note: Same as for second forging.

6. Mechanical properties tests performed on specimens from test ring

7. One-half of the rough-machined forging cut up and mechanical properties tests performed on specimens cut from the same.

   Note: Due to difference in mass of test ring and main part of forging, the cut-up samples had somewhat higher strength properties.

The pressure vessel long cover and the body were assembled as a unit and subjected to a hydrostatic pressure test by Southwest Research Institute at San Antonio, Texas, at the end of the reporting period. The proof pressure test of 11,000 psi external pressure was successfully passed. There was no evidence of leakage into the interior. A preliminary appraisal of the recorded strain gage data indicated excellent linearity of strain vs. applied loading. There appeared to be no evidence of structural instability. Data reduction will be accomplished during the next report period and will be presented in the next quarterly report. A 48-hour hold at 11,000 psi did not produce any measurable creep of the material.

Results of material strength tests are summarized in Table 2-6. Chemical composition of the Berylco-165 material used for the forgings is compared with the specification analysis in the following:

Table 2-6. Strength Test Summary

Forging Number	Test Sample Orientation*	Test Ring				Cut-Up Forging			
		0.20% Offset Tension Yield (Kips)	Elongation (%)	0.20% Offset Compression Yield (Kips)	Charpy Impact at 32°F (ft-lbs)	0.20% Offset Tension Yield (Kips)	Elongation (%)	0.20% Offset Compression Yield (Kips)	Charpy Impact at 32°F (ft-lbs)
1	T	162.0	2.0	173.5	3.5				
	T	161.0	3.0						
	R	158.0	3.0						
	R	156.2	2.0						
2	A					150.8	5.0	165.6	4.0
	A					152.5	3.0	168.6	4.0
	A					144.0	5.0	162.6	4.0
	A					144.0	5.0	171.3	4.5
	T	140.4	11.0	164.1	5.5	156.0	5.0	155.0	5.0
	T	146.0	8.5	154.9	6.0	146.0	5.0	155.5	5.0
	T					150.9	3.5		
	R	142.6	5.0	166.9	5.0			153.5	
	R	145.8	8.5	153.4	5.0			165.7	
	R							160.4	
	R							167.3	
3	T	139.0	11.5	151.0	6.0				
	T	140.0	11.0	149.9	6.0				
	R	141.2	5.0	150.1	5.5				
	R	142.0	7.0	155.5	6.0				

*A – longitudinal
T – Tangential
R – Radial

	Forgings	Specification Min.	Max.
Beryllium (percent)	1.68	1.60	1.80
Nickel + Cobalt (percent)	0.329	0.20	----
Nickel + Cobalt + Iron (percent)	0.419	----	0.6
Copper + Total Named Elements (percent)	99.619	99.5	----

The specification value for tensile yield at 0.20 percent offset is 130,000 psi. A minimum elongation of 3 percent is also specified. Table 2-6 shows that, with one exception, these requirements have been met. Only in the case of the first forging was there a discrepancy.

Actually, the strength values are somewhat higher than the requirements but elongation is lower. This unit is the one which received only the original aging cycle. It was due to this combination of strength and elongation that it was decided to alter the properties of succeeding forgings by changing the aging temperature. The first forging was machined to the final configuration and rather than chance the possibility of distortion during a re-aging cycle, it was decided to accept it in its original condition. The basis for this decision being that elongation is strictly a tensile property and the lower value would not influence the integrity of the complete unit under external hydrostatic pressure loading. A rather extreme example of this philosophy is use of glass for similar loading conditions. Table 2-6 shows that the two units, after re-aging, are well within the specification limits for yield strength and elongation.

Although the specification for Berylco-165 material does not set any values for compression yield strength, it should be noted that a value of 140,000 psi at 0.20 percent offset was used as the design minimum for the pressure vessel calculations. All compression tests reported exceed this value, indicating that the original estimate was both conservative and reasonable.

Ultimate strength values in tension have not been included in the accompanying table. For the pressure vessel design, our interest centers about modulus of elasticity and compression strength in the vicinity of 0.20 percent offset yield. The criteria employed for determination of pressure vessel wall thicknesses are:

1. Buckling of the vessel walls shall not occur when the external pressure loading is 1.50 x 1.10 x working pressure.

2. The design compression yield at 0.20 percent offset shall not be exceeded when the external pressure is 1.50 x 1.10 x working pressure.

The only interest in tension yield and ultimate strengths is in the fact that these values characterize the material very well and are more easily and accurately determined than compression values. The specification limits on ultimate tensile strength are 150,000 to 180,000 psi. The values reported on for the test specimens listed in Table 2-6 vary between 157,000 to 170,000 psi for the two forgings which were re-aged, and from 174,800 to 181,500 psi for the first forging.

During the initial stages of pressure vessel design, no information was available regarding microstructure of forgings made from Berylco-165 in the sizes to be used for the SNAP-21 pressure vessel.

Paragraph 6.4.2 of the material specification, AMS4650E, states that average grain size of forgings shall be "as agreed upon by purchaser and vendor." However, to provide a baseline for grain size acceptance criteria, an arbitrary limit of 0.05 mm was set as the maximum value on the pressure vessel drawing. To provide flexibility in establishing a final acceptance criteria, a stipulation was made in the forging purchase order that the grain size was subject to negotiation.

Apparently the author of the material specification was well aware of the difficulty in establishing maximum grain size in Berylco forgings, since grain size measurements from a single forging have ranged from 0.025 to 0.200 mm. This duplex microstructure is shown in Figure 2-4, which is typical for the three forgings. There is also a random distribution of this duplex type of grain structure which can be clearly seen in Figure 2-5, a reduction from a full scale photograph of the sectioned and polished forging.

From technical discussions with Beryllium Corporation and Wyman Gordon metallurgists, it has been concluded that these variations in grain structure are typical for material which originated as a casting, as is the case for the billets from which the parts were forged. The particular structure has not been found to

Figure 2-4. Macrograph Showing Duplex Microstructure of Test Ring from First Pressure Vessel Forging

be detrimental to performance of the end product. More importance would be attached to the material grain structure for applications involving predominantly tension stresses of varying amplitude or continuous reversals of stress which might lead to fatigue. As previously noted, the SNAP-21 pressure vessel application is one for which only compression is present. During implantment and retrieval there will be stress variation but always compression. The number of implantment and retrieval cycles is not of the order of magnitude likely to lead to any fatigue problems.

In light of the fact that the mechanical properties achieved in the present forgings are excellent, and that the vessel has successfully passed hydrotest, the actual measured grain size is considered satisfactory even though it is in excess of the 0.05 mm that was arbitrarily established as a baseline. Further study of the grain size will be made on the remaining units and the grain size criteria will be established when a final decision is made.

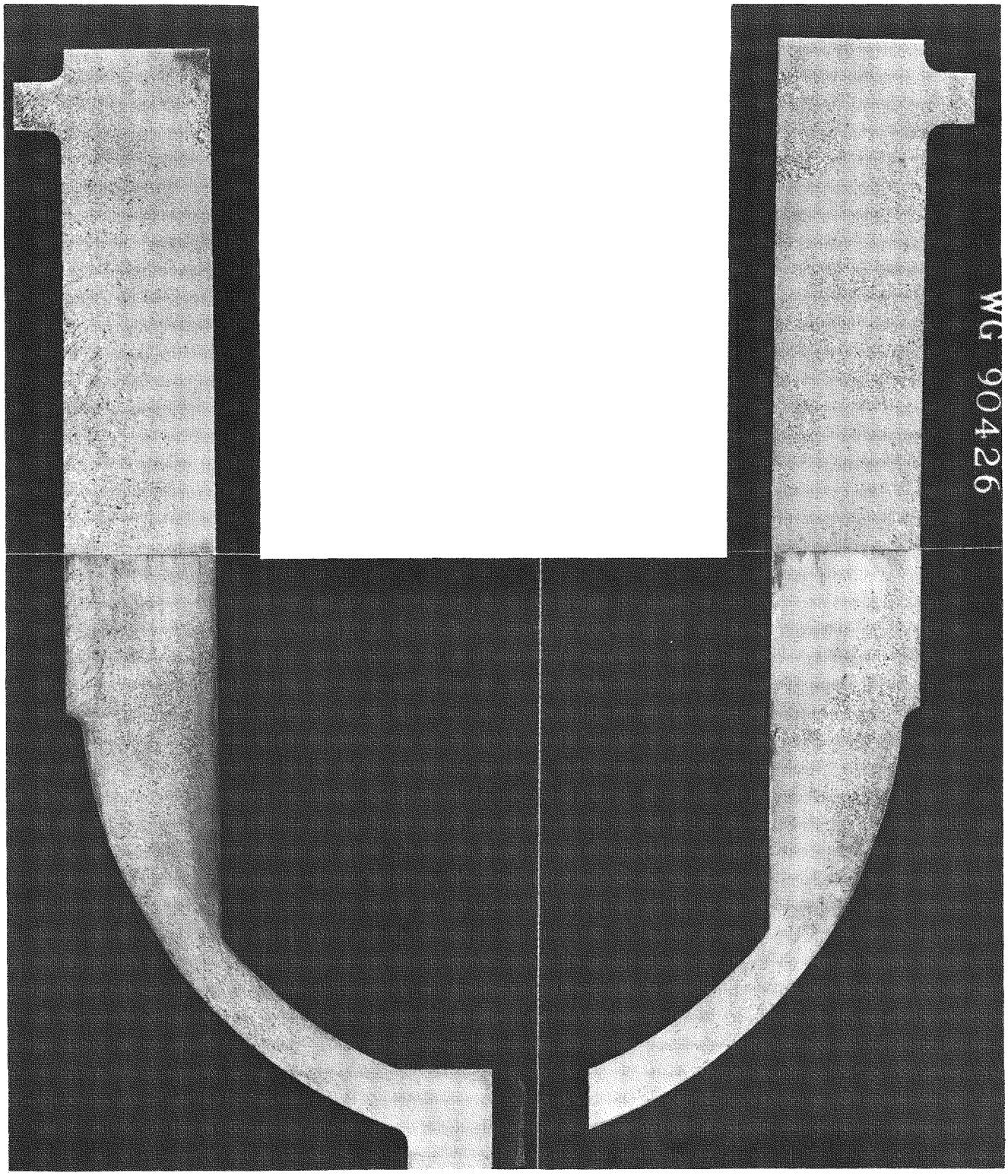

Figure 2-5. Photograph of Sectioned and Polished Pressure Vessel Forging

2.2.6 THERMOELECTRIC GENERATOR

2.2.6.1 Design

During this report period the thermoelectric generator design was finalized. The final design is based on results of the generator development tests and on applicable data from the SNAP-23 and SNAP-27 programs and other 3M Company thermoelectric data.

Complete details of the generator design, including the design basis and rationale, will be presented in a topical report that will be published early in the next report period. Consequently, only a summary of the design and a performance prediction will be included in this report.

A schematic of the final generator design with the basic design features identified is shown in Figure 2-6. A summary of the final thermopile design is presented in Table 2-7 and a detailed breakdown of the final thermoelectric leg design is presented in Table 2-8.

It is important to note from Table 2-7 that the calculated generator load voltage required for maximum efficiency at EOL is 4.73 volts. Since this is different than the optimum load voltage for the previous generator design (5.1 volts), and since it is the power conditioner voltage ratio that determines generator load voltage, it is necessary that the power conditioner design be modified to match it. The power conditioner redesign consists of changing the turns ratio in the transformer. One of the characteristics of the power conditioner is that it maintains a constant load voltage on the generator; consequently, this load voltage must be the voltage required by the generator for maximum efficiency at EOL, since this is the generator design point and the point of minimum generator power output.

A comparison of the development generators with the final generator design is presented in Table 2-9.

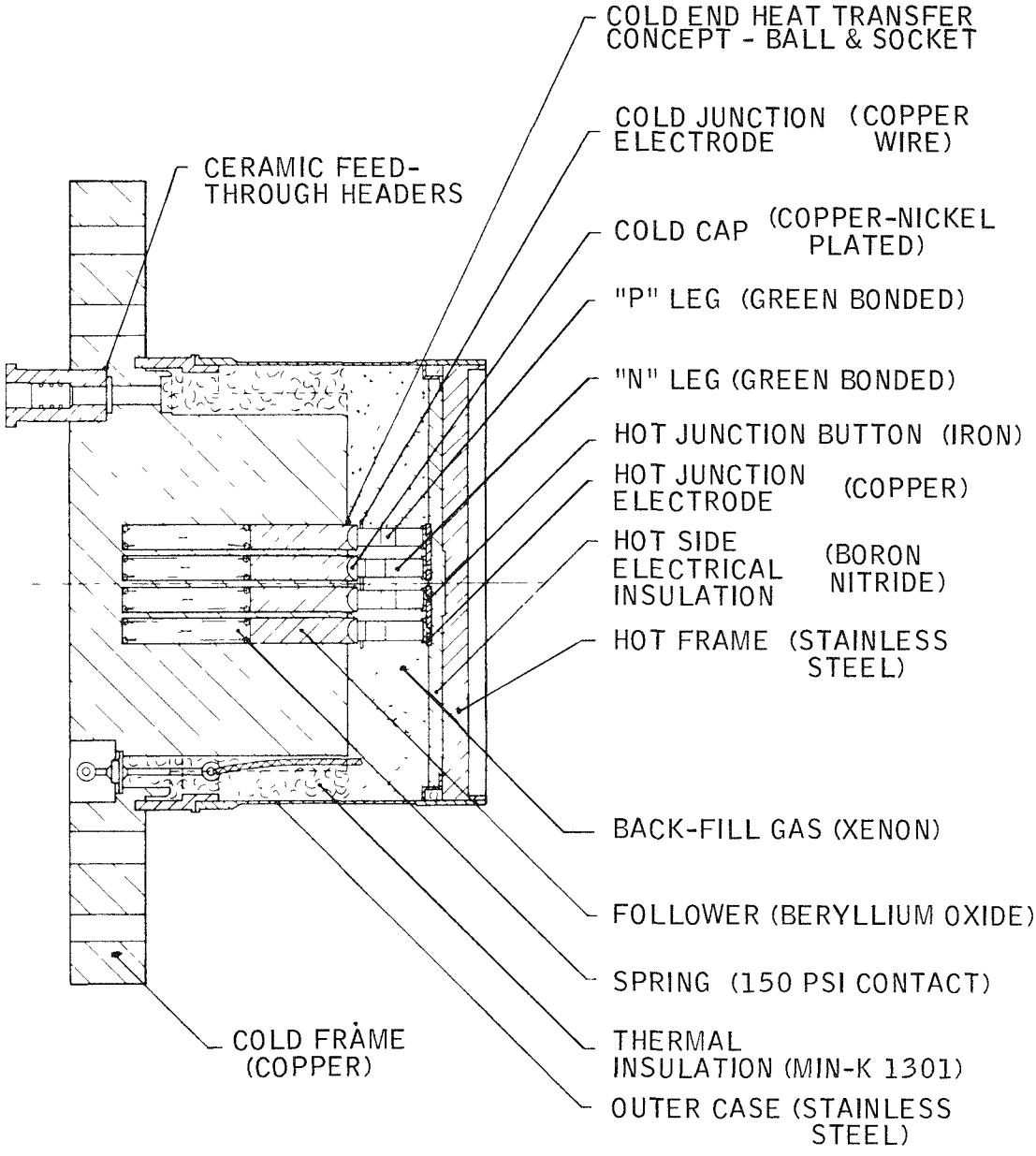

Figure 2-6. Schematic of Final SNAP-21 10-Watt Generator Design

Table 2-10 is a prediction of EOL generator performance at EOL conditions. EOL performance is the only data presented since this is the generator design point. Additional performance data at BOL and intermediate life conditions are being prepared and will be included in the next quarterly report.

Table 2-7. Final Thermopile Design Summary, SNAP-21 10-Watt Generator

Number of Couples	48
Type of Circuit	Series
Hot Junction	Pressure Contact, 150 psi
Cold Junction	Bonded
Load Voltage at Maximum Efficiency, volts (EOL)	4.73
Current at Maximum Efficiency (EOL), amps	2.41
Power at Maximum Efficiency, Pe (EOL) watts (e)	11.4
Heat Absorbed by Legs, Q1 (EOL) watts (t)	119.4
Open Circuit Voltage at EOL, volts	7.99
Circuit Resistance at EOL, ohms	1.35
Thermoelectric Efficiency at EOL $\frac{Pe}{Q1}$ x 100, percent	9.55

Table 2-8. Final Thermoelectric Leg Design Summary, SNAP-21 10-Watt Generator

Parameter		P-Leg	N-Leg
Thermoelectric Material:	Hot Segment	PbSnTe (ES-1110 with "Soft Nose" ES-1111)	PbTe (ES-1103)
	Cold Segment	BiSbTe (ES-1116)	PbTe (ES-1104)
Fabrication Method		Hot segment pressed and sintered. Cold segment pressed and sinter-bonded to hot segment	Both segments separately pressed, then sinter-bonded to form
Hot segment length, inch		0.326	0.329
Cold segment length, inch		0.187	0.184
Total leg length, inch		0.513	0.513
Diameter, inch		0.188	0.188
Length to area ratio 4A, inch		18.48	18.48
Hot junction design temperature,			
	°F EOL	900	900
	BOL	1005	1005
	Max. (during shipment)	1020	1020
Cold junction design temperature,			
	°F EOL	105	105
	BOL	115	115
	Max. (during shipment)**	204	204
Segment temperature,	°F EOL	404	402
	BOL	454	452
	Max. (during shipment)**	560	560
*Open circuit voltage, mv		73.9	93.0
*Load voltage, mv		43.8	54.7
*Average Resistivity, μΩ-in		783	757
*Current, amps		2.41	2.41
*Power, watts (e)		0.091	0.150
*Rate of heat absorption, watts (t)		1.08	1.37
*Rate of heat rejection, watts (t)		0.99	1.22
*Thermoelectric Material efficiency, percent		8.33	10.92

*These parameters apply to maximum efficiency conditions at EOL.
**Short circuit condition.

Table 2-9. Comparison of Development and Final Generator Designs

Design Feature	Development Generators		Final Design
	Design 1	Design 2	Design 3
Cold End Configuration	Ball and socket	In-Line	Ball and socket
Followers	Aluminum with bare and hard-coated sockets	Aluminum with single layer of hardcoat for insulator	Beryllium Oxide
Cold Caps	Bare copper	---	Nickel plated copper
Thermal Insulation	Min-K 1301	Min-K 1301 Min-K 1999 Microquartz	Min-K 1301
Back-Fill Gas	Argon Xenon	Xenon	Xenon
Power and Instrumentation Feed Throughs	Conax	Ceramic (soft soldered)	Ceramic (brazed)
Thermoelectric Legs			
P-Leg Diameter	0.188	0.188	0.188
P-Leg Cold seg. length	0.149	0.149	
P-Leg Total leg length	0.411	0.411	0.513
N-Leg Diameter	0.188	0.188	0.188
N-Leg Cold seg. length	0.202	0.202	
N-Leg Total leg length	0.571	0.571	0.513
Thermoelectric Leg Contact Pressure, psi	150	150	150

Table 2-10. Final SNAP-21 10-Watt Generator Design Performance Prediction

Design Hot Junction Temperature (avg)	900°F (EOL) 1005°F (BOL)
Design Cold Junction Temperature (avg)	105°F (EOL) 115°F (BOL)
(1)Maximum Hot Junction Temperature	1020°F
(1)Maximum Cold Junction Temperature	204°F
(1)Maximum Segment Temperature	560°F
Generator Load Voltage	4.73 volts
Thermopile Resistance	1.35 ohms (EOL)
Total Heat into Generator, Q_t	146.3 watts (t) (EOL)
(2)Shunt Heat Loss, Q_l	26.9 watts (t) (EOL)
Power Out, P_o	11.4 watts (e) (EOL)
Generator Efficiency, $\frac{P_o}{Q_t}$	7.79 percent

NOTES:

(1) Maximum temperatures experienced during shipment in 130°F air with temporary cooling fins attached and generator in short circuit condition.

(2) Generator shunt heat loss includes losses from generator case to insulation system neck tube.

2.2.6.2 Test Fixture

Test equipment effort for the report period consists of the following assemblies:

A test fixture was fabricated along with associated instrumentation to evaluate the insulation system on long-term test. Unfortunately the test is delayed due to a system failure while undergoing a vibration test at Linde. The test plan has been completed for the long-term test.

A dry box was acquired for storage of thermoelectric legs. Some modification and accessories were necessary. Operation will begin early in the next period.

Two power conditioner test cabinets were fabricated, one of which has been pressed into service for the post-assembly tests during power conditioner assembly. The test cabinets will eventually be used for long-term evaluation test.

2.2.6.3 Fabrication

2.2.6.3.1 Generator Fabrication Development and Processing

a) Generator A10D7

The assembly of Generator A10D7 was started on January 5, 1968 and completed on January 10, 1968. This was the last unit in the series of generators using the in-line couple concept. It was packed with Min-K 1999 which increased the packing time by approximately one-third as compared to packing with Min-K 1301. The generator was held in a holding and handling fixture during the external wiring. This fixture greatly simplified the operation by providing accessibility to all external areas of the generator.

Generator A10D7 was processed according to MP-104 (50-hour process) and commenced immediately after the assembly was completed. The pinch-off was made on January 12, 1968. Mapping was started on January 15, 1968.

b) Generator A10D5

Generator A10D5 was returned to Manufacturing from test on January 12, 1968, because of a pressure loss. After having been through shock and vibration testing, it was being heated when the leak occurred. A leak check disclosed the long case was cracked. This crack was evaluated as being non-repairable and replacement of the long case was begun.

The generator was placed into the assembly fixture along with the replacement long case. This leaking long case was removed with a milling operation. After exposing the edge couples for observation by the test group, the new long case was positioned and welded. The generator was then put in the test and process station and reprocessing was begun. The processing was completed on January 21, 1968, without a final pinch-off. Argon was used as backfill gas and the generator was mapped at a steady-state BOL condition for 200 hours. Upon completion of this testing, the generator was purged of its argon backfill gas and refilled with xenon gas. The final pinch-off was then made and the generator returned to the test group for further evaluation.

c) Generator A10D1

The pressure integrity of Generator A10D1 failed while undergoing a series of test procedures in system 10D1. The generator was put in the environmental chamber during cool-down to prevent the entry of contaminating atmosphere. The chamber was filled with argon gas to provide the proper internal backfill gas as the generator cooled to room temperature.

The generator was inspected to determine the reason for the pressure loss. The cause was found to be a mechanical failure of the long case in the transition area between the hot end thick-walled section and the thin (0.005 inch) case section. This is the same area that failed on Generator A10D5.

It was not possible to repair this case, and, since the generator had not been contaminated by the atmosphere, it was decided to seal the generator with a second long case. This case was made of 0.010-inch thick stainless steel sheet and welded over the existing case on the thick sections of both hot and cold ends to determine the weld integrity the unit was pressurized to 1 psig of argon gas and leak checked. No leak was detected. The generator was then returned to the test group for evaluation.

When the final design for generators was released, fabrication and procurement of hardware started immediately. Long lead items such as beryllium oxide (BeO) followers, couples, and cold frames are under close surveillance in an effort to maintain schedule. It appears, at this writing, that the followers will be our pacing item. These are being made for us by the American Lava Corporation of Chattanooga, Tennessee. 3M shop facilities are producing 74 percent of the fabricated components for generators. Within our own shop, we have no schedule problems.

Effort for the next quarter will be concerned with completion of generators A10D8 and A10P1. A10D8 will be instrumented the same as A10D7 whereas A10P1 will have no internal instrumentation.

2.2.6.3.2 Leg and Couple Fabrication Development

Approximately 1000 leg segments of each of the N- and P-leg hot and cold segments and the bonded N- and P-leg segments were pressed. These segments will be bonded early in the second quarter. Since the lengths of the segments have been changed, new bonding molds were manufactured. These molds are in-house and have been inspected. The bonding processes are the same as for the in-line legs and no problems are expected.

The overall length of the couple is unchanged so the same fixture brazing molds and couple soldering molds will be used as were used for the MEL hardware. The processing procedures were established in earlier phases of the program.

2.2.7 POWER CONDITIONER

During this report period three additional power conditioners, H10D2, H10D3 and H10D4, were assembled and subjected to process burn-in for 240 hours. The specified design verification and operational tests have been performed as authorized in the SNAP-21 Power Conditioner Test Plan.

The measured efficiency of these power conditioners is summarized below:

Power Conditioner	Efficiency at Rated Load	Ripple at Rated Load
H10D2	90.06%	62 mv
H10D3	90.51%	50 mv
H10D4	90.82%	50 mv

2.2.7.1 Design

The excess output ripple of 130 mv that was detected in the H10D1 prototype power conditioner has been traced to an unbalance in winding resistance in the transformer introduced by the type of solder terminals used. The terminal arrangement has been revised to correct this problem in the new transformer design.

During performance testing of the units, an excessive voltage spike of 500 mv amplitude of 2 to 3 microseconds duration at each switching period was observed on the extremeties of the output leads. Experimental tests have shown this spike to be due to the inductive reactance of the transformer output leads. This reactance forms a ringing circuit during the switching period of the input transistors. Further tests have shown that the spike can be eliminated by: 1) providing an independent conductor for both the input and the output common negative lead, and 2) by connecting a 27 microfarad capacitor from the input bias transformer lead to the common negative lead. This change will be incorporated in the final power conditioner design.

During this report period the thermoelectric generator design was finalized. As a result of the thermocouple redesign, the calculated generator load voltage required for maximum efficiency at EOL is 4.73 volts. This change requires that the power conditioner transformer be redesigned to match this generator voltage. A prototype transformer has been wound to meet the revised requirements and preliminary tests indicate efficiency comparable to the 5.1 volt design.

The necessary drawing changes for defining the components for the production run of six power conditioners have been made and procurement has started. The necessary changes in the assembly drawings will be made during the next report period.

2.2.7.2 Fabrication

The process routings for H10D2, H10D3, and H10D4 and the various subassemblies were completed, and fabrication of the subassemblies was completed. Developmental work was done on the welding of the container and the potting of the conditioners with epoxy, an electrical foam 3M XR 5017. Both worked quite successfully.

During the actual assembly of the conditioners two major problem areas were discovered:

1. A dielectric breakdown when subjected to the dielectric withstanding voltage specified for application between the input/output leads commoned together and the mounting plate.

2. A dielectric breakdown of the fusite terminals after welding, when subjected to the same test as given above.

Power conditioner H10D2 was completely torn down in the effort to determine the cause of these problems.

The cause of the dielectric breakdown indicated in No. 1 above, was found to be a combination of two things: minimum coverage of the necessary area by the mica washers under the transistors, and lack of proper cleanliness during assembly of these components. To eliminate the problem special insulating washers were ordered and a laminar flow ultra-clean bench will be used during assembly.

The cause of the breakdown of the fusite terminals was traced to the use of water as a heat sink during welding. In the future, water will not be used as a heat sink and to assure that no moisture will come in contact with the terminals, epoxy will be used to pot the terminals after installation in the lid.

After tearing down power conditioner H10D2 the decision was made to discontinue any further work on it. H10D3 and H10D4 were repaired and finalized.

The parts for power conditioners H10D5, H10D6, H10P1, 2, 3, and 4 were also ordered during this past report period.

2.2.8 ELECTRICAL RECEPTACLE AND STRAIN RELIEF PLUG

There was no significant design or development effort on this component during the period covered by this report.

2.3 COMPONENT AND SUBASSEMBLY TESTING

2.3.1 FUEL CAPSULE

A fuel capsule test plan for Phase II of the SNAP-21 Program was published in late December 1967. However, the necessity for performing tests on the empty capsules is presently being re-evaluated.

2.3.2 BIOLOGICAL SHIELD

The 500- and 2000-hour test phases of the isothermal test are completed. The last test (5000 hours) will be completed May 11, 1968.

Visual inspection of the 500- and 2000-hour tests show slight oxidation due to a small amount of air in the fixtures. The test specimen containing the aluminum oxide (Al_2O_3) barrier was metallographically mounted. The results of the emission spectrographic analysis showed that uranium oxide (U_3O_8) was found only on the surface of the Al_2O_3, a natural result of the slight oxidation of the U-8 molybdenum disc adjacent to the Al_2O_3 coated Hastelloy-X disc. A specimen showed no significant uranium diffusion through the Al_2O_3 barrier into the Hastelloy-X.

2.3.3 INSULATION SYSTEM

2.3.3.1 Dynamic Test to Failure of Unit 10D1

After the thermal retest of insulation system 10D1 the dynamic test to failure was conducted according to the development test plan, "Dynamic Shock to Failure." Following the completion of the shocks specified in the test plan (12g max) the unit had not failed. The decision was made to vibration test the unit at higher g levels rather than continue to increase the shock g level. The unit failed during a 4.5g vibration test (50 cps max) as evidenced by a loss of vacuum.

The dynamic failure tests were conducted on the unit Y-Y axis only. In this axis one support rod is in the plane of the axis with the other two support rods being 60° from the plane of the axis. This axis was used for the failure test because the support rods exhibit the lowest spring constant in one direction of the axis resulting in maximum deflections of the shield.

Three shocks in each direction of the Y-Y axis were performed at input g levels of 7-1/2g, 9g, 10-1/2g and 12g. All shocks had a nominal duration of 6 milliseconds. The unit was leak checked with helium after each g level shock sequence, except the 10-1/2g level, with no evidence of unit failure.

At the conclusion of the above shock tests a design factor of 2.0 in shock was established. It was decided that if unit modifications were to be made as a result of the failure test, it would be necessary to vibration test the unit to the 6g level to establish a 2.0 design factor in vibration. Present plans call for first testing the unit at 4.5g in vibration and then 6.0g in vibration.

The unit was vibration tested on the Y-Y axis according to the following schedule: 5-8 cps at 0.4-inch double amplitude to 8-21 cps at ±4.5g and return to 5 cps in the reverse of this procedure. Total test time was 15 minutes, 7-1/2 minutes for 5-50 cps and 7-1/2 minutes for 50-5 cps. Following this test the unit vacuum gauge was turned on and it was noted that the unit had lost vacuum. The unit was removed from the test machine and placed in a helium filled bag to cool. After cooling, the unit was placed in the shipping container and returned to Linde Division, Tonawanda.

The results of the failure test show that the unit failed in vibration at a level predicted during the calculations (3g design by 1.5 design factor = 4.5g). The exact g level causing failure is, however, not known as there was no failure during the 3g vibration tests, but the unit did fail during the 4.5g vibration tests. In addition, there is a possibility that the 12g shock level started a failure which was not of sufficient magnitude to cause leakage and allow detection. As a result of the dynamic tests (shock and vibration) to specification level and the dynamic test to failure, the unit structural design will not be changed on future units.

Upon return of the unit to Linde Division, Tonawanda, New York, the Min-K insulation system was removed from the inner liner. Examination revealed that the failure had occurred in the inner liner neck tube as predicted. The failure was caused by shear buckling, as evidenced by 45° wrinkles in the inner liner. The inner liner was cracked open for approximately two-thirds of the circumference. This large failure was no doubt caused by continued testing after initial failure occurred. Figure 2-7 shows the inner liner failure.

2.3.3.2 Dynamic Test of Unit 10D3

Unit 10D3 successfully passed the vibration test (3g at 50 cps) and the shock test (6g at 6 ms) during this reporting period.

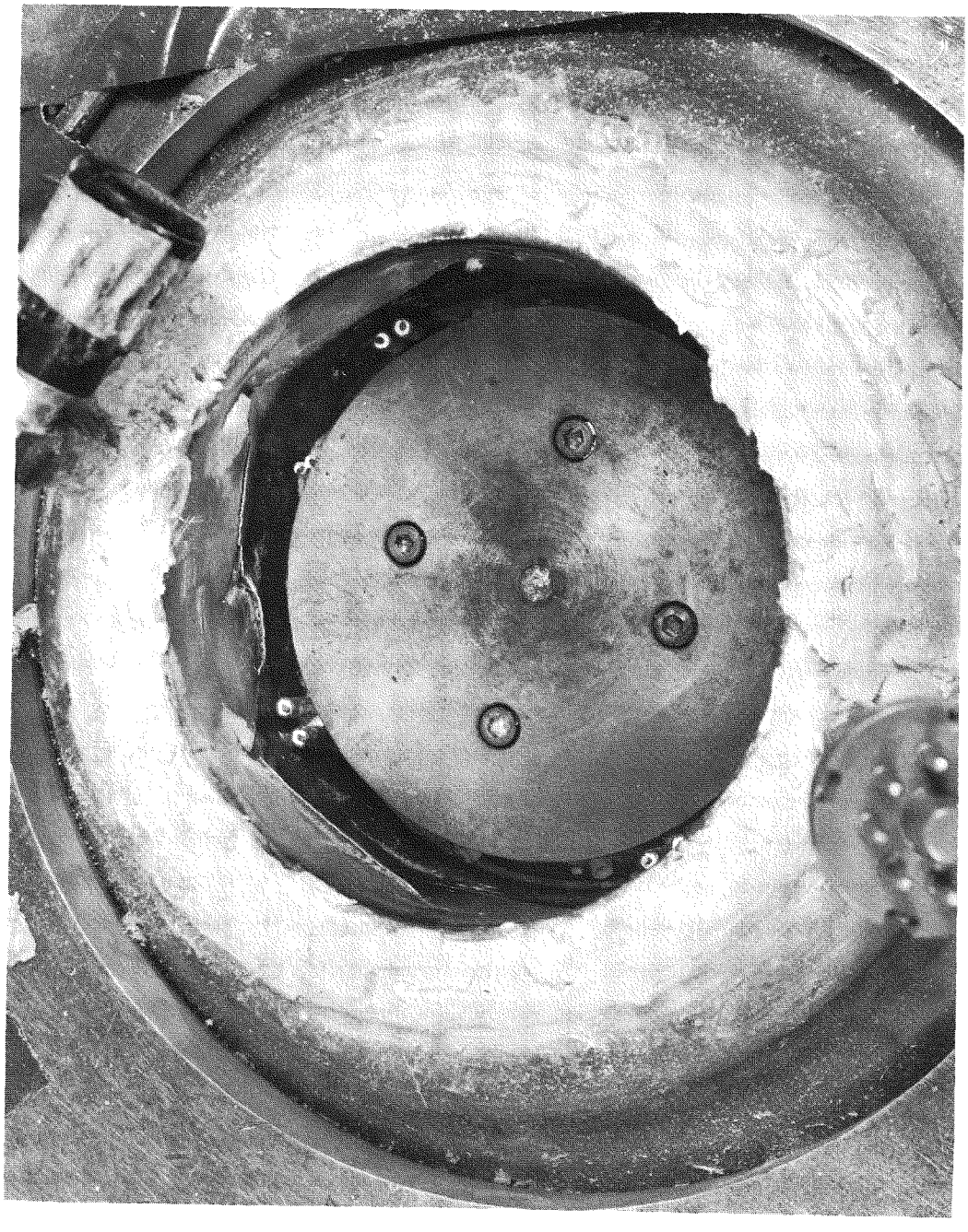

Figure 2-7. Failed Inner Liner Unit 10D1 View from Vacuum Gauge

After the thermal performance test the unit was cooled to ambient temperature and placed in the unit shipping container. The unit was transported to the dynamic test facility (Ogden Technology Laboratories - Deer Park, Long Island, New York) by Linde personnel. Nothing of significance occurred while transporting the unit to the test facility.

Upon arrival, the unit was removed from the shipping container and installed in the dynamic test fixture. The electrical wiring was connected as shown in the development test plan, "Dynamic Vibration Test," and power was supplied to the unit to bring the temperature at the bottom of the neck tube to 1285°F operating temperature. When the operating temperature was reached, the 1/2-inch diameter copper rod was installed in the unit to increase the system heat loss. It was found that with this redesigned copper rod system, the unit heat loss could be maintained at 200 watts with 1285°F at the bottom of the neck tube.

The dynamic vibration test was conducted as specified in the development test plan (three sweeps at 3g maximum for 15 minutes on each axis). Following each sweep the unit was bagged in a helium atmosphere for 1/2 hour and unit pressure was monitored. The unit pressure remained below 0.2 micron during the times that the unit was bagged in helium. From this, the conclusion was drawn that no failure occurred during the dynamic vibration test.

The dynamic shock test was conducted as per the development test plan (three shocks each direction each axis — 6g peak sawtooth at 6 ms). Following each axis test the unit was bagged in a helium atmosphere for 1/2 hour and the unit pressure was monitored. As for the vibration tests, the unit pressure remained below 0.2 micron at all times, leading to the conclusion that no failure occurred during the dynamic shock test. The profile achieved during the shock tests was out of specification with MIL-STD-810A, Figure 516-1, in that the negative g level after the 6g peak was reached exceeded the specified 1.2g.

A complete test report of the dynamic tests on unit 10D3 has been prepared by Ogden Laboratories. At the completion of the dynamic test, the unit was cooled and the Min-K neck tube insulation system was removed. The unit was installed in the shipping container and transported by common carrier to 3M Company.

2.3.3.3 Dynamic Test of Unit 10D4

The insulation system neck tube of unit 10D4 failed during the first specification vibration sweep made during this report period.

Following the thermal performance test the unit was cooled to ambient temperature and placed in the unit shipping container. The unit was shipped to the dynamic test facility by common carrier. Upon arrival at the dynamic test facility the unit was placed in the dynamic test fixture, the electrical connections were completed and power was supplied to the unit. On March 25, when the operating temperature was reached, the unit was subjected to a 1g vibration sweep to ensure that the control accelerometer and the unit accelerometer were both reading the same. At this point everything was normal. The unit pressure was checked and it too was normal.

The unit was then subjected to the vibration test to specification along an axis perpendicular to the neck tube. The specification for vibration testing is as follows:

5-8 cps	0.4 inch double amplitude
8-26 cps	1.3g peak
26-40.5 cps	0.036 inch double amplitude
40.5-50 cps	3g peak

Upon completion of the sweep the unit vacuum was monitored and it was found that the unit had lost vacuum. The unit was removed from the test machine, cooled, placed in the unit shipping container and returned to Linde.

When the truck arrived at Linde from the test facility, it was noted that the shipping container was intact with no evidence of mishandling. The container was removed from the truck and placed in the laboratory where disassembly was started.

Upon removal of the Min-K it was noted that the neck tube was buckled and that many small cracks had formed in the middle of the neck tube about 75 percent of the way around it.

Photographs were taken of the unit during various stages of the disassembly. A crust approximately 0.020 to 0.030 inch thick was found around the copper block which was bolted to the emitter plate. The bolts were removed from this copper block but the block itself was frozen to the emitter plate. Penetrating oil was poured into the bolt holes and a special tool was made to lift on the outside edge of the block. This was successful and the block was removed.

All of the six bolts fastening the emitter plate to the inner liner were loose. During assembly of the system the bolts were staked after being torqued. The stake marks were still in their original location and so it can be assumed that the bolts stretched during heat-up. The bolts were tightened and the amount of looseness was estimated as follows, starting from the bolt adjacent to the vacuum gauge and going clockwise:

Bolt Number	Angle of Looseness
1	40°
2	100°
3	40°
4	25°
5	30°
6	20°

The emitter plate and the heater block were removed from the unit. A plate with an evacuation port was placed on top of the unit and sealed to the unit using an RTV sealing compound. The purpose of this setup was to evacuate the unit to determine if the unit had developed any further leaks. The leak check was performed and it was found that there are no other leaks in the unit.

The accelerometer traces were examined. The trace indicates 1.3g up to 15 cps. At this point the trace became erratic. From 15-20 cps the g level increased to 5 to 6 g's. The test was continued and the g levels remained high.

The traces of all previous dynamic vibration tests were examined. They all appeared normal except the final sweep on the destruct unit 10D1. On this sweep, with a 1.3g input between 15 and 16 cps, the unit accelerometers showed g levels

up to about 5. This lasted only a short time, approximately 4 inches of trace, and then became normal again.

This failure occurred late in the report period and the analysis of the failure is not yet complete. Details of this failure will be reported on in the next report period.

Further details of the shock and vibration tests can be found in Appendixes B and C.

2.3.4 SEGMENTED RETAINING RINGS

All testing on this component has been completed.

2.3.5 PRESSURE VESSEL

Pressure vessel D10D1 has completed hydrostatic testing at Southwest Research Institute, San Antonio, Texas. The pressure vessel was instrumented with strain gauges, total deformation potentiometers and leak detectors. Pressure was incrementally increased to 11,000 psi. A medium of chilled salt water was used. Three cycles to 11,000 psi were conducted, followed by a 48-hour creep test at 11,000 psi.

Instrumentation data is presently being reduced and calculations made regarding stress-strain curves and total deformation at pressure. Strain readings were linear with pressure and repeatability was excellent. No leakage was indicated by the detector. This indication was verified when the pressure vessel was disassembled. The creep test data revealed no creep or material yield during the 48 hours at 11,000 psi.

The pressure vessel is presently being measured for post-test total permanent deformation. A formal test report including photographs and stress-strain curves is being prepared by Southwest Research Institute.

The next quarterly report will contain the finalized test information of pressure vessel D10D1 and also include the hydrotesting results of pressure vessel D10D2.

2.3.6 THERMOELECTRIC GENERATORS

2.3.6.1 Ball and Socket Configuration

a) Generator A10D1

This thermoelectric generator has completed all short-term dynamic testing to specification level. In addition, the unit was integrated into system S10D1 to obtain shipping container design characteristics and fuel loading requirements. During the final hours of system testing, a leak developed at the transition area of the long outer generator case. Upon discovery of the thermoelectric generator leak, the system was dismantled and argon was used to pressurize the generator.

The generator was maintained at a positive argon pressure greater than atmospheric during the disassembly operation. The unit was transferred to a dry-box where, after some development weld processes were investigated, a repair procedure was instituted. The repair consisted of attaching over the existing external case a second case of 10 mil stainless steel of a rolled construction. End closure welds were made by TIG welding within the dry box. A 48-hour surveillance in a vacuum chamber revealed no loss of generator pressure. This indicates a leak-free generator.

The thermoelectric generator was placed on test again. The generator has again stabilized at operational design temperatures. Table 2-11 shows generator performance pre- and post-case failure:

Table 2-11. Generator A10D1 Performance Before and After Long Case Failure

Date	Test	Cold Cap	Hot Button	R_{Pile}	P_{Out}	Gas Pressure
10/24/67	Generator	102	1100	1.77	16.63	25.75
12/16/67	System	130	1048	1.509	14.88	26.5 psia
1/25/68	System	185	1048	1.67	13.11	*19.0 psia
3/18/68	Generator	106	1101	1.72	16.73	24.75

*Removed from system test due to a leak — backfilled at this point in test.

b) Generator A10D2

This generator has completed all short-term and dynamic testing. Currently the generator is on long-term test.

c) Generator A10D4

Short-term testing, dynamic testing and system S10D1A integration and evaluation test has been completed for this generator. Currently the unit is being run in the efficiency fixture, and early in the next report period the unit will be installed in system S10D2.

2.3.6.2 In-Line Configuration

a) Generator A10D5

Generator A10D5 was returned from specification level dynamic test and operated at BOL conditions for 200 hours. This stabilization was necessary to determine the degradation rate of the generator from two separate losses of backfill gas incidents during earlier test procedures (see SNAP-21, Monthly, January 1968).

The thermopile resistance was gradually increasing and affecting generator output. Therefore, the unit was returned to Environ Laboratories for dynamic testing to destruct.

At the close of 20g level dynamic test the generator exhibited an increase in thermopile resistance to a value of 2.71 ohms, compared to an initial resistance of 1.83 ohms early in the test sequence and prior to any type failure mode.

This increase in thermopile resistance is most probably due to oxidation at the hot junction which occurred during the loss of backfill gas from the generator. The degradation caused by increasing pile resistance and decreasing generator power output dictated the end of test for this generator. The unit was removed from test on February 14, 1968.

Refer to SNAP-21 Program, Phase II, January 1968 Monthly Report for a more detailed discussion of Generator A10D5.

b) Generator A10D6

All short-term and dynamic testing has been completed for this generator. The unit is currently on long-term test. Its performance is normal.

c) Generator A10D7

This generator has completed all short-term and specification level dynamic testing. The unit is currently at design temperature conditions and is awaiting system S10D2 integration. A complete and detailed topical report on all generators is being prepared. This report will compare the performance of SNAP-21 Phase II and Phase I generators.

2.3.6.3 Generator Development Testing

The following section is a synopsis of the development testing on SNAP-21 generators. The section includes the test results and test efforts for the SNAP-21 generators. A complete and detailed analysis of SNAP-21 Phase II generators will be completed at a later date. The outcome of this analysis will result in a final design configuration for system integration.

2.3.6.3.1 Thermal Insulation

The thermal insulation to be used in the final design generator was evaluated by studying the effect on the cold end thermal performance of the generators, the electrical performance and its effect on overall generator efficiency (a measure of its total heat leak). Effects on cold end thermal performance caused by the thermal insulation is considered pertinent only when grease is present in the follower cold frame interface such as in the in-line series of generators. The only effect insulation has on cold end performance is to raise the cold end thermal impedance by soaking the grease from the follower cold frame interface. Of the in-line series of generators, 10D5 had microquartz as the thermal insulation around the thermoelectric legs, Generator 10D6 had Min-K 1301 and 10D7 Min-K 1999. Microquartz and Min-K 1999 both have a lower initial cold end temperature drop, as shown in Figure 2-8.

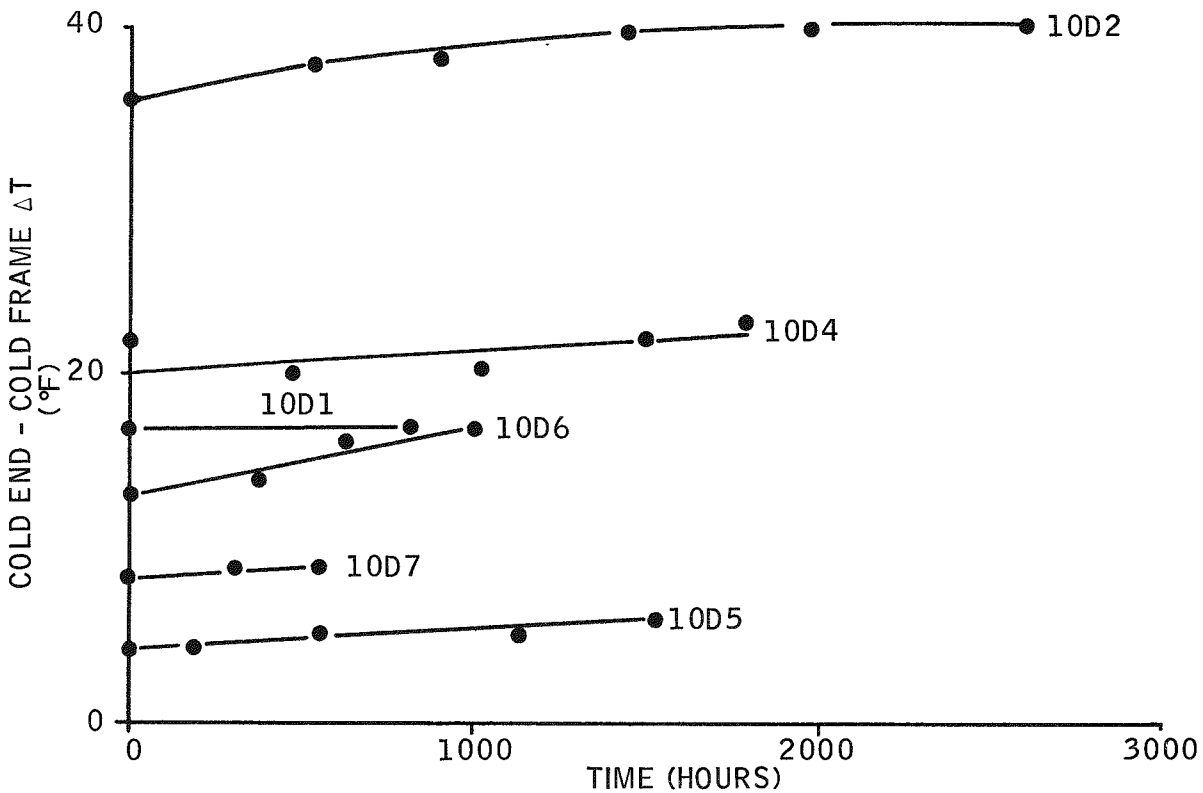

Figure 2-8. Cold End Thermal Stability, Phase II Generator

The stability of the generators using Microquartz and Min-K 1999 appeared superior to that of Generator 10D6 which used Min-K 1301. It should be noted, however, that the performance of Generator 10D6 was not unacceptable in either capacity. Both the initial cold end temperature drop and the stability were far superior to the Phase I generators. This is shown in Figure 2-9.

The effects of the thermal insulation on the electrical performance are much less discernible than on the cold end thermal performance. The Min-K 1999 generator, 10D7 has been the most stable SNAP-21 generator to date, with only 300 hours of life test available. The thermal insulation used in generator 10D7 was processed at 650°F prior to placement in the generator. Data from the SNAP-23 10-couple modules, however, shows a large degree of P-leg degradation with Min-K 1999. Thermal insulation in these modules, however, was merely ground and used in keeping with the recommendation of Johns-Mansville. It is suspected that some water was present in the Min-K 1999 put in the SNAP-23 module which caused the P-leg degradation. The electrical stability characteristics of Min-K 1301 are well known and at an acceptable level. Since contradictory evidence exists on the thermal insulations and only short-term data is available on the SNAP-21 Min-K 1999 generator, Min-K 1301 must be favored on the basis of thermoelectrical stability.

Thermal insulation also has an effect on generator efficiency caused by total heat leak. The thermal conductivity of Microquartz is about twice that of either Min-K 1301 or Min-K 1999 at the temperature conditions at which SNAP-21 generators run. This should be reflected in the efficiency of the Microquartz generator as compared to that of the other two.

This difference is not readily apparent. It is felt that this is caused by a change in the thermal impedance of the legs in Generator 10D5. A drastic increase in the electrical resistance of the legs was noted when the generator was inadvertently exposed to air. The efficiency of this generator was measured after this failure occurred. Since the electrical resistivity of the legs was so affected, it is not unreasonable to assume that the thermal impedance was similarly affected since in nearly all materials known, a higher electrical conductance implies a higher thermal conductance. An increase in the thermal resistivity of the legs would be reflected in a decrease in heat flow through the legs. Thus, the total heat flow through Generator 10D5 may not reflect the increase in heat flow through the

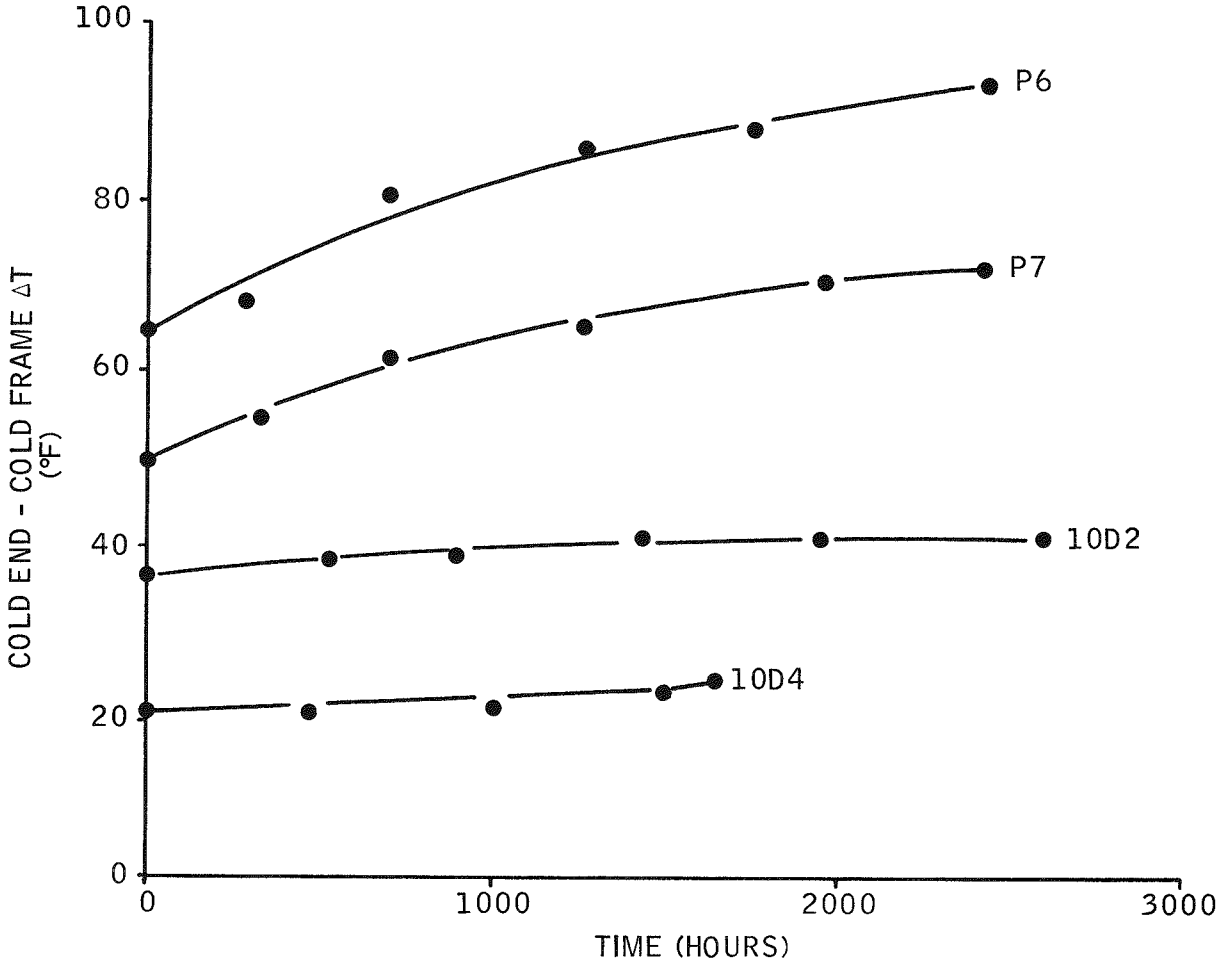

Figure 2-9. Cold End Thermal Stability, Phases I and II Generators

insulation around the legs. It can further be noted from Table 2-12 that Generator 10D7 requires slightly less heat at the EOL condition than does 10D6, even though it required more at BOL conditions. This indicates the possibility of a lower insulation thermal conductivity from Min-K 1999 at EOL average temperature conditions.

Table 2-12. Results of Generator Efficiency Tests

Generator	BOL		EOL	
	Q_{GEN} (w)	η (percent)	Q_{GEN} (w)	η (percent)
10D2	201.8	7.46	170.6	7.09
10D4	208.7	8.07	175.7	7.72
10D6	203.7	7.88	170.9	7.22
10D7	204.9	8.16	167.9	7.82
BOL = 1100°F T_h, 80° T_{cf} EOL = 1000°F T_h, 75° T_{cf}				

From the foregoing discussion it is apparent that the technical value of Min-K 1999 is close to that of Min-K 1301. Thus considering the aforementioned contradictory data on Min-K 1999, Min-K 1301 has been selected as the thermal insulation to be used on the SNAP-21 final design generators. However, because of the known degradation of Min-K 1301, Min-K 1999 should be re-evaluated when long-term data becomes available.

2.3.6.3.2 Cold End Thermal Mechanism

To evaluate the comparative thermal performance of the in-line generator and the ball and socket generators, one must investigate the initial cold end temperature drop and the stability characteristics. From the standpoint of initial cold end thermal performance, the in-line generators have a lower cold end temperature drop (see Figure 2-8). However, the stability of the ball and socket generators is expected to be better than that of the in-line generators. The cold end temperature drop of Generator 10D2 is stable after only 1500 hours of test. Generator 10D1 showed no instability at all from initial start-up. Generators 10D5, 10D6 and

10D7 all have a noticeable instability. This is probably caused by the grease in the follower cold frame interface. The only other stability data to date on generators with grease at the cold end is from the Phase I generators, as shown in Figure 2-9.

The cold end temperature drops of Phase I generators did not stabilize until approximately 2500 hours after start-up (see Figure 2-9).

Bell jar tests on the ball and socket concept using a beryllium oxide follower yielded a cold end temperature drop of about 10°F. The stability of this concept can be assumed good as indicated by Generators 10D1, 10D2, and 10D4. Thus, if on Figure 2-8 this were compared to the in-line and ball and socket development generators from the standpoint of cold end thermal performance, this must be the recommended configuration. For this concept, ring contact between the ball and follower socket, that is, where the cold cap ball is larger in radius than the follower socket, appears to be desirable. The nominal design, therefore, will incorporate a cold cap with a spherical radius 0.002 inch larger than that of the follower.

Beryllium oxide is a ceramic and is an excellent electrical insulator. The other acceptable cold end configurations, the bare aluminum socket or the in-line design, offer only one thin layer of hardcoat for an electrical barrier between the leg and the cold frame. If a hardcoated follower is scratched, there is an increased possibility of shorting to the cold frame. A short occurred in a Phase I generator and it was never determined whether it was due to a mislaid instrumentation wire or a shorted follower. Thus, reliability of electrical isolation strongly favors a beryllium oxide follower.

A nickel plated cold cap will be necessary on the final design generators. SNAP-21 systems are expected to be delivered in a short circuit condition with no external cooling except natural convection to the atmosphere. Under these conditions, it is entirely possible for the cold end of these generators to exceed 200°F, the maximum allowable temperature with copper cold caps. Thus, nickel plated cold caps will be necessary to deter copper migration into the thermoelectric legs.

2.3.6.3.3 Generator Backfill Gas

With the improved design of the cold end thermal mechanism on the SNAP-21 generators very little heat is conducted through the gas at the cold cap follower spherical interface. Thus, as this cold end mechanism is improved, the difference between the effects of generator backfill gasses on cold end thermal impedance is diminished. Two other effects of the generator backfill gas are, however, very important. From SNAP-27 10-couple module tests, the SNAP-21 P3 post-test investigation and other tests connected with the SNAP-23 program, xenon was noted to restrict the sublimation of the N legs to a much greater degree than was argon (see Figure 2-10). It appeared, in fact, that with xenon the sublimation was approximately half what it was when argon was used as a backfill gas. This effect is suspected to be a function of the gas molecular weight. Xenon has a greater molecular weight than does argon and a correspondingly lower gas mobility. The aforementioned effect on thermoelectric sublimation is expected to be attributed to this property.

The other key factor in evaluating generator backfill gas is that of the heat loss through the thermal insulation packed around the thermoelectric legs. In the SNAP-27 thermal insulation stability fixture testing and in subsequent thermal insulation analytical investigations, it was noted that the thermal conductivity of Min-K 1301 insulation is inversely proportional to the square root of the backfill gas molecular weight. Thus, xenon backfill gas gives the thermal insulation a lower effective thermal conductivity than does the argon; thus, the heat leak through the thermal insulation would be less. Xenon has therefore been selected for use in final design generators.

2.3.6.3.4 Leg Manufacturing Technique

The leg manufacturing technique must be analyzed by studying the electrical performance of the thermoelectric generators; specifically the thermopile power output. Since the in-line series of generators is the best performing series that we have today, the new 3M proprietary press-bond-sinter technique will be used for the legs in the final design generators. In this technique, after the end leg segments are pressed, they are bonded green and then the entire leg assembly is sintered. After the P-leg segments are pressed, however, the hot segment is individually sintered. Then the segments are bonded and the entire leg is sintered.

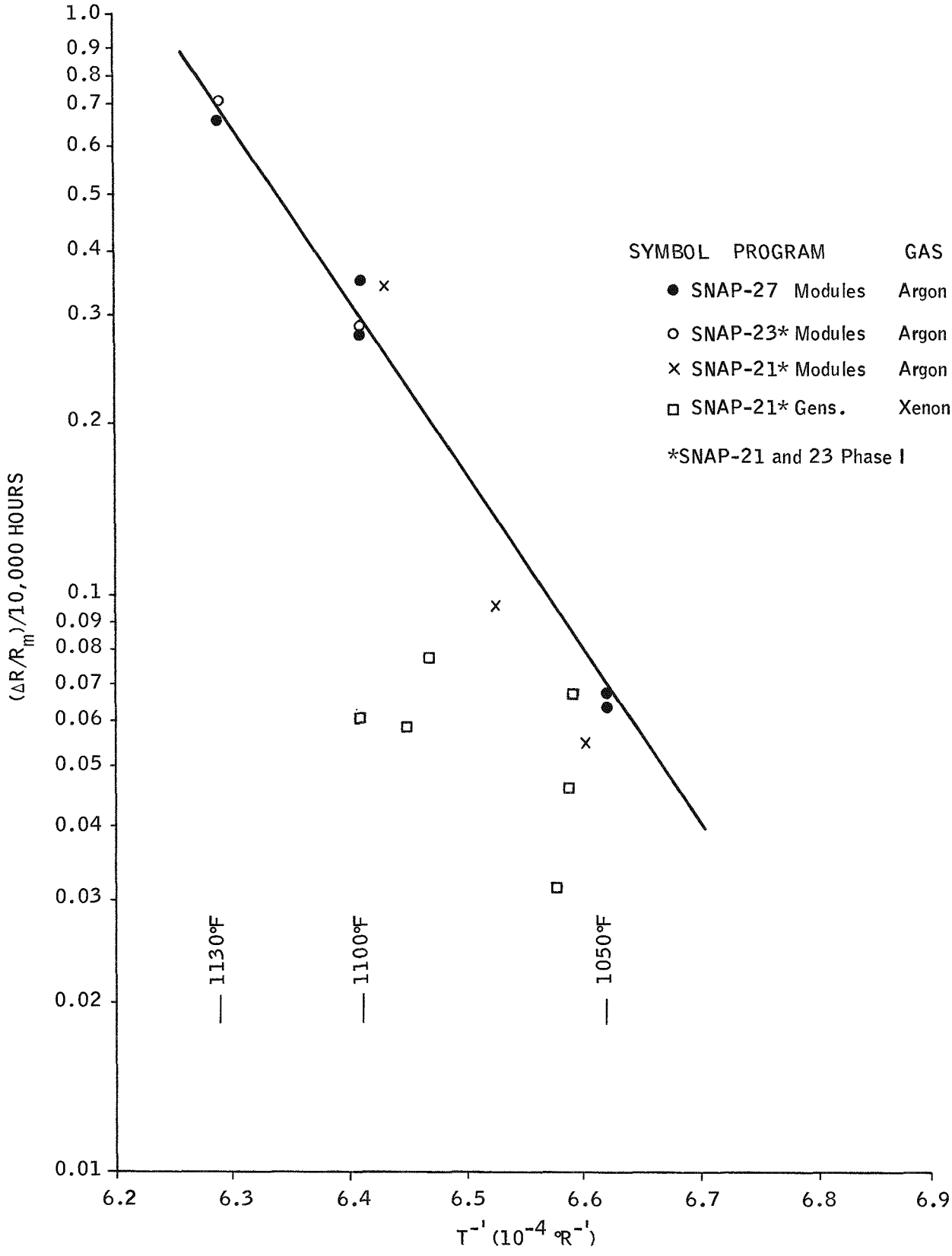

Figure 2-10. Effects of Argon and Xenon Backfill Gasses on N-Legs Degradation Rate

2.3.6.4 Efficiency Testing

Generator efficiency testing was initiated in the first quarter of 1968. Task accomplishments for this quarter include:

- Assembly of test fixture.
- Fixture calibration.
- Efficiencies measured on Generators 10D2, 10D4, 10D5, 10D6, and 10D7.

The following paragraphs describe the work performed in the first quarter.

a) Test Fixture

Figure 2-11 depicts the efficiency test fixture. It consists of a Linde HTVIS mounted on a stand with the segmented retaining ring attached to facilitate generator placement. A Min-K plug was also fabricated to calibrate the fixture (Figure 2-12).

b) Fixture Calibration

To calibrate the system, the plug was installed in place of the generator. A range of emitter temperatures was swept, holding the copper plate at the top of the plug at 80°F. The heat conducted through the plug was calculated for each emitter temperature and subtracted from the respective input power to determine fixture heat loss as a function of emitter temperature. This method of calibration conveniently accounts for any loss through heater leads, and/or instrumentation leads, as they are part of the fixture. The effective thermal impedance of an assembled generator is much less than that of a Min-K block; thus, the temperature profile of the system will be different from calibration to operating conditions. This will cause heat leaks in two areas which must be accounted for; generator side losses, and HTVIS support tube losses.

1) Generator Side Heat Loss – The thin walled neck tubes of the generator long case and the HTVIS lie in close proximity, approximately as shown in Figure 2-13.

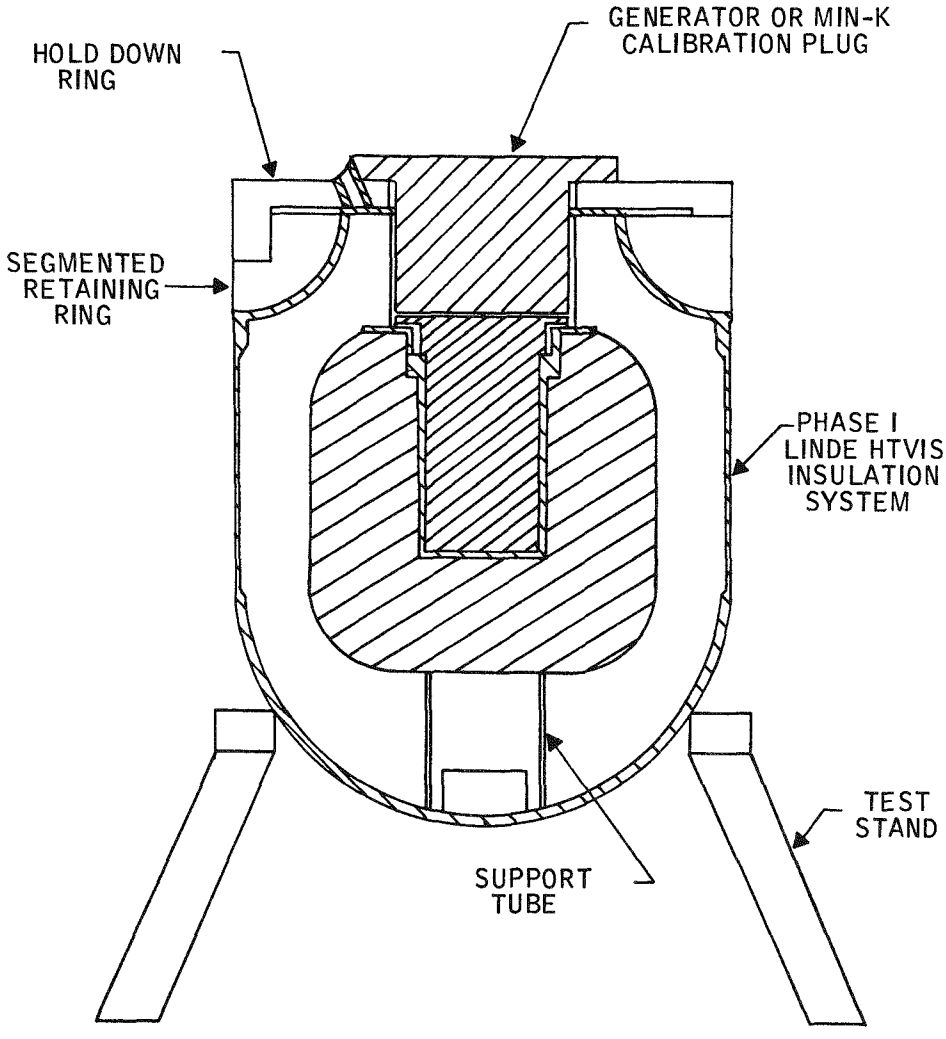

Figure 2-11. Efficiency Test Fixture

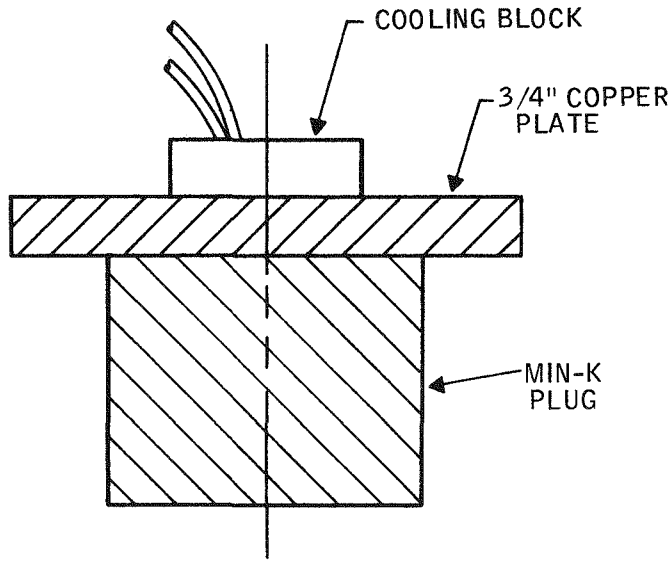

Figure 2-12. Calibration Plug

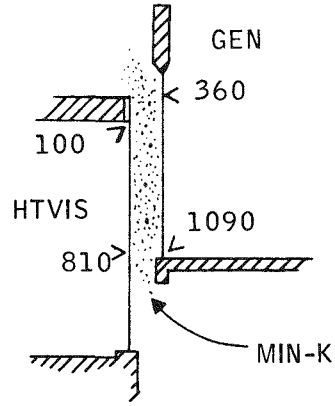

Figure 2-13. Area of Interaction Between Generator and HTVIS

They are separated by powdered Min-K. Temperatures shown on this sketch indicate approximate values at BOL conditions for the locations shown. Obviously, heat will flow from the generator surface to the insulation system through the annular gap. Annular heat flow can be defined by:

$$q = \frac{2\pi k \ell}{n\,(r_2/r_1)} \quad (T_1 - T_2) \tag{1}$$

where:

k = Average thermal conductivity of Min-K

ℓ = Length of interaction

r_2 = Radius of HTVIS neck tube

r_1 = Radius of generator long case

T_1 and T_2 are the average temperatures of the long case and neck tube, respectively (refer to sample calculation, at the end of this section). For our configuration, equation (1) becomes:

$$q = 0.1367k\,(T_1 - T_2)$$

T_1 and T_2 in this equation are defined in Figure 2-14. The quantity X represents an arbitrary length dimension; if the generator long case is represented by the length X = 0.5 to X = 2.5, the HTVIS neck tube falls from X = 1 to X = 3.6 inch. In this example, $T_1 - T_2$ represents the average temperature difference between these two surfaces on which the heat leak calculation is based.

2) Support Tube Heat Leak Change — With a generator in the efficiency fixture, the temperature at the base of the biological shield is much higher than when a Min-K plug is in it. Thus, the heat loss through the support tube is different for these two cases, and the difference can be written as:

$$\Delta q = \frac{k_{st} A_{st}}{\ell_{st}} \quad (T'_{top} - T_{top})$$

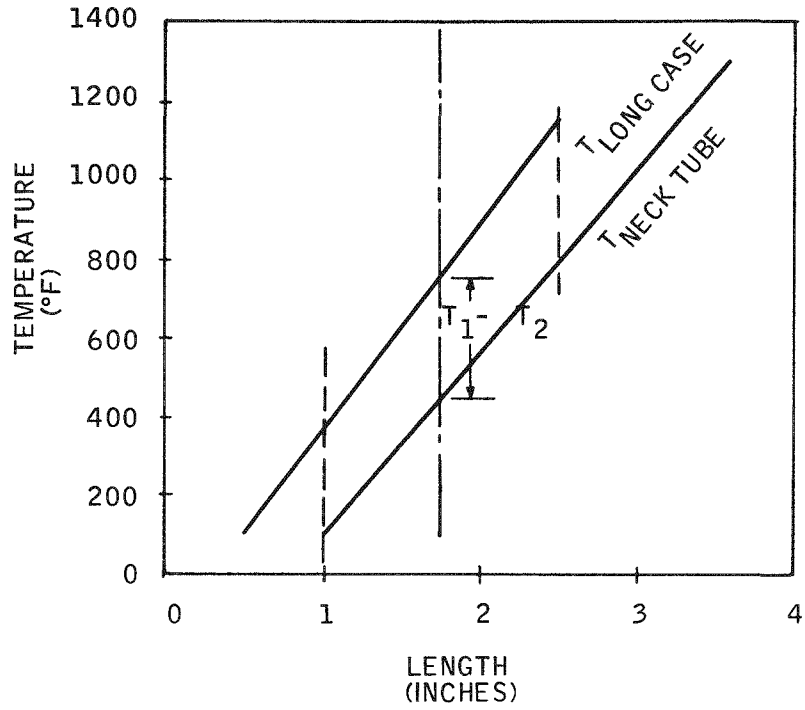

Figure 2-14. Temperature Distribution of Long Case and Neck Tube

where:

k_{st} = Conductivity of the support tube

A_{st} = Cross sectional area of the support tube

ℓ_{st} = Length of the support tube

T'_{top} = T_{top} with generator in fixture

T_{top} = T_{top} with Min-K plug in fixture

The temperature of the top of the support tube, T_{top}, was not monitored, but it is assumed that this temperature will linearly follow that of the base of the hot block. This assumption is fair since the thermal path out the bottom of the system is much smaller than that at the top. The relationship then becomes:

$$\Delta q = \frac{k_{st} A_{st}}{\ell_{st}} \quad (T'_{hb} - T_{hb})$$

Where T_{hb} represents the temperature at the bottom of the hot block. The following section of sample calculations includes this correction and also the one on side losses to the fixture heat loss.

c) Sample Calculation (10D6, BOL)

Necessary Data:

Average Emitter Temperature	1290°F
Average Cold Frame Temperature	80°F
T'_{hb}	1547°F
T_{hb}	1312°F
Hot Button Temperature	1048°F
Heater Power (gen.)	279.6 watts
Generator Power Out	16.03 watts
Fixture Loss (from 2.4.0)	61.8 watts

Generator Side Loss

$$q = 0.1367k\,(T_1 - T_2)$$
$$= 0.1367 \times 0.21\,(298)$$
$$= 8.47 \text{ watts}$$

Support Tube Change

$$\Delta q = \frac{k_{st} A_{st}}{\ell_{st}} \quad (T'_{hb} - T_{hb})$$

$$= 5.58 \text{ watts}$$

Total Loss = Fixture Loss + Side Loss + Support Loss
= 61.8 + 8.47 + 4.48
= 75.85

$$Q_{gen} = \text{Heater Power - Total Loss}$$
$$= 203.7$$

$$\eta = \frac{\text{Gen. Power Out}}{Q_{gen}}$$

$$= \frac{16.03}{203.7}$$

$$\eta = 7.88\%$$

d) Efficiency Tests

Efficiency tests were run on Generators 10D2, 10D4, 10D5, 10D6, and 10D7 at BOL and EOL temperature conditions. Two intermediate hot junction temperatures were also run on 10D7 to determine the shape of the η vs. T_H curve. Generator efficiency and heat flow into the generator hot frame are presented in Table 2-13 and efficiency is plotted in Figure 2-15.

2.3.6.5 Conax Leakage

As discussed in SNAP-21 Quarterly Report No. 6(MMM 3691-26) dated February 1968, a systematic sequence of applied torque to all ball and socket generators containing Conax (feed-through) fittings has continued. This effort has minimized the loss of gas pressure from each respective unit. A bi-monthly retorquing of all ball and socket generators containing Conax fittings has been instituted on the SNAP-21 program. The long-term test data thus accumulated will be helpful in obtaining a realistic solution to the leak problem present in the Phase II ball and socket generators.

2.3.6.6 Phase I Continuation Testing

During this period the test group continued to monitor and analyze the thermoelectric test work initiated during Phase I. The units being tested and the accumulated hours on test are:

A1 – 32,085
A3 – 30,753
A4 – 29,913

Table 2-13. SNAP-21 Generator Efficiency and Heat Flow Into Hot Frame

Generator		Hot Junction Temp (°F)			
		1050 (BOL)	995	957	925 (EOL)
10D2	Q_{gen}	201.8			170.6
	η	7.46			7.09
10D4	Q_{gen}	208.7			175.7
	η	8.07			7.72
10D5*	Q_{gen}	207.4			167.0
	η	6.29			5.45
10D6	Q_{gen}	203.7			170.9
	η	7.88			7.22
10D7	Q_{gen}	204.9	191.5	178.9	167.9
	η	8.16	7.99	7.93	7.82

*Generator 10D5 had a failure in the generator case and the leg resistance rose due to oxidation. All this occurred prior to efficiency test. Refer to 3691-0986 for details on 10D5 failure.

Prototype generator on test and the hours accumulated are:

P5 – 25,193
P6 – 24,564
P7 – 24,717

All generators are operating with no significant change in performance. Performance data for the modules and generators listed is given in Figures 2-16 through 2-19 and in Tables 2-14 and 2-15.

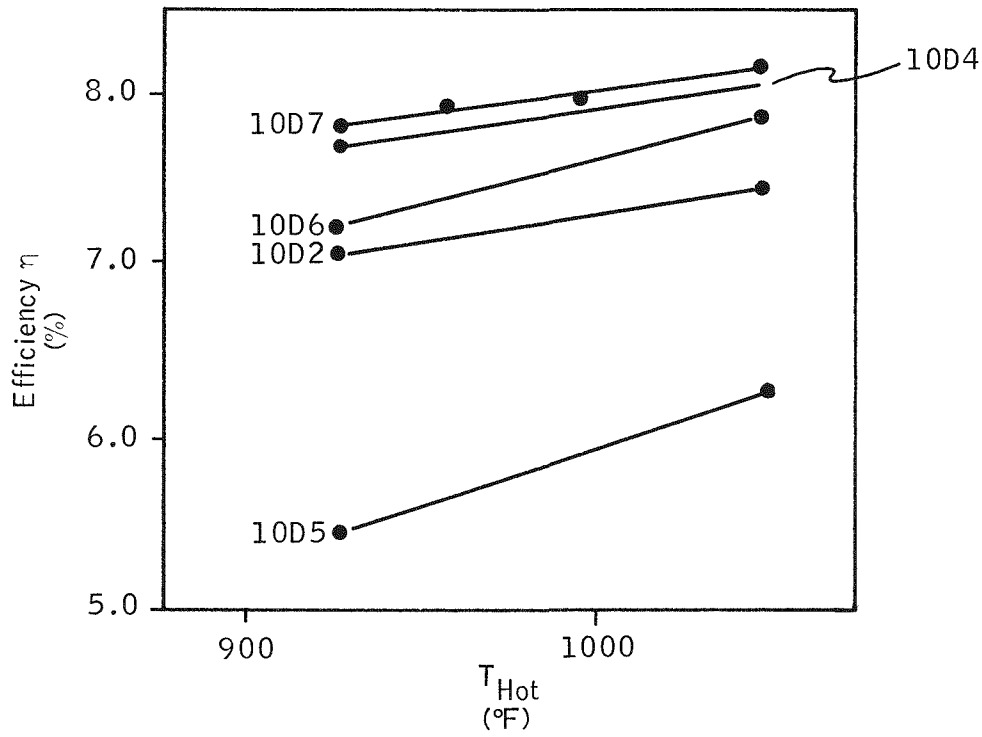

Figure 2-15. Generator Efficiency vs. Hot Junction Temperature

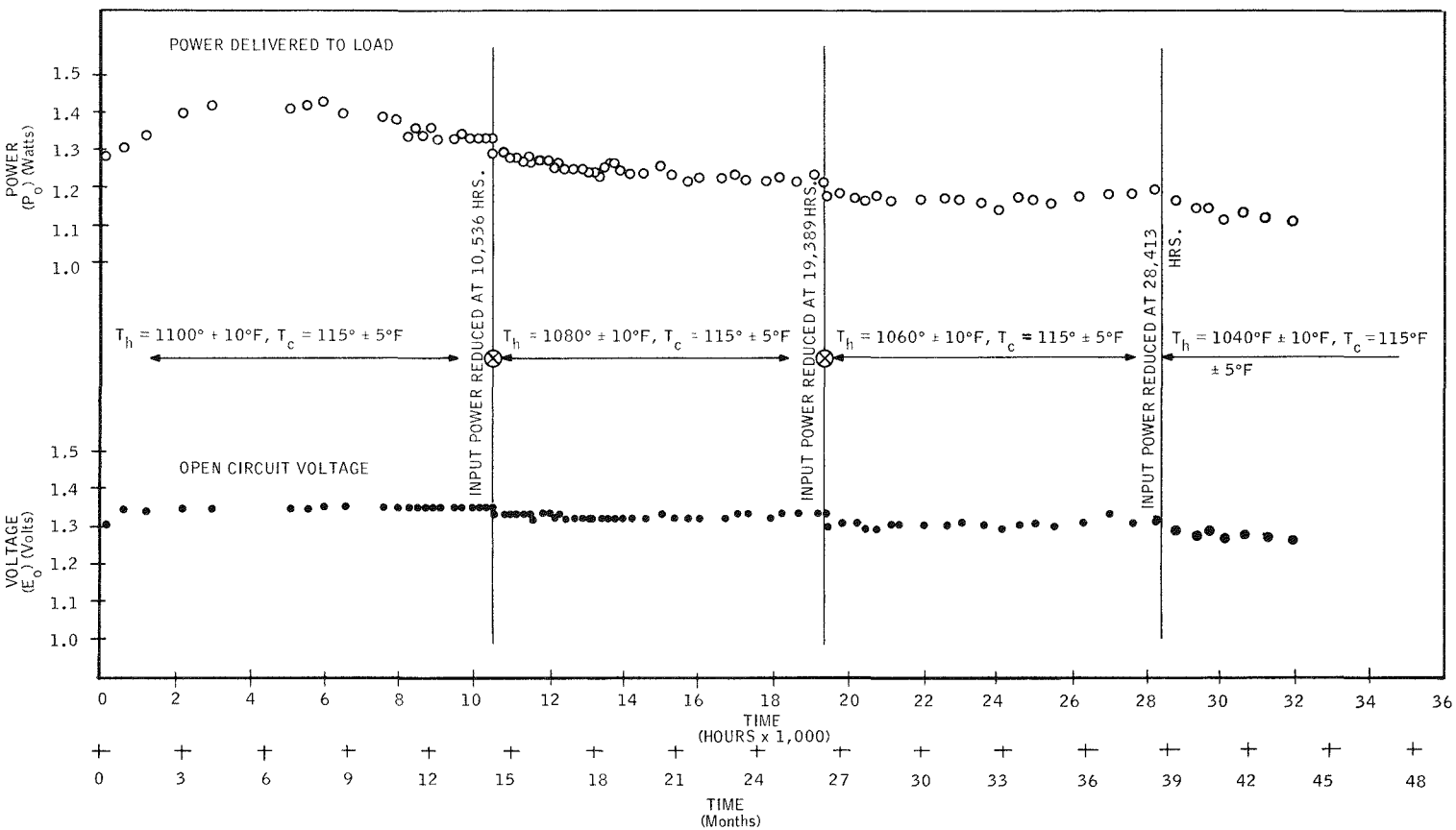

Figure 2-16. Performance of SNAP-21B 6-Couple Module A1

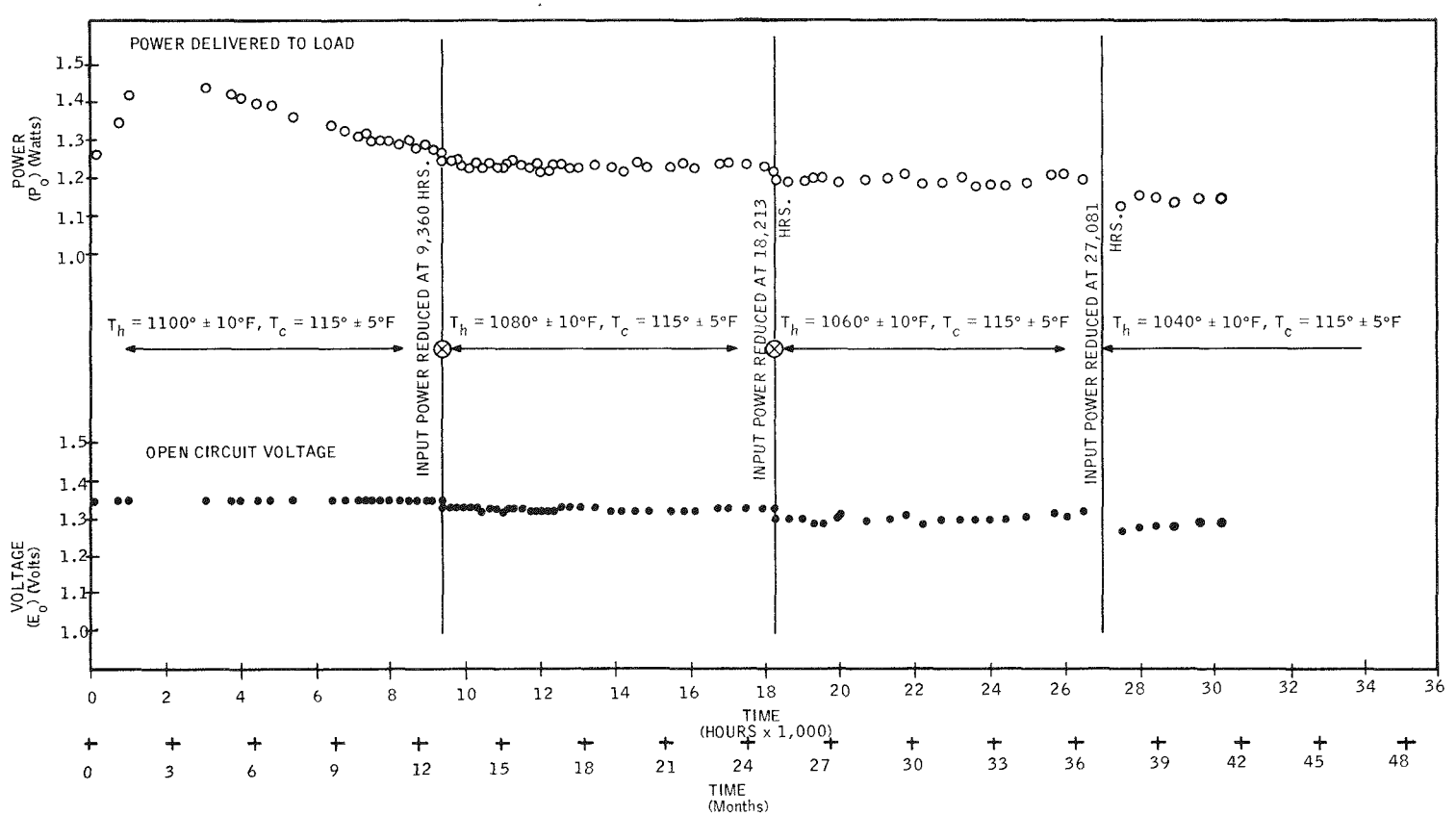

Figure 2-17. Performance of SNAP-21B 6-Couple Module A3

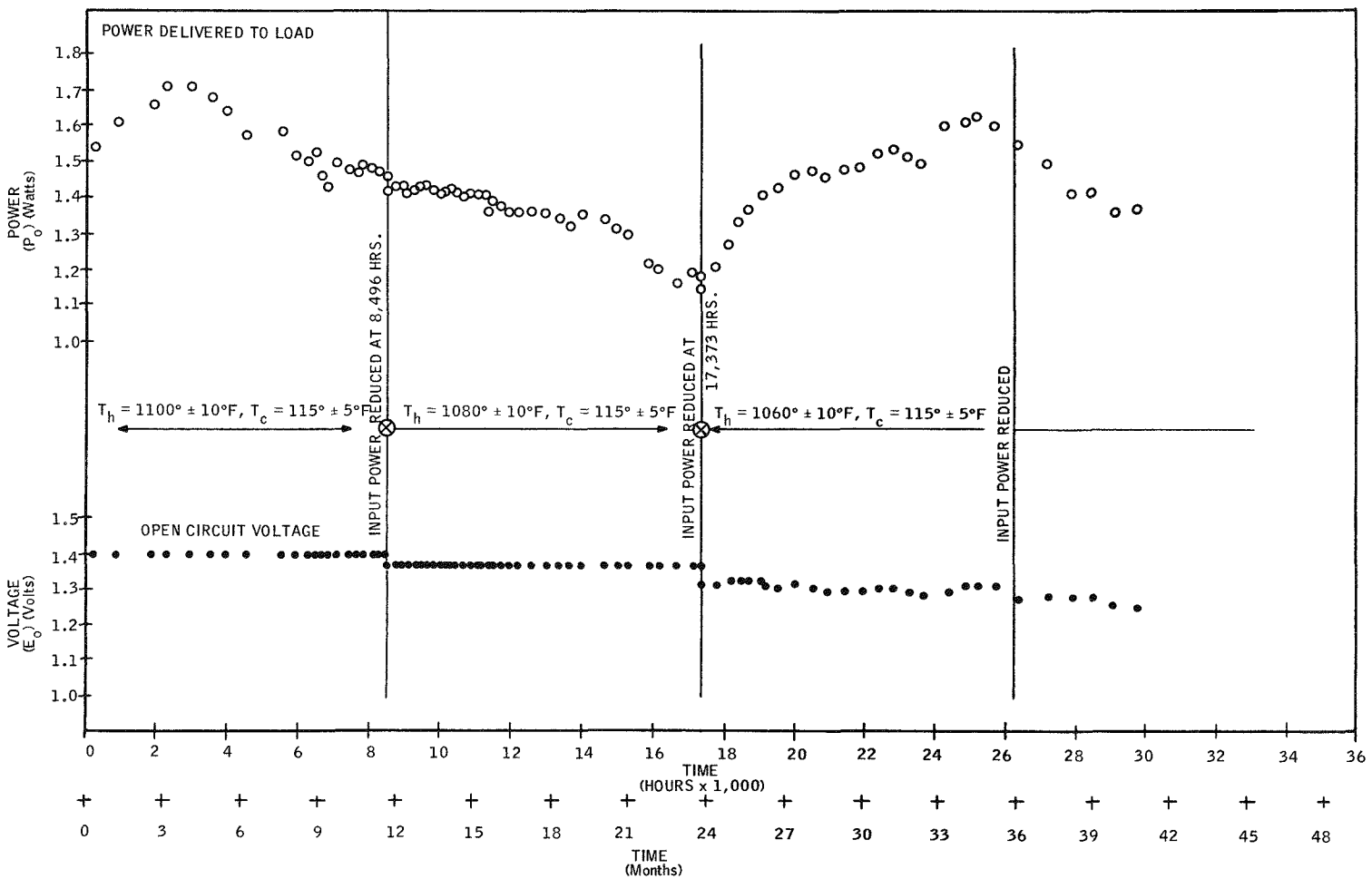

Figure 2-18. Performance of SNAP-21B 6-Couple Module A4

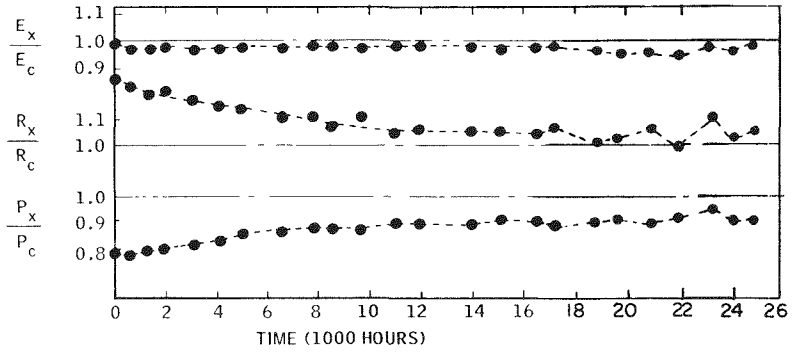

Prototype 3M-37-P5

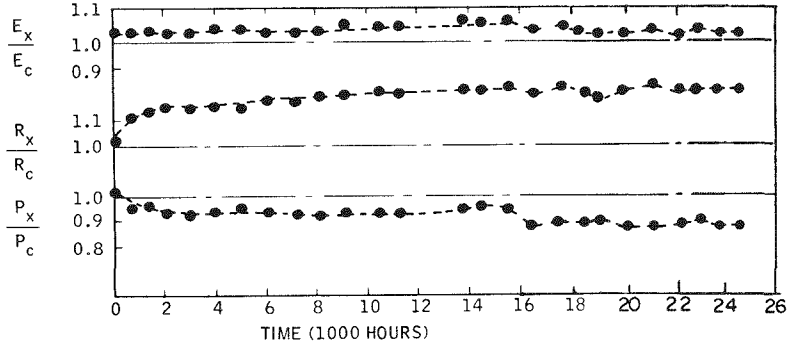

Prototype 3M-37-P6

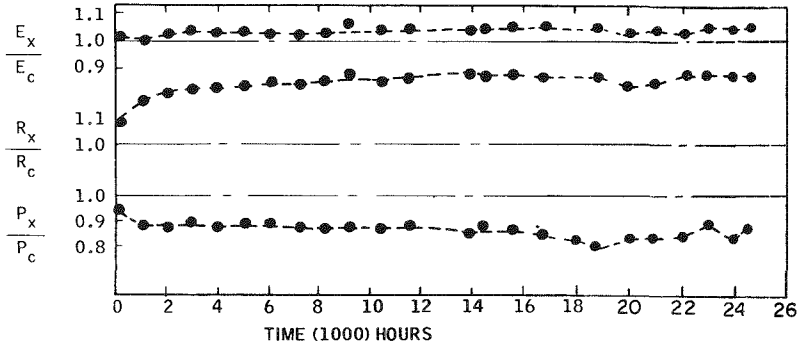

Prototype 3M-37-P7

Figure 2-19. Performance of Prototype 48-Couple Generators 3M-37-P5, P6, P7 (E = voltage, R = resistance, P = power, x = experimental, C = computer)

Table 2-14. Performance Data of SNAP-21 6-Couple Modules

Module	Date	T-Hot (est)	T-Cold	E_o (volts)	E_L (volts)	I_L (amps)	P_o (watts)	R (M-ohms)	P_I (watts)	Hours
A1	1-15-68	1040	Building power was off and emergency power came on for 1 hour.							
	1-17-68	1040	114	1.27	0.63	1.79	1.12	359	32	30,573
	1-30-68	1040	115	1.27	0.63	1.79	1.12	360	32	30,885
	2-15-68	1040	116	1.26	0.62	1.78	1.11	357	32	31,269
	2-17-68	1040	Building power was off and emergency power came on for 5 hours.							
	2-19-68	1040	115	1.27	0.62	1.78	1.11	363	32	31,365
	3-14-68	1040	113	1.26	0.62	1.78	1.11	358	32	31,941
	3-20-68	1040	113	1.26	0.62	1.76	1.09	365	32	32,085
A3	1-15-68		Building power was off and emergency power came on for 1 hour.							
	1-17-68	1040	120	1.29	0.64	1.79	1.13	361	46.5	29,241
	1-30-68	1040	120	1.28	0.63	1.79	1.14	360	46.5	29,553
	2-15-68	1040	119	1.28	0.63	1.79	1.14	364	46.0	29,937
	2-17-68		Building power was off and emergency power came on for 5 hours.							
	2-19-68	1040	120	1.29	0.64	1.79	1.14	365	46.0	30,033
	3-14-68	1040	119	1.28	0.63	1.79	1.13	361	46.0	30,609
	3-20-68	1040	120	1.09	0.63	1.78	1.13	363	46.5	30,753
A4	1-15-68		Building power was off and emergency power was on for 1 hour.							
	1-17-68	1040	119	1.27	0.61	2.32	1.41	286	38.5	28,401
	1-30-68	1040	119	1.25	0.59	2.27	1.35	289	38.5	28,713
	2-15-68	1040	116	1.25	0.60	2.25	1.35	290	38.0	29,097
	2-17-68		Building power was off and emergency power came on for 5 hours.							
	2-19-68	1040	116	1.26	0.60	2.26	1.36	292	38.0	29,193
	3-14-68	1040	118	1.25	0.60	2.26	1.36	287	38.5	29,769
	3-20-68	1040	119	1.26	0.60	2.27	1.37	290	39.5	29,913

Table 2-15. Performance Data, SNAP-21 Prototype Generators

Module	Date	T-Hot (est)	T-Cold	E_o (volts)	E_L (volts)	I_L (amps)	P_o (watts)	R (M-ohms)	P_I (watts)	Hours
P5	1-15-68		Building power was off and emergency power came on for 1 hour.							
	1-17-68	1064	153	10.04	5.02	2.23	11.19	2.25	176	23,681
	1-30-68	1070	151	9.90	4.95	2.21	10.94	2.26	175	23,993
	2-15-68	1062	150	10.00	5.00	2.21	11.05	2.26	175	24,377
	2-17-68		Building power was off and emergency power came on for 5 hours.							
	2-19-68	1068	149	10.10	5.05	2.17	10.96	2.33	177	24,473
	3-14-68	1052	156	9.96	4.98	2.19	10.91	2.27	177	25,049
	3-20-68	1046	151	10.00	5.60	2.17	10.85	2.30	173	25,193
P6	1-15-68		Building power was off and emergency power came on for 1 hour.							
	1-17-68	1055	166	10.04	5.02	2.03	10.19	2.47	192	23,052
	1-30-68	1055	171	10.00	5.00	2.03	10.15	2.46	190	23,364
	2-15-68	1055	165	9.90	4.95	2.03	10.05	2.44	192	23,748
	2-17-68		Building power was off and emergency power came on for 5 hours.							
	2-19-68	1055	166	10.00	5.00	2.05	10.25	2.44	192	23,844
	3-14-68	1055	171	10.02	5.01	2.04	10.22	2.46	192	24,420
	3-20-68	1055	168	10.00	5.00	2.04	10.20	2.45	192	24,564
P7	1-15-68		Building power was off and emergency power came on for 1 hour.							
	1-17-68	1055	169	10.40	5.20	1.92	9.98	2.71	177	
	1-30-68	1055	184	10.20	5.10	1.91	9.74	2.67	177	
	2-15-68	1055	165	10.20	5.10	1.92	9.79	2.66	178	
	2-17-68		Building power was off and emergency power came on for 5 hours.							
	2-19-68	1055	164	10.20	5.10	1.92	2.66	2.66	9.79	23,997
	3-14-68	1055	170	10.28	5.14	1.92	2.68	2.68	9.87	24,573
	3-20-68	1055	169	10.28	5.14	1.92	2.68	2.68	9.87	24,717

2.3.7 POWER CONDITIONER

Power conditioner testing during this period consisted primarily of evaluating the data from power conditioners H10D2, H10D3, and H10D4 prior to encapsulation. Wave form photos, starting characteristics, and efficiency percentages were recorded. This data was compared to the original design expectations and to H10D1 performance to determine if the unit characteristics were satisfactory for completion of assembly. Figure 2-20 shows the power conditioner test circuit. Wave forms taken from power conditioners H10D2 and H10D3 are shown in Figures 2-21 and 2-22. Power conditioner test and efficiency data is given in Tables 2-16 through 2-19.

Unit H10D2 did not pass the voltage insulation test after encapsulation and H10D3 will replace H10D2 for the dynamic test. H10D1 is undergoing additional starting characteristic testing plus other testing.

Two test panels for long-term testing are 90 percent complete. Each has a capacity of three power conditioners. One panel is currently in use for evaluation and assembly mode testing. The panels will be extremely useful for ensuring exact test conditions for each power conditioner tested. The beginning-of-life (BOL) and end-of-life (EOL) test parameters can be varied to match predicted value conditions. The output load has two variable loads to simulate varying conditions and the effect on the power conditioner.

Efficiency values for EOL only are listed for the various power conditioners. The BOL efficiency value is not a true representation of power conditioner efficiency.

The residual Phase I power conditioners and related electronic equipment have accrued 26,000 hours of test time. Exception to the hourly total is the automatic selector switch. This was shut down on February 28, 1968, to improve the breadboard layout.

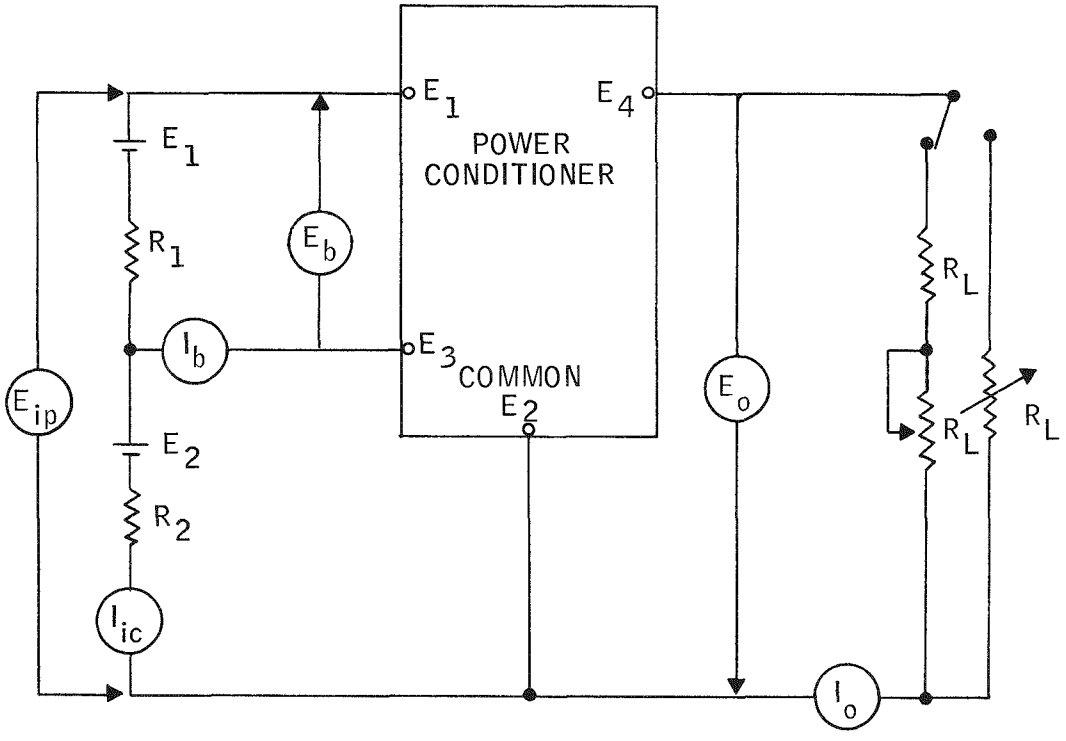

Figure 2-20. Power Conditioner Test Circuit

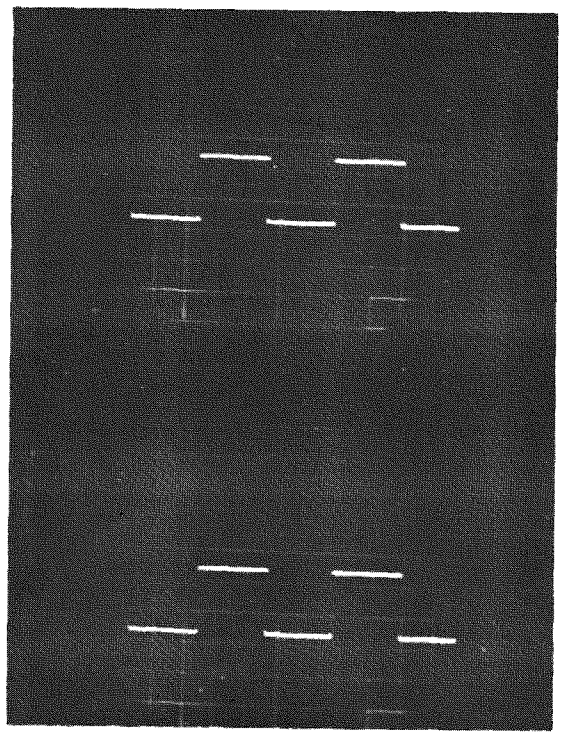

a) Emitter to collector of Q_1 and Q_2

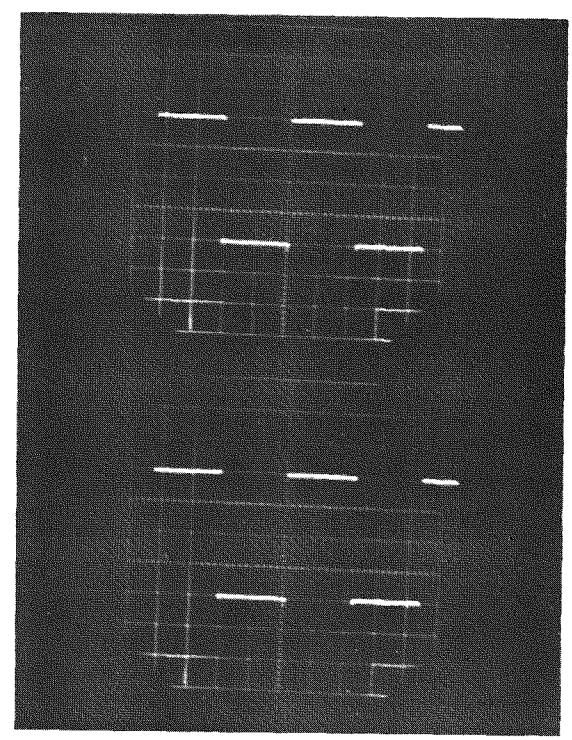

b) Collector to base Q_3 and Q_4

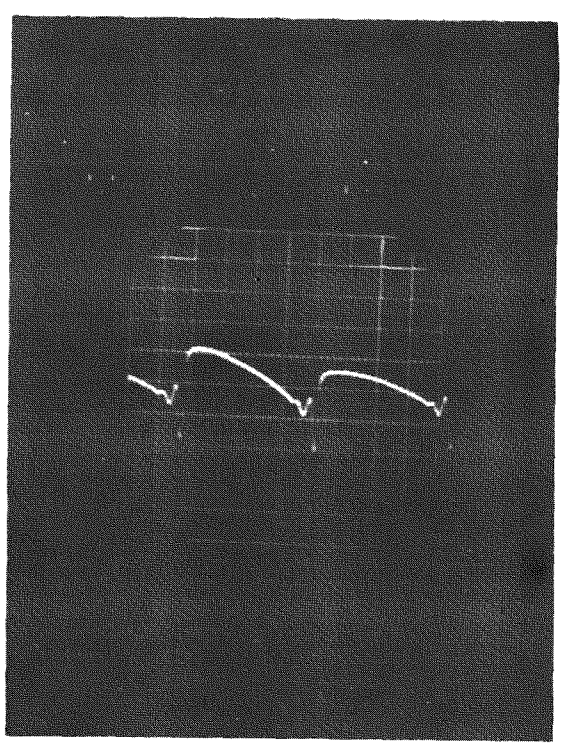

c) Rated load output ripple

Figure 2-21. Voltage Waveform from Power Conditioner H10D2

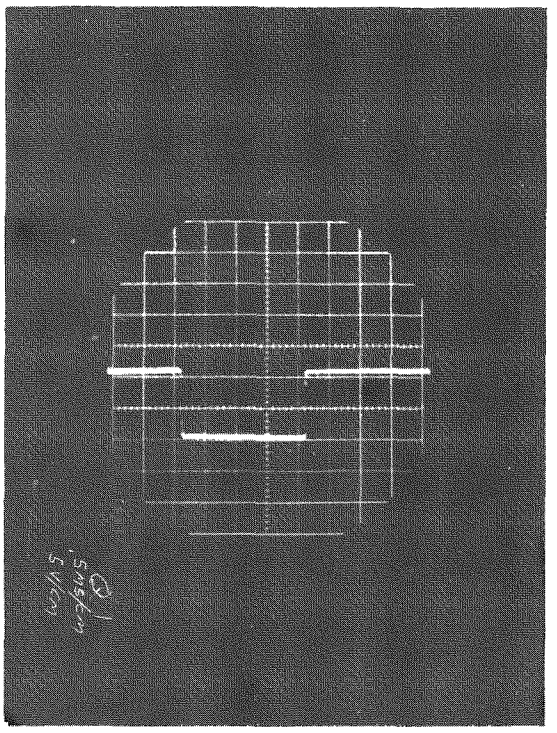

a) Emitter to collector of Q_1 and Q_2

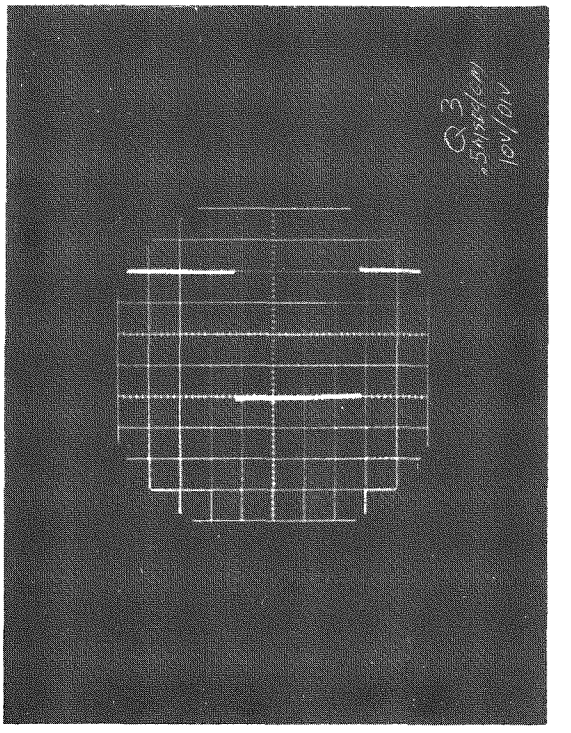

b) Collector to base Q_3 and Q_4

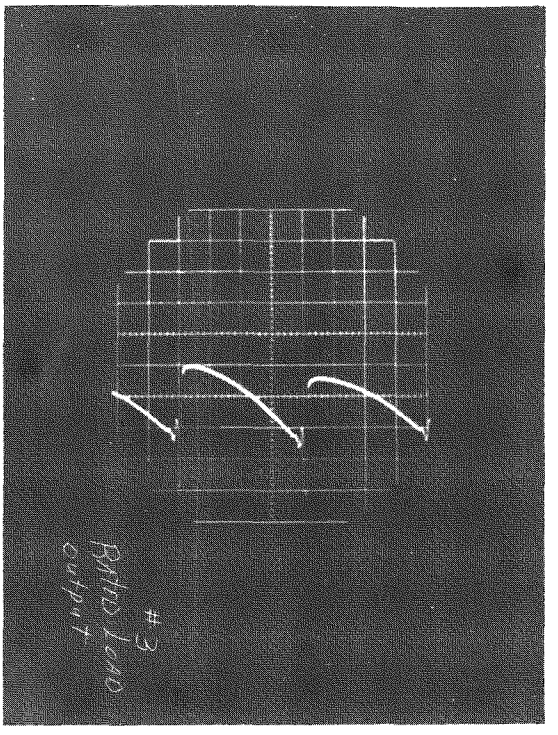

c) Rated load output ripple

Figure 2-22. Voltage Waveform from Power Conditioner H10D3

Table 2-16. Automatic Selector Switch: Output Voltage vs. Time on Test

Time (Hours on Test)	Output Voltage		Remarks
	Conditioner MP-A	Conditioner MP-D	
13,583	24.54	24.59	
13,943	24.55	24.60	
14,471	24.56	24.60	
14,615	24.55	24.59	
15,095	24.62	24.58	Note: System turned off from 4-24-67 to 6-6-67
15,479	24.62	24.58	
15,887	24.50	24.59	
16,343	24.46	24.58	
16,799	24.45	24.57	
17,327	24.47	24.55	
17,951	24.50	24.55	
18,479	24.47	24.59	
18,959	24.47	24.57	
19,319	24.48	24.59	
19,631	24.48	24.58	
20,111	24.47	24.58	
20,687	24.45	24.56	
20,999	24.48	24.56	Note: At 22,367 hours the system was shut down to install into cabinet.
22,367	24.49	24.60	

Table 2-17. Regulator Test Fixture Performance Data

Operating Hours	A	C	D	F	HPR-A Operating Hours	HPR-A
18,369	21.75	21.86	22.49	21.93	17,552	26.78
18,729	21.72	21.79	22.47	21.90	17,912	26.77
19,257	21.72	21.78	22.46	21.89	18,440	26.80
19,401	21.72	21.78	22.46	21.88	18,584	26.81
19,881	21.54	21.63	22.41	21.88	19,064	26.46
20,265	21.53	21.55	22.42	21.90	19,448	26.51
20,673	21.53	21.46	22.42	21.88	19,856	26.51
21,117	21.49	21.39	22.40	21.84	20,360	26.51
22,161	21.52	21.37	22.39	21.85	21,344	26.51
22,617	21.60	20.79	22.40	21.88	21,800	26.48
23,145	21.46	21.45	22.35	21.82	22,328	26.45
23,769	21.46	21.13	22.31	21.82	22,952	26.36
24,297	21.35	21.52	22.41	21.82	23,480	26.31
24,777	21.43	20.93	22.33	21.76	23,960	26.34
25,137	21.49	21.00	22.36	21.83	24,320	26.47
25,449	21.49	21.00	22.39	21.84	24,632	26.53
25,929	21.50	20.97	22.39	21.83	25,112	26.56
26,381	21.51	20.95	22.40	21.84	25,564	26.60
26,693	21.74	21.81	22.46	21.92	25,876	26.93
28,061	21.52	21.30	22.41	21.83	27,244	26.52
28,541	21.51	21.27	22.38	21.81	27,724	26.56

Table 2-18. Performance of Power Conditioners MP-B and MP-C

Converter Performance Power Conditioner	E-In (volts)	I-In (amps)	P-In (watts)	E-Out (volts)	I-Out (amps)	P-Out (watts)	Efficiency Percent	Hours on Test
MP-B	4.844	2.491	12.167	24.00	0.451	10.824	88.96	16,212
	4.839	2.456	11.986	24.00	0.444	10.656	88.90	16,572
	4.842	2.471	12.066	24.00	0.447	10.728	88.91	17,100
	4.843	2.470	12.063	24.00	0.447	10.728	88.93	17,244
	4.841	2.464	12.029	24.00	0.446	10.704	88.98	17,724
	4.840	2.463	12.022	24.00	0.445	10.680	88.84	18,108
	4.838	2.443	11.920	24.00	0.442	10.608	88.99	18,516
	4.843	2.478	12.102	24.00	0.449	10.776	89.04	19,020
								19,620
Note: Unit shut down for experimental testing 6-7-67.								
MP-C	4.913	2.395	11.809	24.00	0.436	10.464	88.61	15,783
	4.908	2.360	11.606	24.00	0.429	10.296	88.71	16,143
	4.909	2.374	11.757	24.00	0.432	10.368	88.19	16,671
	4.910	2.378	11.779	24.00	0.433	10.392	88.22	16,815
	4.906	2.372	11.740	24.00	0.432	10.368	88.31	17,295
	4.905	2.374	11.747	24.00	0.432	10.368	88.26	17,679
	4.904	2.353	11.642	24.00	0.428	10.272	88.23	18,087
	4.909	2.389	11.831	24.00	0.439	10.416	88.04	18,591
	4.912	2.395	11.867	24.00	0.436	10.464	88.18	19,575
	4.913	2.396	11.878	24.00	0.436	10.464	88.10	20,031
	4.910	2.375	11.764	24.00	0.432	10.368	88.13	20,559
	4.908	2.371	11.740	24.00	0.431	10.344	88.11	21,183
	4.909	2.375	11.762	24.00	0.432	10.368	88.15	21,811
	4.909	2.376	11.767	24.00	0.432	10.368	88.11	22,098
	4.910	2.375	11.764	24.00	0.432	10.368	88.13	22,485
	4.912	2.403	11.907	24.00	0.438	10.512	88.28	22,770
	4.911	2.377	11.776	24.00	0.433	10.380	88.92	23,250
	4.909	2.357	11.674	24.00	0.428	10.270	87.99	24,066
	4.908	2.368	11.725	24.00	0.431	10.344	88.22	25,434
	4.908	2.368	11.725	24.00	0.430	10.320	88.02	25,914
Note: Unit accidentally shut down, discovered on 12/21/67. Power restored 12/22/67.								

Table 2-19. Power Conditioner Test Efficiency

Unit	Condition	E_o	I_o	E_b	I_b	E_{ip}	I_{ic}	Efficiency (percent)
H10D2	EOL	24.0	0.465	0.732	0.137	5.14	2.43	90.06
H10D3	EOL	24.0	0.5015	0.708	0.1379	5.161	2.55	90.51
H10D4	EOL	24.0	0.449	0.659	0.1336	5.12	2.30	90.82
	Efficiency $= \frac{E_o I_o}{E_b I_b + E_{ip} I_{ic}}$							

2.4 SYSTEM TEST

2.4.1 PHASE I SYSTEM TESTING

Phase I System B-1 came off test on December 4, 1967 after logging over 23,496 hours of test time. For a history of the components refer to SNAP-21B Program Phase I, Final Summary Report No. MMM 3321-19, C-92a M3679 (44th Edition). This section contains an analysis of the test data for some of the major components and the system as a whole.

2.4.1.1 Insulation System

The insulation envelope used in this system was never hermetically sealed. Because of this it had to be continuously pumped to maintain the desired vacuum. No post-test analysis was done on this system. At the present time, this insulation envelope is being used for generator efficiency studies.

2.4.1.2 Thermoelectric Generator

Figure 2-23 shows the operating thermal conditions for the generator during the test period. Throughout most of the test period the hot electrode temperature was determined from the cold electrode temperature and the N-leg Seebeck voltage. Therefore, it should be remembered that the hot electrode temperature is an approximation. The changes in power input at 10,000 and 18,000 hours of test were made to simulate the radioisotopic fuel decay after a year of operation. The system power input shown on this graph is corrected to take into consideration the extraneous losses due to instrumentation. A major concern of the thermal operating conditions was that the cold electrode temperature was somewhat higher than expected (cold electrode design temperature is 115°F). It is believed that this was caused at the cold cap follower interface. This problem has been corrected in subsequent Phase II systems.

Figure 2-24 shows the normalized performance data for the generator in the system. Shown here is the ratio of the experimental data to the calculated expected performance* for the Seebeck voltage, internal resistance, and power (matched load) for the generator. Ideally, these ratios should be 1.00. It can be seen that the major cause for the decrease in power output was the increase in internal resistance. Further analysis of the data indicates that the increase in resistance was due primarily to the N-leg. It should be noted that prototype P4 was on bench test for over 1400 hours and had indicated stable performance prior to incorporation into the system. After the test was terminated the generator was put into bonded stock.

2.4.1.3 Power Conditioner

Since the power conditioner for this test was treated as a "black box" the only performance value that may be determined is the converter efficiency (see Figure 2-25). From Figure 2-25 it can be seen that the converter efficiency

*Theoretical resistance is material resistance only.

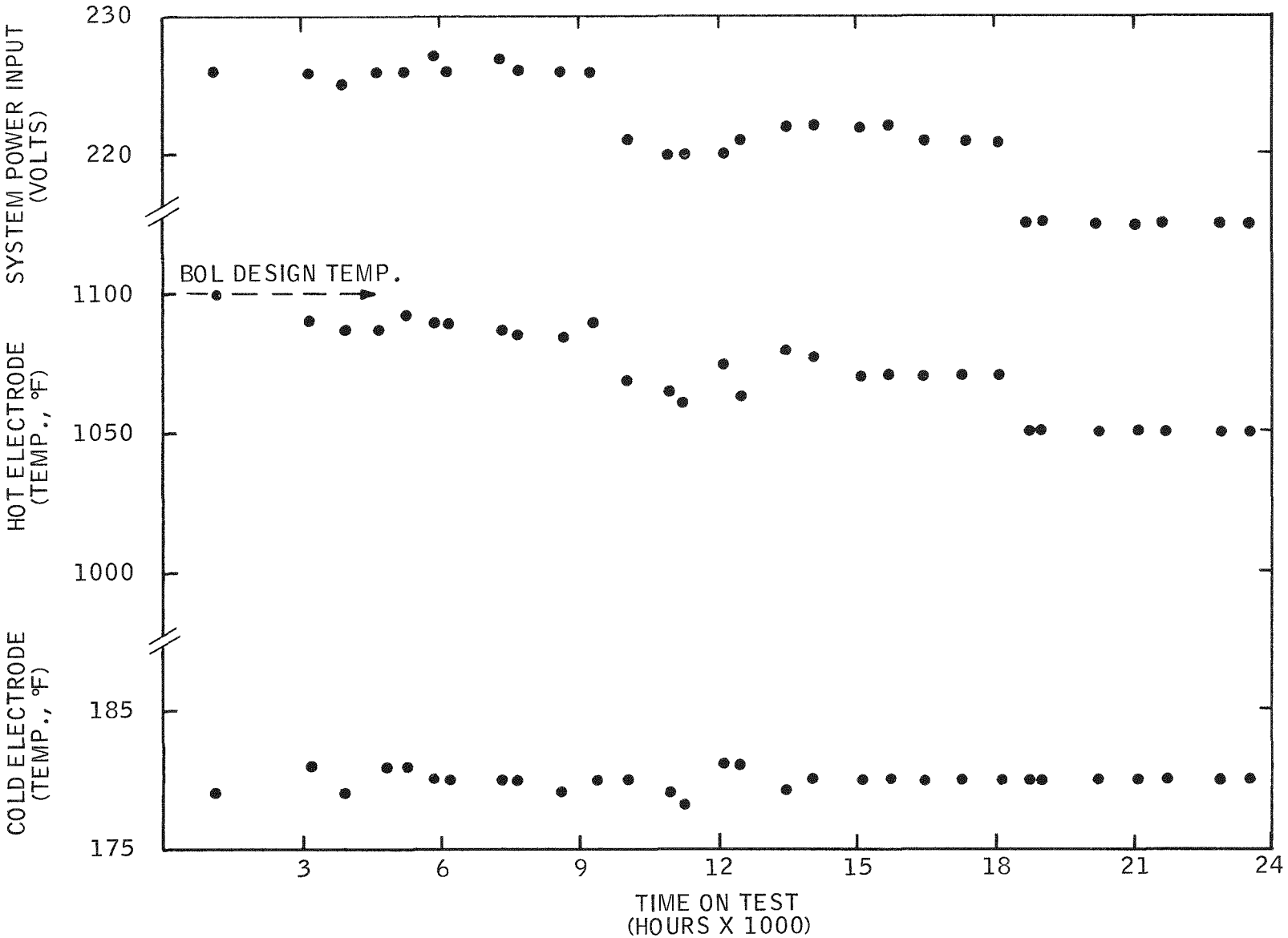

Figure 2-23. Operating Thermal Conditions for Prototype Generator P4

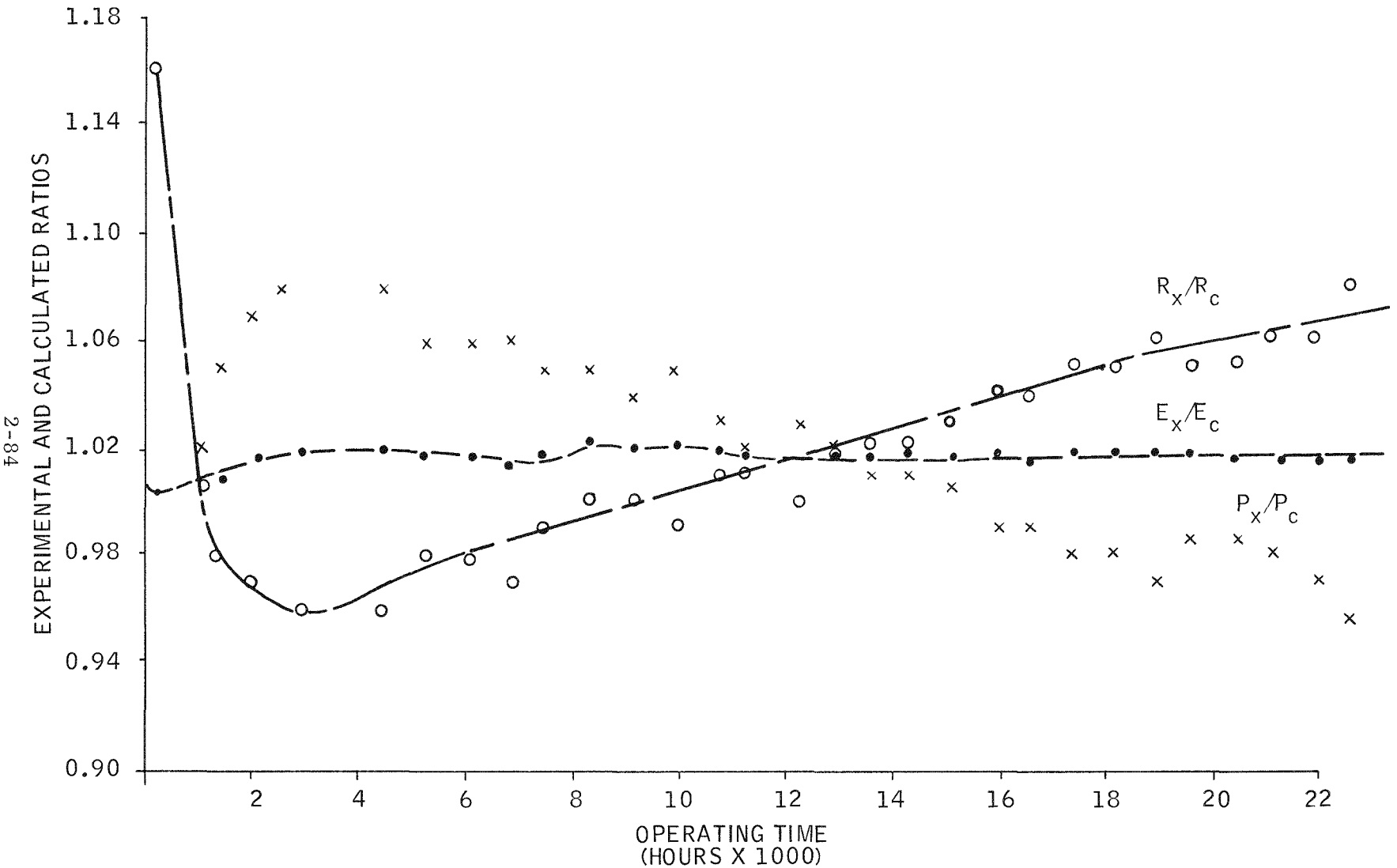

Figure 2-24. Normalized Data, Prototype Generator P4

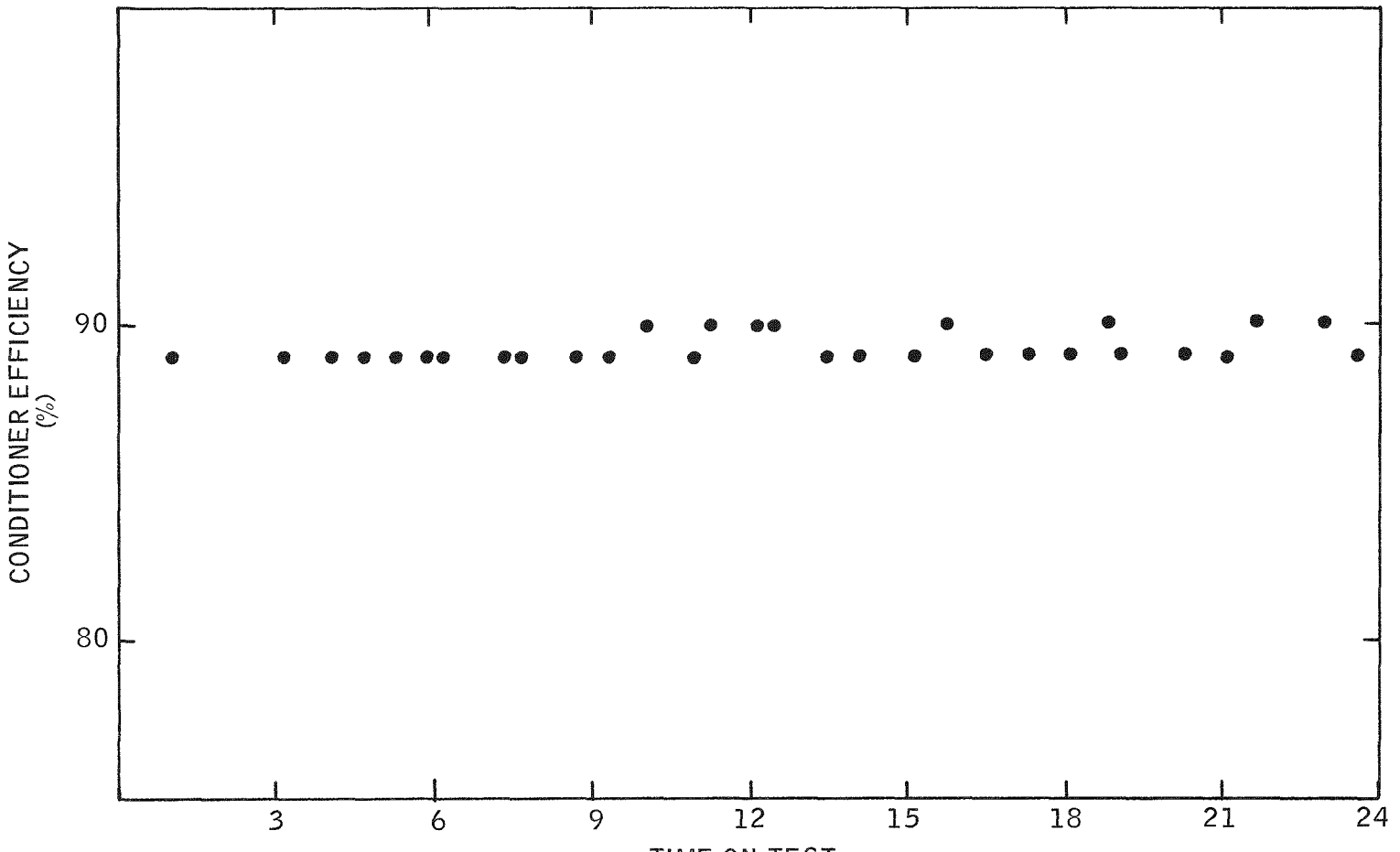

Figure 2-25. Conditionier Efficiency vs. Time

was very stable throughout the test period. Note that prior to system integration the power conditioner was on bench test for about 792 hours. During this time its performance was stable.

No detailed post-test analysis was conducted on this component. After termination of test, this conditioner was incorporated into Phase II System S10D1A for short-term test (see Section 2.2.3).

2.4.1.4 Pressure Vessel

A cast pressure vessel of type CFSC (AISI-347) stainless steel was used in this test. The only monitoring of the pressure vessel was the temperature profile (see Section 2.4.3).

2.4.1.5 System Performance

Figure 2-26 shows performance curves for the system. Shown is the system load current, system power out, and system efficiency. The system load voltage was 24 ± 0.1 volts. From this figure it can be seen that the system power out had decreased. The cause of this is the decrease in generator power output (see Section 1.2). Some of the fluctuations in the system power out were caused by changes in the load resistance. The operation of the system is at a constant system load voltage of 24 volts, but the current can be varied over a small range, thereby causing variations in power output for the same load voltage. Further analysis of this graph shows that as the system power input decreased (simulated yearly fuel decay) the system performance became more stable. It is suspected that this is caused by the decrease in change of the generator power output.

Prior to system shut down the system power input was restored to BOL value and the system stabilized. (Refer to SNAP-21 Program Phase II Quarterly Report No. 6 (MMM 3691-26) for a discussion of this test.) The System power out shown on this graph is corrected to account for extraneous losses due to insulation.

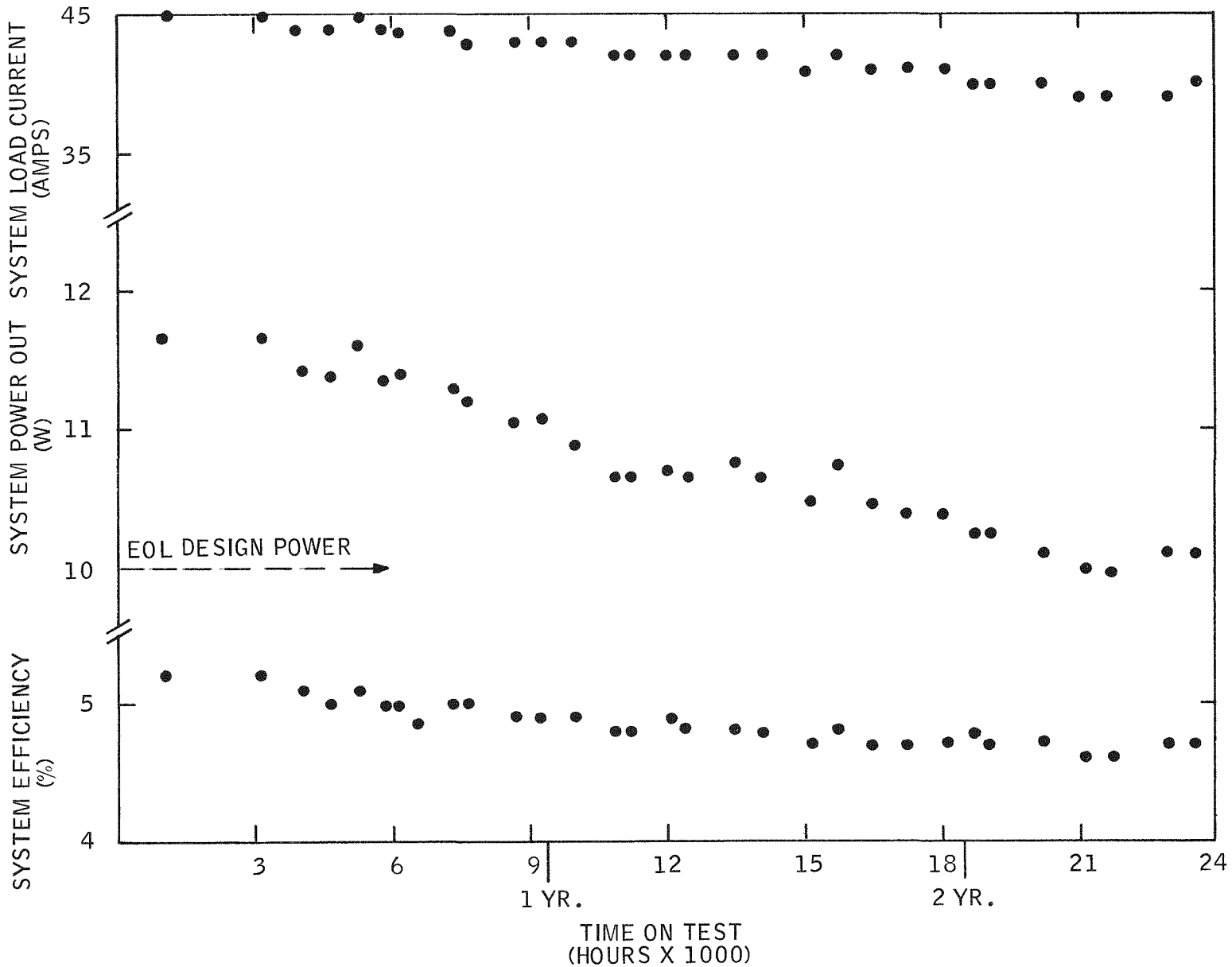

Figure 2-26. Performance of System B-1, SNAP-21, Phase I

2.4.2 PHASE II SYSTEM TESTING

2.4.2.1 System S10D1

System S10D1 was taken off test on January 29, 1968 after accumulating about 1460 hours of test time. Refer to SNAP-21 Program Phase II Quarterly Report No. 6 (MMM 3691-26) for system component history and system assembly. The test was terminated when the generator pressure transducer indicated a leak in the hermetic seal. After cooling to room temperature, the generator was inspected. A hole in the long case was found in the area where the long case and hot frame meet.

The system was dismantled with full power being applied to the heater block. This was done to preclude any pressure decrease due to a drop in temperature. To prevent an increase in temperature, a polyflow cooling manifold was connected around the pressure vessel in the vicinity of the flange.

No detailed post-test analysis is planned for the system components. The following paragraphs give analysis of the test data for some of the major components and the system as a whole.

2.4.2.1.1 Insulation System

The insulation system used in this test was of the Phase II design. Throughout most of the test period the active getter inside the insulation envelope kept the vacuum below 10 microns, keeping the insulation thermal losses low. The only time the vacuum was above 10 microns (high of 15 microns) was during heat-up. Thermal performance of the insulation system appeared to be good.

2.4.2.1.2 Thermoelectric Generator

Operating temperatures during most of the test period were approximately 1040 ± 10°F and 130 ± 10°F at the hot and cold electrodes, respectively. The exception to this is when the environment temperatures were changed and when the system was put through simulated shipping thermal conditions (see Section 2.4.2.1.5).

Figure 2-27 shows the ratio of experimental to theoretical value of Seebeck voltage and internal resistance for the generator*. Ideally, these ratios should be 1.00. Included in this graph is the time the generator was on bench test. It can be seen that generator performance was stable when on bench test and system test, except that there is a decrease in Seebeck voltage and resistance when the generator was transferred into the system. The exact cause for this decrease is not known at this time.

Because disassembly of the system was done with full system power still applied, the generator was backfilled (argon with 1 percent helium) at operating temperature and then allowed to cool to room temperature. After cooling to room temperature, a new long case was welded over the old case. The generator is presently on life test.

2.4.2.1.3 Power Conditioner

The power conditioner used in this system was a Phase I residual conditioner (MP-F). Since the conditioner was treated as a black box, about the only performance value that may be determined is the converter efficiency (see Figure 2-28). This curve shows that the conditioner was fairly stable at about 85 percent efficiency. No post-test analysis is planned on this component.

2.4.2.1.4 Pressure Vessel

The pressure vessel used in this test was fabricated from titanium 621. The only monitoring on the pressure vessel was the temperature profile (see Section 2.4.3). At the present time this pressure vessel has been put into bonded stock.

*The theoretical resistance is material resistance only.

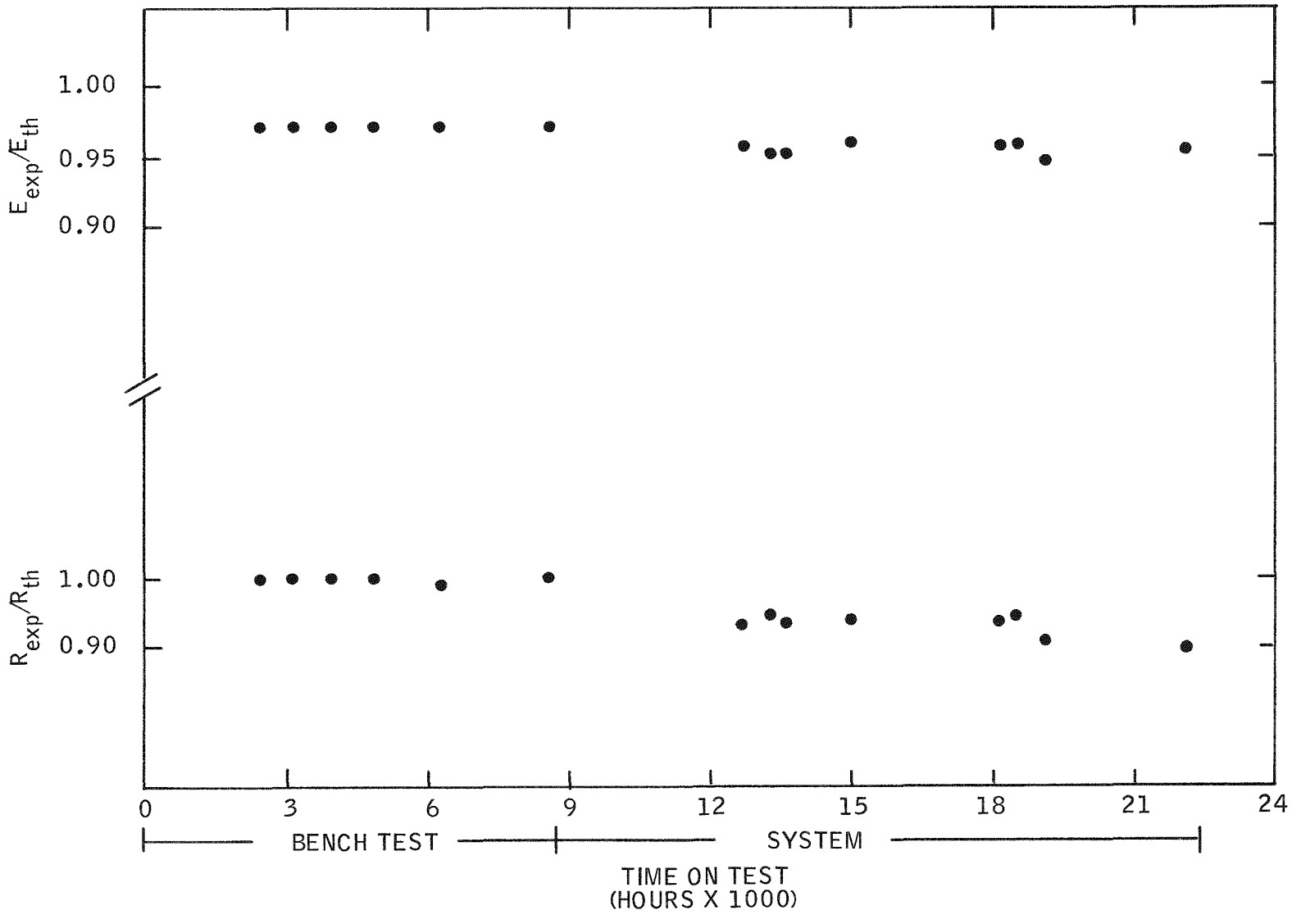

Figure 2-27. Seebeck Voltage/Resistance Ratio vs. Time, Generator 10D1

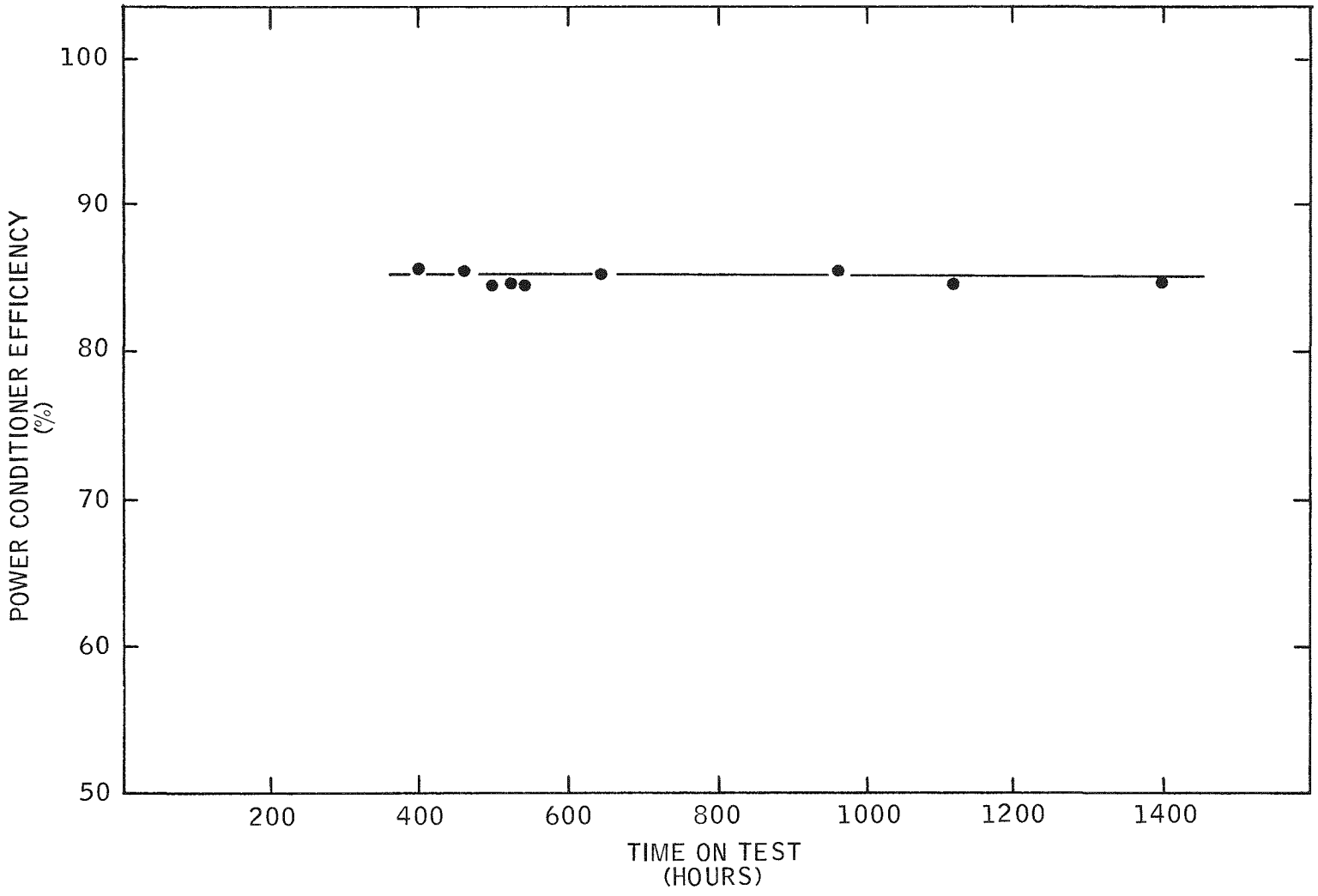

Figure 2-28. Power Conditioner Efficiency vs. Time, System S10D1

2.4.2.1.5 System Performance

2.4.2.1.5.1 System Testing

System testing on S10D1 is divided into three parts. The three segments, in order of progression, are:

a) System response to changes in input power

b) System response to various environment conditions

c) Simulated shipping conditions tests

a) System Response to Changes in Input Power

Figure 2-29b shows the hot and cold electrode temperatures at varying input power. Since the environmental water temperature was not held exactly at 38°F, the cold electrode did not vary as it should have with a constant environmental water temperature. The dotted line in Figure 2-29b shows cold electrode temperature corrected to a constant 38°F environmental water temperature.

Figure 2-29a shows the efficiency and power output as a function of power input. The plot indicates that for the operating range of the system, there is a change of 0.94 watt output power per watt of input power.

b) System Response to Various Environmental Conditions

Response to environmental temperature change is shown in Figure 2-30. Curves with the triangles indicate empirical data in water. The two dashed curves represent analytically derived relationships for a mean pressure vessel temperature. Average heat transfer coefficients were calculated for free convection over the entire pressure vessel in air and in water for the temperature range from 0 to 100°F (see Figure 2-31). These coefficients were used with the total surface area to derive pressure vessel mean temperatures as a function of environment temperature for air and water. The empirically obtained temperature of the pressure vessel was taken in the bolt hole at the top of the cylindrical section. This is different from the theoretical mean temperature because of the low thermal conductivity of the titanium. Since pure conduction is the mode of heat

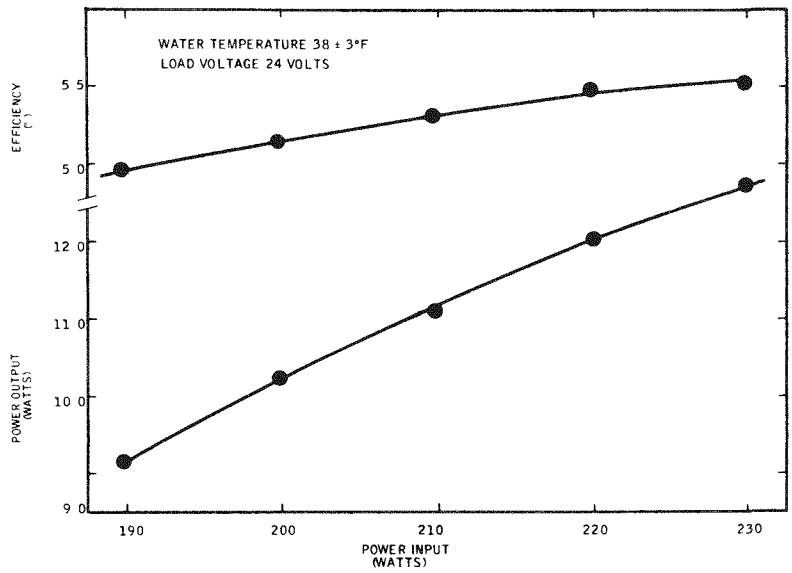

a. Power Output and Efficiency

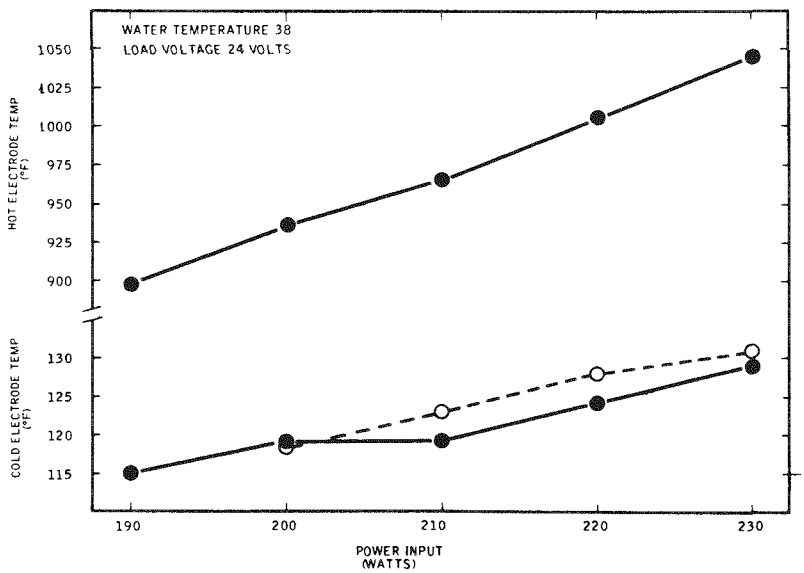

b. Hot and Cold Electrode Temperatures

Figure 2-29. Reduced Power Input Test, System S10D1

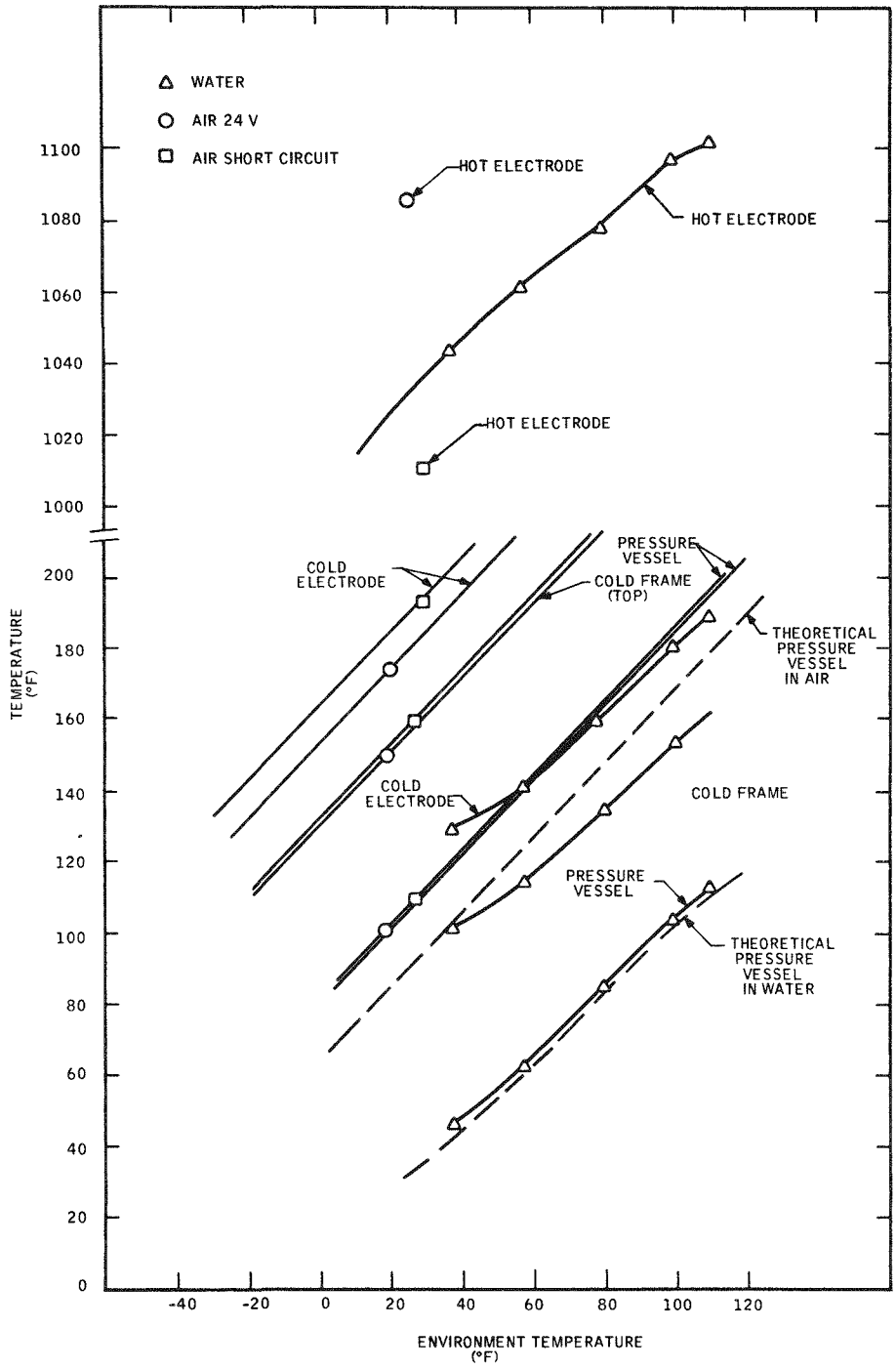

Figure 2-30. Response to Change in Environmental Temperature, System S10D1

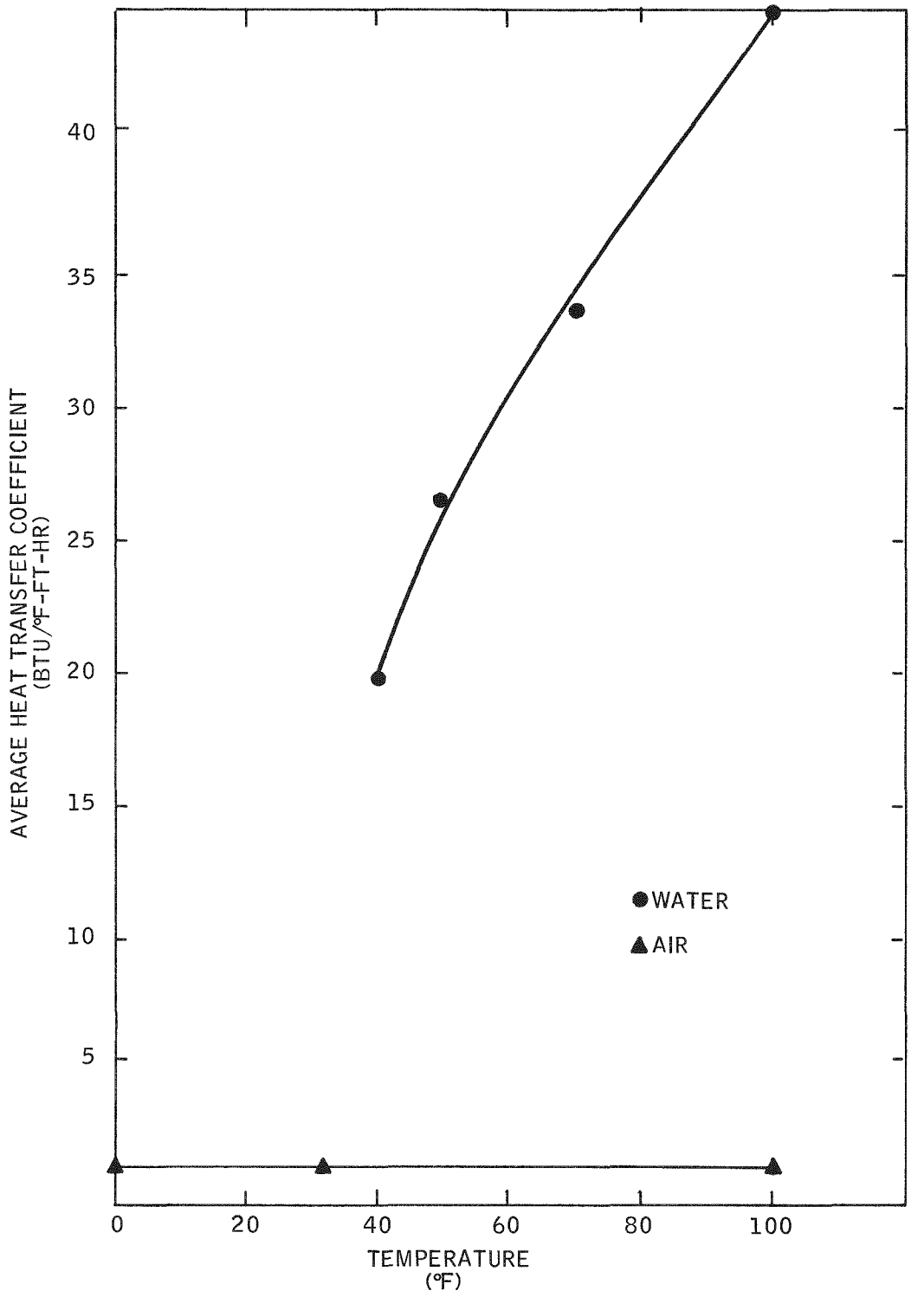

Figure 2-31. Heat Transfer Coefficient Temperature, System S10D1

transfer between the cold frame and pressure vessel top, these three curves can be drawn parallel.

It is interesting to note at this time that if the pressure vessel were made of beryllium-copper, the experimental pressure vessel curve would fall within one degree of the theoretical curve presented. The conductivity is high enough that thermal gradients from top to bottom would be very small, thus pulling down the temperature of the top of the cylindrical portion and thus the cold frame temperature also. Thus, the cold electrode temperature would be over 15 degrees lower in air with a Berylco pressure vessel than with a titanium one. This difference will not be as great in water, as the two bottom curves in Figure 2-29 show. The only points shown are for hot electrode temperatures in air, since at this writing a good correlation is not available. This will be investigated at a later date.

c) Simulated Shipping Conditions Test

The final test before terminating performance testing of System S10D1 was to simulate shipping conditions for a system. This was done to determine what effects, if any, shipment would have on the system. To accomplish this, System S10D1 was operated in air (about 25°F) with the generator short circuited for approximately two weeks (see Figure 2-30). Data from this test appears in the SNAP-21 January 1968 Monthly Report (MMM 3691-28). Further analysis of the data shows that shipment of the system under these conditions has no detrimental effects on the system.

2.4.2.1.5.2 Overall System Performance

Figure 2-32 shows the overall performance of the system during its entire test period. The load voltage for the system was 24 ± 0.1 volts. Since the load current may be varied while the system load voltage is at 24 ± 0.1 volts, the power out from the system can also vary. It is suspected that this was part of the cause for the decrease in system power output. It can also be seen that the efficiency of the system was fairly constant. System efficiency was using a corrected value of power input to account for extraneous heat losses (6.34 watts).

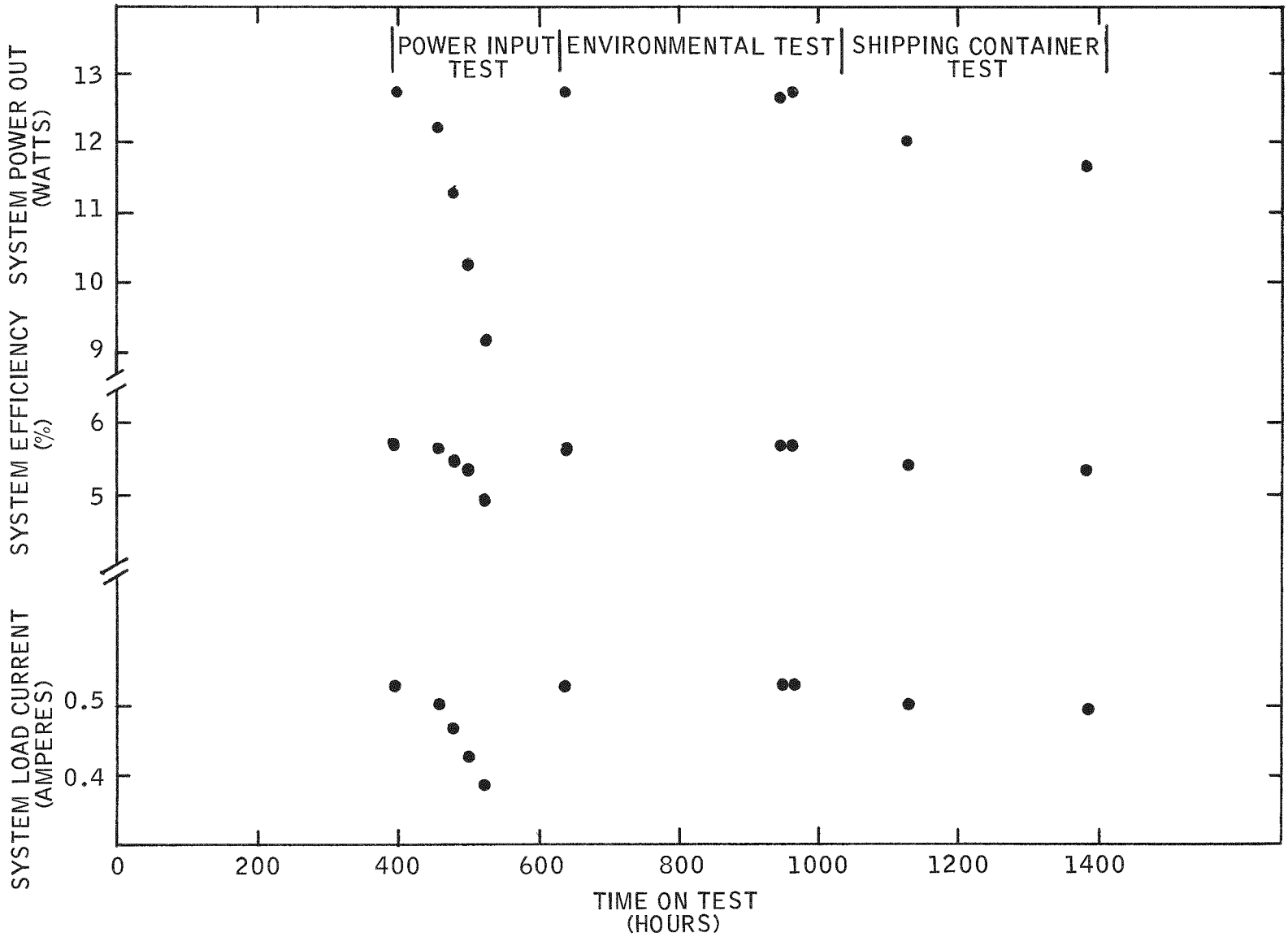

Figure 2-32. Overall Performance, System S10D1

Table 2-20 shows reasonably good correlation between experimental and theoretical temperature distribution. However, some significant differences do exist. The following comments can be made regarding those differences:

a) The experimental cold end temperatures are about 20-30°F higher than the theoretical. One of the factors contributing to this difference was a small metal chip found in the interface between the generator mounting plate and the pressure vessel cover flange. This chip, which was 0.008-inch thick, prevented a good heat transfer interface between the pressure vessel cover and the generator mounting plate.

b) The experimental temperature drop across the emitter plate-to-generator hot frame was 56°F greater than theoretical. It is felt that this was caused by Min-K 1301 thermal insulation material found between the emitter plate and generator hot frame upon disassembly of the system.

After the test was terminated System S10D1 was disassembled. Regarding disassembly, the following major points should be reiterated:

a) System S10D1 was disassembled with full power input to the system to prevent any loss of TEG pressure due to a decrease in temperature.

b) A metal chip (0.008-inch thick) was found between the pressure vessel cover flange and the generator mounting plate.

c) Min-K 1301 thermal insulation was found between the emitter and collector plates. This probably collected there during system assembly.

Table 2-20. Comparison of Theoretical and Experimental Temperature Distribution Data, System S10D1

Location	Experimental Temperature (°F)	Theoretical Temperature (°F)
P.V. Cover – Upper Hemisphere	46	42
P.V. Cover – Flange	49	45
Seg. Ring – Generator Mounting Plate	86	68
Seg. Ring – Interface with P.V. Wall	80	51
Cold Frame – Interface with Mounting Plate	98	71
Neck Tube – Top	152	174
Emitter Plate	1324	1336
Generator Hot Frame (external)	1137	1205
Generator Hot Frame (internal)	1072	1170
Hot Button	1040	1140
Cold Cap	130	113
Cold Frame (internal)	116	82
Fuel or Heater Assembly	1445	1450
Water Temperature	40	40

2.4.2.2 System S10D1A

System S10D1A was taken off test on March 11, 1968 after logging about 1352 hours of test time. This system was the early fueled system and was tested at Oak Ridge National Laboratories. For assembly details refer to Appendix D. (This information is reprinted from the SNAP-21 Program, Phase II Monthly Report, MMM 3691-28, January 1968.) The fuel loading for this system was only about 186.72 watts. As a result, the hot and cold electrode temperatures were about 838°F and 84°F, respectively. The following is an analysis of the test data for some of the major components and the system as a whole.

2.4.2.2.1 Insulation System

The insulation system used in this test was of the Phase II design. Throughout the test period the active getter inside the insulation envelope kept the vacuum below 10 microns. It appears that the insulation system had good thermal performance.

2.4.2.2.2 Thermoelectric Generator (Generator 10D4)

The operating conditions for the generator while in the system were about 838°F and 84°F at the hot and cold electrodes, respectively. While on bench test the hot and cold electrodes operated at 1090 ± 10°F and 100 ± 10°F, respectively. Figure 2-33 shows the ratio of experimental to theoretical value for Seebeck voltage and internal resistance for this generator*. Figure 2-33 shows that the performance of Generator 10D4 was quite stable.

Before terminating the test, short circuit and open circuit tests were conducted on the generator. These tests were conducted to obtain data on the extent of change in hot junction temperature under these conditions. This data is used to predict the effectiveness of short circuiting the generator to lower the hot junction temperature during system handling, storage and shipping.

*Theoretical resistance is only material resistance.

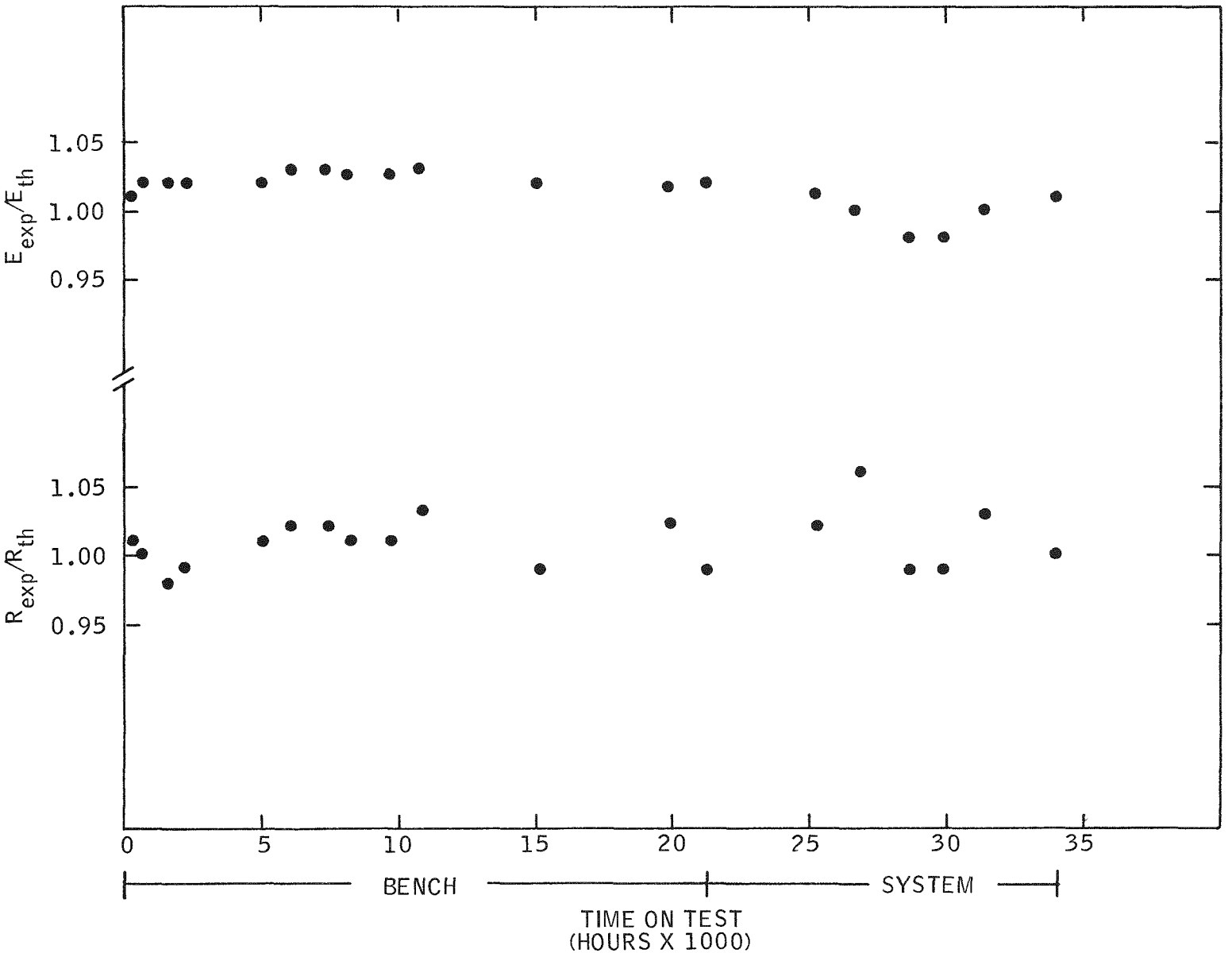

Figure 2-33. Seebeck Voltage and Resistance Ratios vs. Time, System S10D1A, Generator 10D4

The tests were conducted by electrically disengaging the power conditioner from the generator and then operating the generator in either a near short circuit condition or open circuit condition and recording the change in hot junction temperature. Since the test was conducted at ORNL and it required that 3M personnel be in attendance, it was necessary from a cost standpoint to define a condition under which the system could be considered thermally stable. These conditions were arbitrarily defined as follows:

Short Circuit Test – The system is considered stable when the rate of change of the average hot junction temperature is less than 3°F/hour.

Open Circuit Test – The system is considered stable when the rate of change of the average hot junction temperature is less than 5°F/hour.

The short circuit test consisted of electrically stopping the power conditioner by applying a reverse bias to the converter circuit, then loading the generator output with a 0.1 ohm resistor. A 0.005 ohm, 50 millivolt shunt in series with the resistor provided the voltage source readout for current calculations. These conditions remained in effect until the average hot junction temperature did not lower more than 3°F per hour. The results of the test are noted in Figure 2-34. The Digitec voltmeter used to measure voltage drop across the shunt became erratic towards the end of the test, therefore only three points of data are correct for the current curve. The power conditioner was then restarted and the system was operated normally for three hours before the open circuit test was conducted.

The open circuit test was conducted in the same manner as the short circuit test except that the generator was operated in an open circuit condition. At the start of this test, the hot junction temperature was 10°F below the stable temperature that existed before any of the tests were started. The generator open circuit voltage and average hot junction temperature as a function of time is shown for the open circuit test in Figure 2-35.

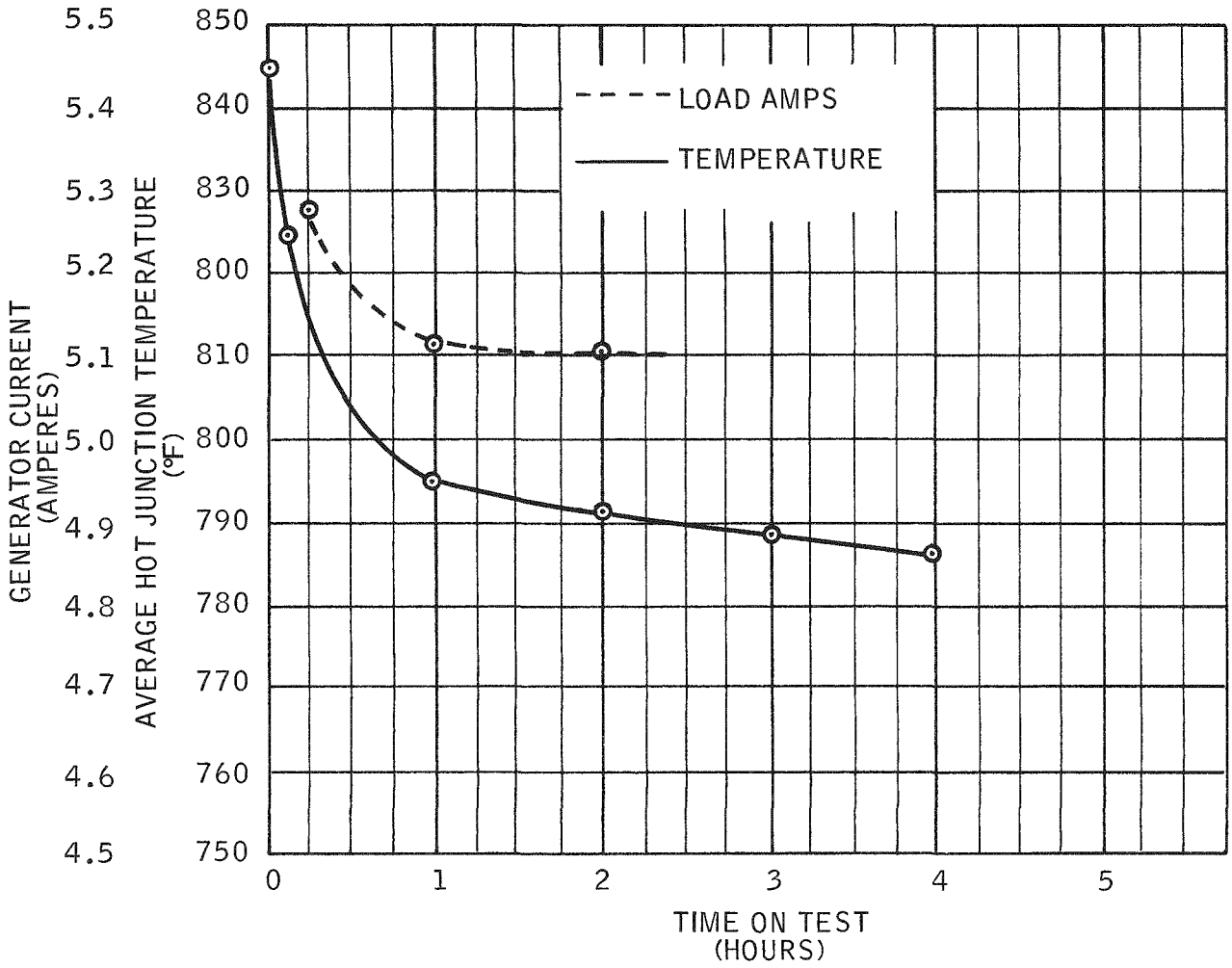

TIME	LOAD CURRENT (0.1 OHM LOAD)	AVERAGE HOT JUNCTION TEMPERATURE (°F)
PRE-START 0850		845
0900	5.280	825
1000	5.116	795
1100	5.106	712
1200	4.80*	788.8
1300		786.5

*Not valid - Digitec Voltmeter faulty requiring new meter.

Figure 2-34. Generator Short Circuit Test, System S10D1A

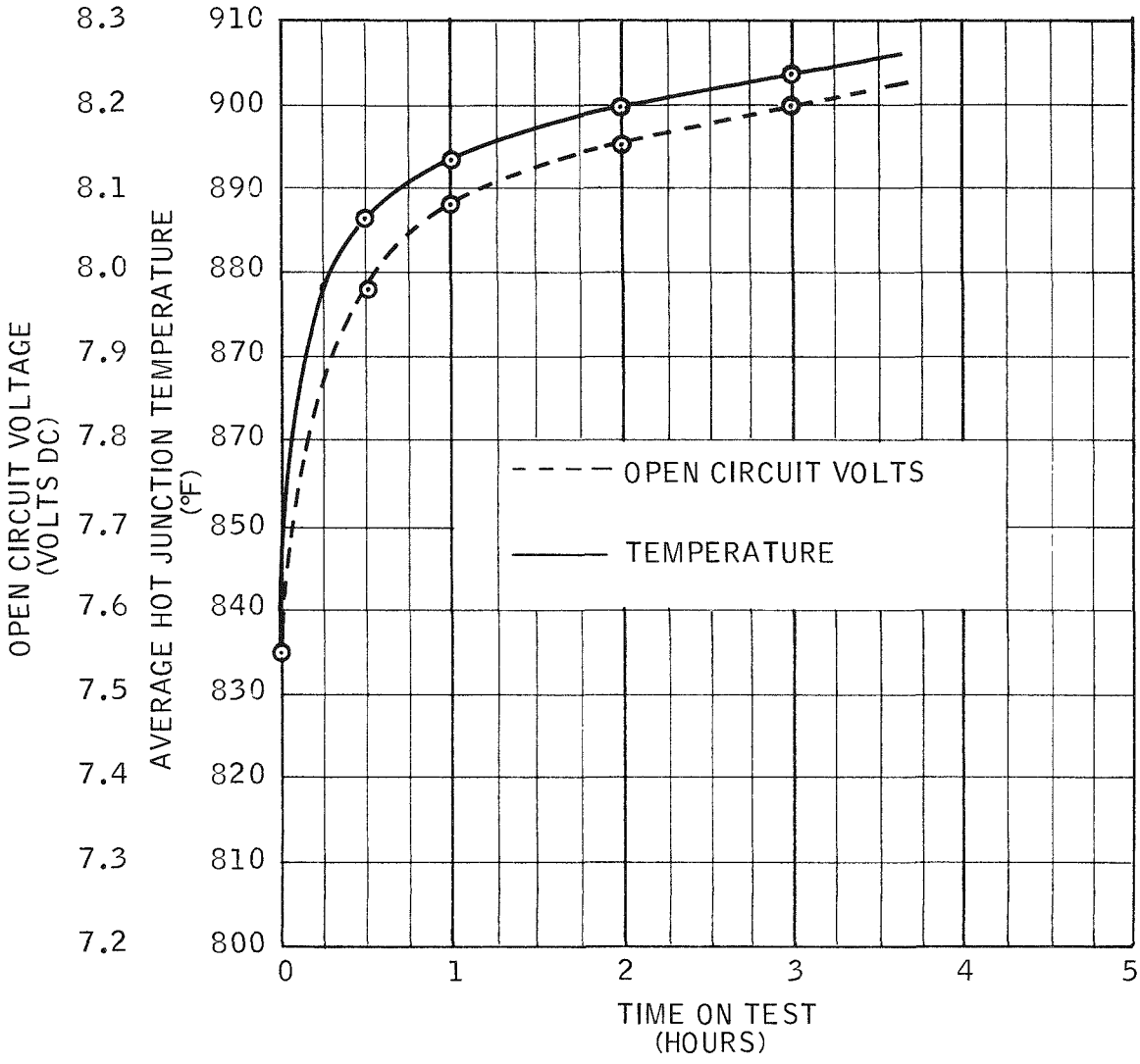

TIME	VOLTS	AVERAGE HOT JUNCTION TEMPERATURE (°F)
1600	7.38	835.0
1630	7.98	886.6
1700	8.08	893.1
1800	8.15	899.1
1900	8.20	903.0

Figure 2-35. Generator Open Circuit Test, System S10D1A

2.4.2.2.3 Power Conditioner

The power conditioner used for this test was the same one used for Phase I System B-1. Figure 2-36 shows the conditioner efficiency. From the graph it appears that the performance of the conditioner is comparable to the Phase I System B-1.

2.4.2.2.4 Pressure Vessel

The pressure vessel used in this test was the same one used for Phase I System B-1. The pressure vessel is of a cast type CFSC(AISI-347) stainless steel vessel. Only the temperature profile of the pressure vessel was monitored.

2.4.2.2.5 System Performance

Figure 2-37 shows overall System S10D1A performance. It can be seen that the system performance was very stable while on test. The fuel loading on the system was 186.72 thermal watts. The system efficiency was calculated to account for 1.22 watts of extraneous losses due to instrumentation.

From Table 2-21 it is apparent that a reasonably good correlation exists between the experimental and the theoretical values of temperature distributions. The only exception to this is the neck tube top. It is felt that this difference is caused by a difference in measuring point.

2.4.3 COMPARISON OF SYSTEMS B1 AND S10D1

In general the components for both systems were from Phase I hardware. Table 2-22 summarizes the components which comprised Systems B1 and S10D1. The major difference between the two systems was in the fabrication of the thermoelectric generator, the difference being between the hardcoated and non-hardcoated follower sockets at the cold end.

No comparison with System S10D1A will be made because of its lower operating conditions.

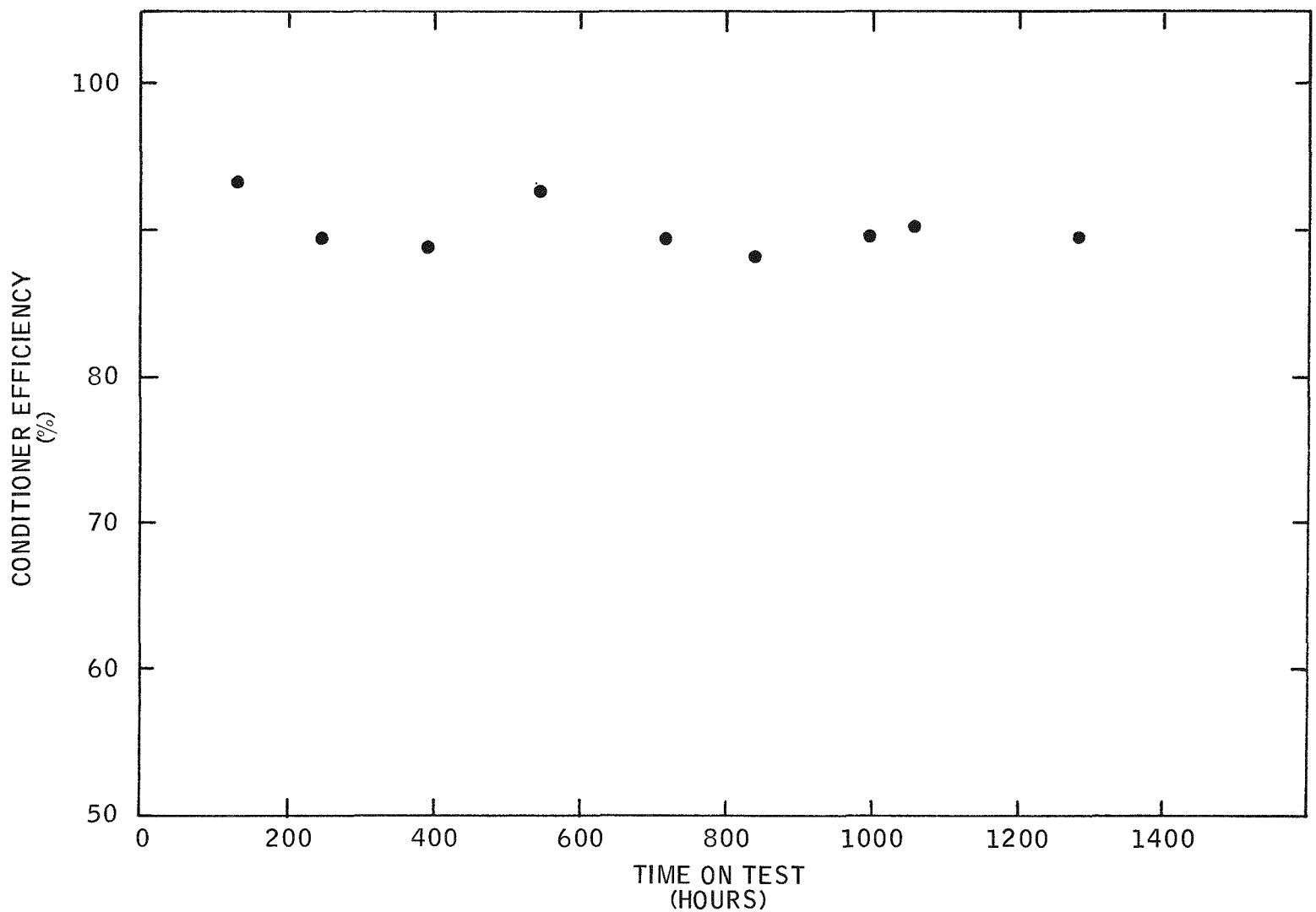

Figure 2-36. Power Conditioner Efficiency vs. Time, System S10D1A

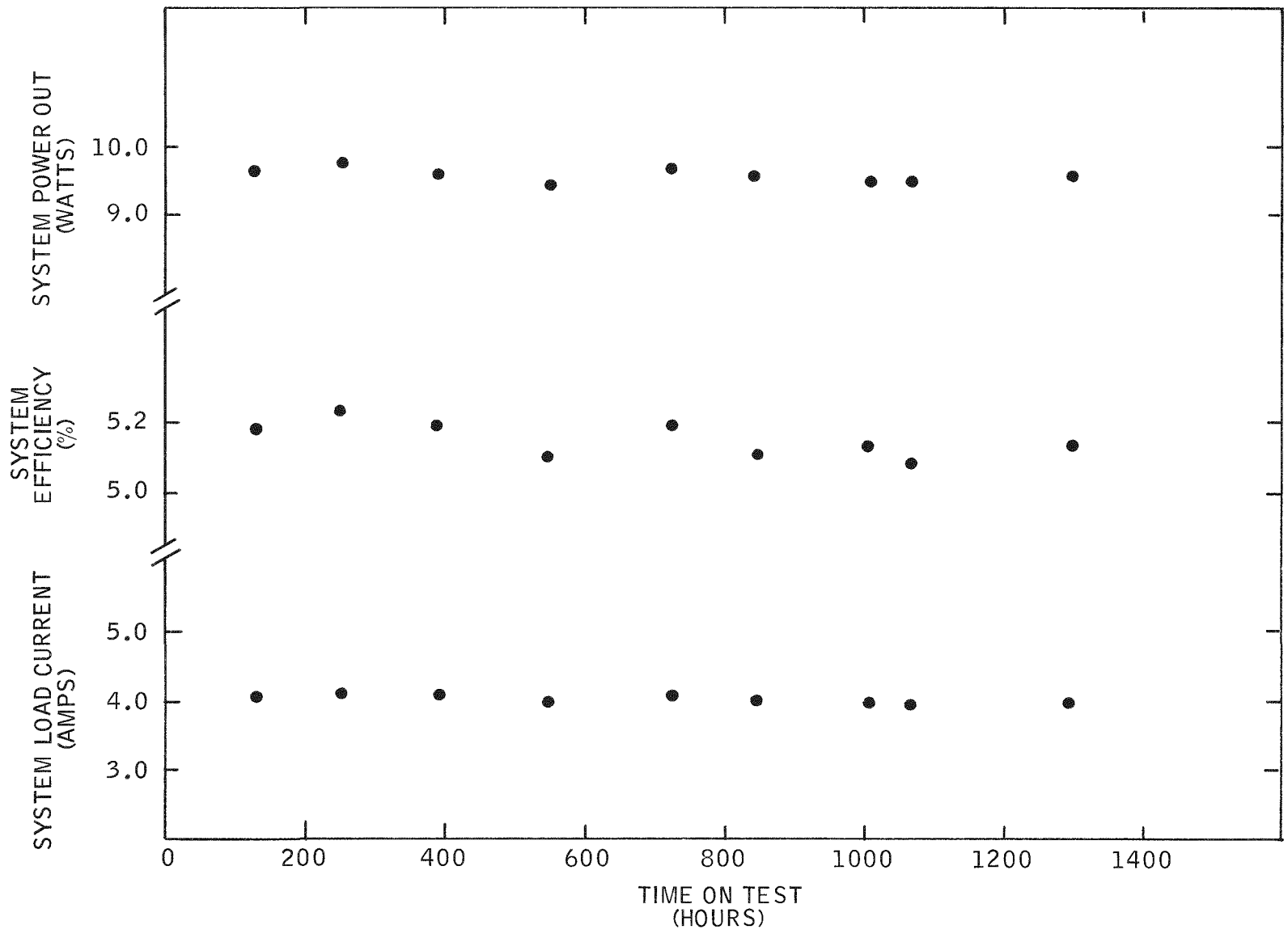

Figure 2-37. Overall Performance, System S10D1A

Table 2-21. Comparison of Theoretical and Experimental Temperature Distribution Data, System S10D1A

Location	Experimental Temperature (°F)	Theoretical Temperature (°F)
P.V. Cover – Upper Hemisphere	49	50
P.V. Cover – Flange	51	50
Seg. Ring – Generator Mounting Plate	70	65
Seg. Ring – Interface with P.V. Wall	Not instrumented	51
Cold Frame – Interface with Mounting Plate	70	68
Neck Tube – Top	92	155
Emitter Plate	1120	1105
Generator Hot Frame (external)	900	895
Generator Hot Frame (internal)	850	855
Hot Button	830	832
Cold Cap	100	101
Cold Frame (internal)	80	77
Fuel	Not instrumented	1225
Water Temperature	42	40

Table 2-22. Component Summary and Comparison of Systems B1 and S10D1

Component	B-1	S10D1	Comments
Pressure Vessel	Phase I (stainless steel)	Phase II (titanium)	
Retaining Ring	Phase I	Phase I	
Insulation System	Phase I	Phase I	S10D1 – Operated with active getter. B-1 – Insulation system had to be continually pumped.
Thermo-electric Generator	Phase I	Phase II	B-1 – Prototype 4 - hardnose P type thermoelectric material, hardcoated followers with hardcoated sockets, silicon heat transfer grease used completely over follower, Xenon backfill gas S10D1 – Softnose P type thermoelectric material, hardcoated followers with non-hardcoated sockets, no heat transfer grease used, argon backfill gas
Power Conditioner	Phase I	Phase I	B-1 – MP-E S10D1 – MP-F
Heater Block	Phase I	Phase II	

Table 2-23 contains the thermal data for both systems and should be used in conjunction with Figure 2-38. The following comments can be made for the systems:

a) The pressure vessel temperature profiles agree fairly closely.

b) S10D1 retaining ring and external cold frame temperatures are higher than for B-1. This is suspected to be due to the chip of metal (0.008-inch thick) that was found between the pressure vessel cover flange and the retaining ring. This impeded the transfer of heat at the cold end.

c) S10D1 heater block and emitter operated at higher temperatures than did the same components of B-1. This could be due to the Min-K insulation found between the emitter and collector in S10D1. It should be pointed out that the value for thermocouple 18 on S10D1 is an erroneous reading.

d) The operating temperatures for the thermoelectric generator are lower for S10D1. It is felt this is due to the non-hardcoated follower sockets used in S10D1 to decrease the cold electrode temperature.

The following comments can be made with regard to the thermoelectric generator used for these systems (see Table 2-24):

a) The Seebeck voltage for S10D1 is lower than for B-1. It is suspected this is due to a slight difference in material.

b) The internal resistance for S10D1 is lower than for B-1. One of the contributing factors for this is that S10D1 is operating at a lower temperature and the temperature distribution is different than for B-1.

c) It is felt that the higher power output for S10D1 is due to the lower resistance.

Table 2-23. Thermal Comparison of Systems B-1 and S10D1

Thermocouple Location (see Figure 2-38)	System B-1 Temperature (°F)	System S10D1 Temperature (°F)	Identification
1	45	42	Pressure vessel – cover upper
2	45	40	Pressure vessel – cover middle
3	52	46	Pressure vessel – cover bottom
4	50	49	Pressure vessel – flange
5	50	44	Pressure vessel – body upper
6	43	42	Pressure vessel – body lower
7	43	44	Pressure vessel – body sphere upper
8	46	NI	Pressure vessel – body sphere middle
9	NI	43	Pressure vessel – body sphere bottom
10	46	45	Pressure vessel – power conditioner
11	65	78	Retaining ring – lower outer
12	65	80	Retaining ring – top outer
13	73	88	Retaining ring – top inner
14	75	99	Cold frame – outer
15	79	102	Cold frame – center
16	(out)	154	Neck tube – top
17	1285	1146	Heater block – side top
18	1437	1524	Heater block – bottom
19	1332	NI	Heater block – top edge
20	NI	1375	Heater block – top center
21	1276	NI	Emitter – edge
22	NI	1324	Emitter – center
23	1120	1102	Collector – edge
24	(out)	1060	Hot electrode – edge
24a	1091	1035	Hot electrode – center
25	179	132	Cold electrode – edge
25a	179	127	Cold electrode – center
26	115	111	Cold frame – center internal
27	39	41	Water – top
28	39	40	Water – middle
29	39	44	Water – bottom

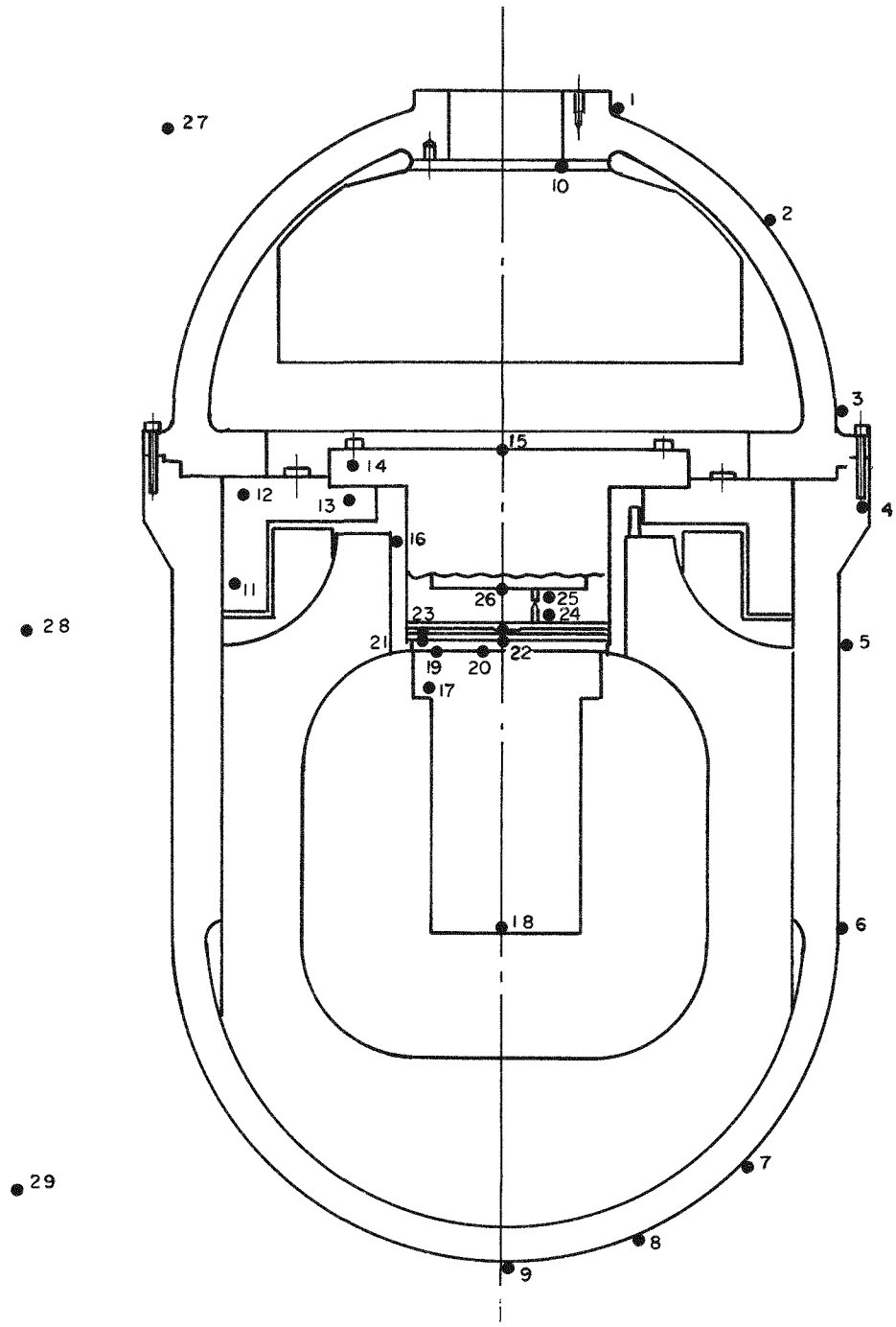

Figure 2-38. Thermocouple Location Points

Table 2-24. Electrical Comparison of Thermoelectric Generators, Systems B-1 and S10D1

Item	B-1	S10D1
Open Circuit Voltage	10.48 vdc	9.76 vdc
Primary Load Voltage	5.23 vdc	5.17 vdc
Primary Load Current	2.49 amps	2.86 amps
Internal Resistance	2.11 ohms	1.59 ohms
Total Power Output	13.02 watts	14.88 watts

Table 2-25 contains a summary of the electrical performance for both systems. The following comments can be made for the systems:

a) System S10D1 has a higher power output. This appears to be due to a larger power output from the thermoelectric generator.

b) As a result of the lower power output for System B-1, the efficiency of the system is slightly lower.

c) The power conditioner for System B-1 appears to have a higher efficiency than the power conditioner for S10D1. The exact cause for this is not known at this time.

In conclusion it appears that the BOL performance for S10D1 was better than the BOL performance for B-1. No attempt will be made to compare the performance vs. time characteristics for the systems due to the small amount of test time for S10D1.

2.4.4 QUALITY CONTROL

The Vendor Qualification Survey Team visited eight potential suppliers during this report period. The efforts of this group have resulted in a good cross-section of approved vendors available for use. Survey effort is now being focused on more specific product or parts needs. In keeping with this philosophy, source inspection

Table 2-25. Electrical Comparison of Systems B-1 and S10D1

Item	System	
	B-1	S10D1
System Power Input (Corrected)* (watts)	226	223.7
Generator Primary Load Voltage (vdc)	5.23	5.17
Generator Bias Load Voltage (vdc)	0.728	0.727
Generator Primary Load Current (amperes)	2.47	2.86
Generator Bias Load Current (amperes)	0.146	0.134
Generator Primary Power Output (watts)	12.92	14.80
Generator Bias Power Output (watts)	0.106	0.097
Generator Total Power Output (watts)	13.026	14.897
Conditioner Primary Voltage Input (vdc)	4.91	5.15
Conditioner Bias Voltage Input (vdc)	0.603	0.698
Conditioner Primary Current Input (amperes)	2.47	2.86
Conditioner Bias Current Input (amperes)	0.146	0.134
Conditioner Primary Power Input (watts)	12.10	14.71
Conditioner Bias Power Input (watts)	0.088	0.093
Conditioner Total Power Input (watts)	12.188	14.803
System Load Voltage (vdc)	24.0	24.0
System Load Current (amperes)	0.452	0.530
System Load (ohms)	53.1	45.3
System Power Output (Measured)* (watts)	10.84	12.72
Conditioner Efficiency (percent)	89.3	86.0
System Efficiency (percent)	4.8	5.7
Test Hours	1176	409

*Note: System power out is actual measured output, not corrected for instrumentation losses.

is being performed on the pressure vessel at Wyman Gordon and resurveys have been made at Vector Cable Company, receptacle supplier, and Linde Corporation, insulation system supplier. The Quality Plan of Linde Corporation was also approved.

A two-week surveillance inspection was performed at Linde Division, March 18 through 28. Intermittent surveillance for the rest of the program was subsequently recommended as a cost and time saving factor.

Surveillance at Linde concluded with a trip to National Lead, Albany, New York, (3/29/68) to establish tightened inspection controls as a result of un-noted discrepancies on National Lead inspection documents.

The SNAP-21 Quality Program Plan has been revised and reviewed by Space and Defense Products management. The final draft is complete and has been signed by appropriate managers and the Manager, Space and Defense Products Department. This document will be submitted to the AEC in the next reporting period.

Positioning and alignment of the legs in a thermopile has been one of the most difficult features to inspect on a thermoelectric module. This alignment must be held to a few thousandths of an inch, and many of the legs are effectively hidden within the thermopile, where normal inspection methods cannot be applied. This problem has been essentially overcome by the acquisition of a borescope. This instrument can be inserted into the pile and both ends of the legs individually inspected for correct positioning.

2.5 SAFETY ANALYSIS AND TESTING

2.5.1 RADIATION MEASUREMENTS, SYSTEM S10D1A

External radiation levels were determined in conjunction with the assembly and testing of System S10D1A at ORNL. The system was fueled with a 187-watt strontium titanate ($SrTiO_3$) heat source. Two sets of radiation measurements were taken. The first was done using a "cutie pie" survey meter and the second used personnel type film packs. The average radiation levels obtained are shown in Figure 2-39. Readings correspond to system surface and at one meter from

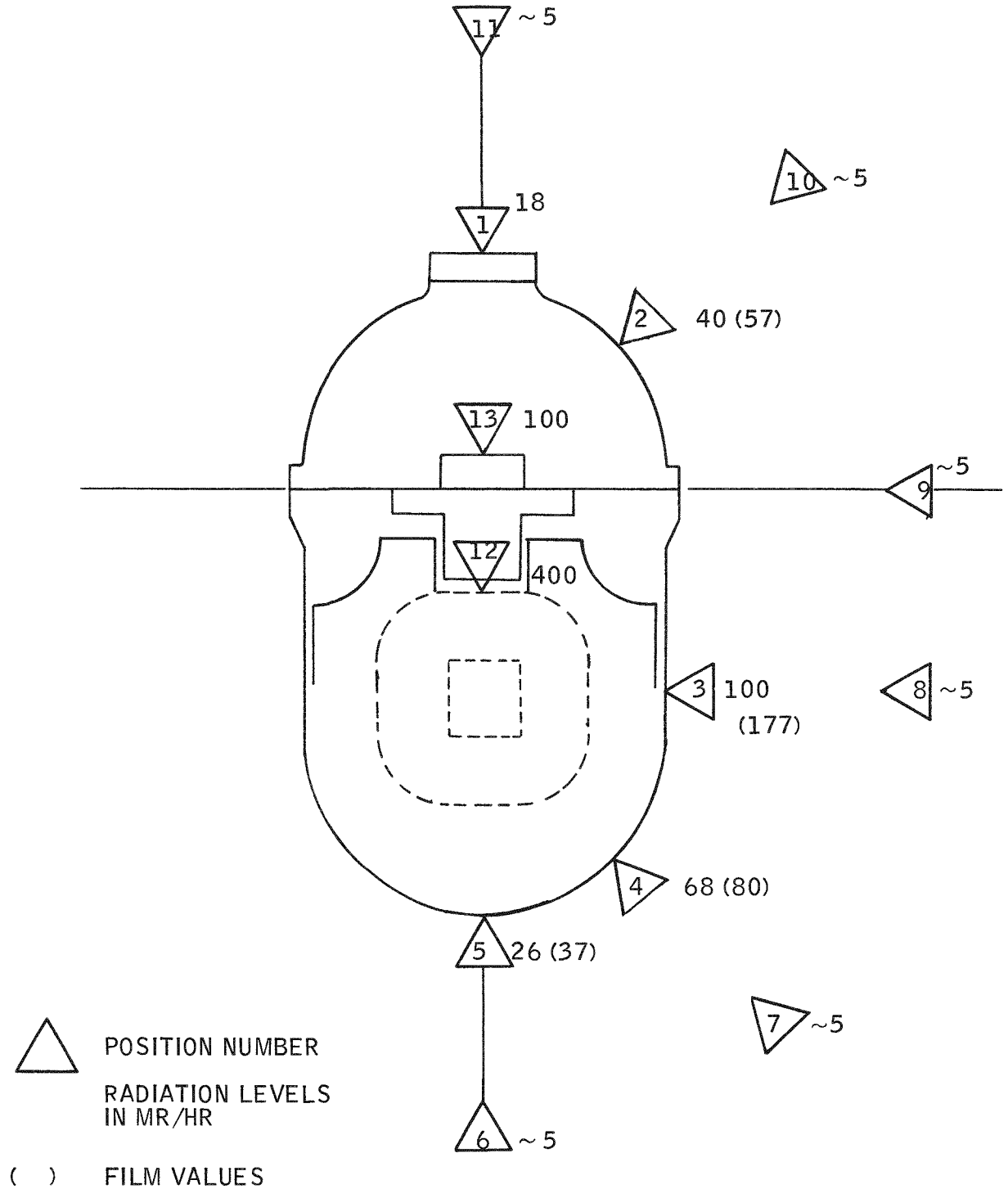

Figure 2-39. Radiation Measurements on Mock-Up System

the surface. Film packs were placed only at surface positions. The readings from the film were predictably higher than from the survey instrument since the centroid of the sensitive volume of the ionization chamber is about 2 inches further from the surface. The levels are well within the technical specification limits of 200 mr/hr at the surface and 10 mr/hr at one meter from the surface. The stainless steel pressure vessel used in this assembly is considered equivalent in shielding ability to the Berylco 165 alloy which will be used in the prototype systems.

2.5.2 ELECTRICALLY HEATED FUEL CAPSULES

On January 24, 1968, four electrically heated fuel capsules were implanted in the ocean off San Clemente Island. NRDL personnel were in charge of the implantment.

The operation was effected from a 70 foot by 25 foot barge on which a 10-ton converted crawler crane was mounted. The anchor for the test units was a 5000-pound block of concrete. The depth of the water at the point of implantment is 110 feet. Although the test plan states that the water depth will be 150 feet, the Navy limitation for divers is 130 feet. A location was chosen which was somewhat less than the maximum depth.

The power cable had previously been connected to the instrumentation panels in the trailer on shore and was spooled on a reel on the barge. As the barge left the pier, the power cable was payed out until the desired implantment location was reached. The crane then lifted the concrete anchor and swung it over the end of the barge. A one-inch diameter, 60-foot long wire rope pendant was attached to the anchor and to a buoy. Two of the capsules were temporarily attached to the anchor and one was attached to the cable six feet from the anchor. The anchor was lowered to a position where the fourth capsule could be attached to the cable ten feet from the top of the cable. The buoy, which has approximately 2300 pounds of buoyancy, was then attached to the end of the cable and the load was transferred from the crane to the barge hoist drum. Prior to placing the anchor on the bottom, the two divers went down to ensure that the cable was free of the anchor. When the anchor was lowered to the bottom the divers disconnected the hoist cable from the buoy, buried one capsule in six inches of bottom material and the other capsule on the

bottom. The divers then followed the cable back to the pier. The entire operation took 2-1/2 hours. The power was turned on at the trailer and everything worked satisfactorily.

Figure 2-40 shows the concrete anchor, the electrically heated fuel capsules attached to the pendant, and the buoy.

2.5.3 SYSTEM OCEAN EXPOSURE TESTS

Planning for system ocean exposure testing continued this quarter between 3M and NRDL. At a meeting on March 5, 1968, between 3M and NRDL personnel the details of the 3M/NRDL interface relative to the SNAP-21 system ocean testing were outlined. The areas of work covered were shipping container shipment, unit handling, implantment structure, generator performance data, system temperature data, data acquisition system, electrical receptacle and the test plan.

3M has prepared specifications for the shipping container. The job of design and fabrication will be subcontracted. The approximate size is approximately 5 feet x 5 feet x 5 feet. It will weigh between 1500 and 2000 pounds and will be capable of being lifted by a forklift truck or an overhead crane. The system will withstand a one-month shipping cycle with a maximum temperature of 130°F for four hours per day. For extended storage the maximum temperature is 95°F. There must be close supervision during any handling operation, since the unit in the shipping container will only attenuate a 3-inch flat drop and a 6-inch edge drop to the specified shock load of 6 g's.

Fins will be attached to the system inside the shipping container. There will be three fin sections on the system: one on the pressure vessel body, one on the flange portion and one on the pressure vessel cover. Each section will be constructed in segments and will be bolted together to form a complete ring.

The conceptual design of the implanted structure consists of four bars forming a cage around the system with support members contacting the system at the lower spherical surface and at the strain relief plug.

a) Anchor

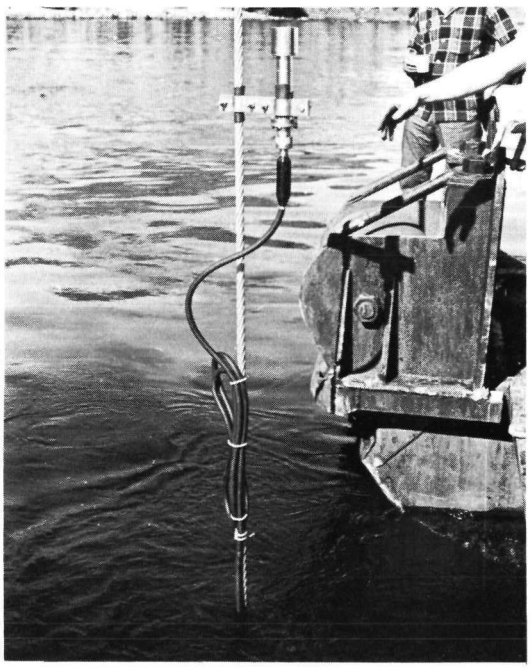

b) Electrically Heated Fuel Capsule Attached to Pendant

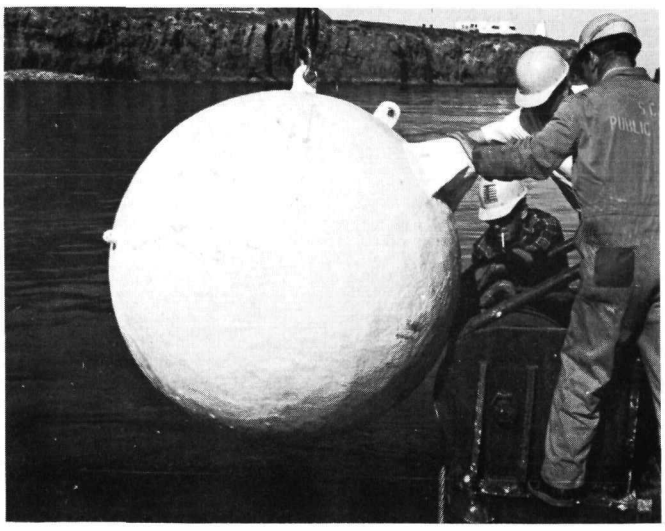

c) Buoy

Figure 2-40. Stages of Implantment of Electrically Heated Fuel Capsules for Sea Environment Testing

During transfer from the shipping container to the implantment structure, the unit would either have to be cooled or the implantment structure would have to be made to accommodate the unit with the fins attached. Details of this interface area will be defined during the next quarter.

A "maximum g" accelerometer and a recording thermometer will be provided with the systems. These will require monitoring and the charts on the temperature recorder will have to be changed at approximately one-week intervals. A thermoelectric checkout would be made at each point of termination of transportation.

The NRDL data acquisition system and the 3M instrumentation will be checked out at NRDL and at San Clemente Island.

There will be six type K thermocouples in the system. They will be distributed as shown in Table 2-26.

Table 2-26. SNAP-21 System Test Thermocouple Locations and Approximate Temperature Performance

Parameter	Thermocouple* Amount	Location	Range
Cold End			40°F-200°F 0.18 mv-3.82 mv**
Pressure Vessel	1	1	
Seg. Retaining Ring	1	2	
Cold Frame	1	3	
Hot End			1050°F-1350°F 23.4 mv-30.4 mv**
Hot Frame External	2	4, 5	
Emitter	1	6	

*Chromel-alumel sheath thermocouples

**Cold junction at 32°F reference

Table 2-27 shows the electrical parameters which will be monitored and the approximate electrical performance. The electrical performance values shown are based on data from the laboratory test of System S10D1 at a system load voltage of 24 volts, a water temperature of 40°F, a hot junction temperature of 1050°F and a cold junction temperature of 130°F.

Table 2-27. SNAP-21 System Test Electrical Parameters and Approximate Readings

Parameter	Symbol	Value (BOL)
System Power Output	P_{SO}	12.6 watts
System Load Voltage	V_{SL}	24.0 vdc
System Open Circuit Voltage	E_{SL}	9.7 vdc
System Shunt Voltage	V_{SR}	0.052 vdc
System Load Current	I_{SO}	0.53 amp
TEG Primary Power Output	P_{GP}	14.8 watts
TEG Primary Load Voltage	V_{GPL}	5.1 vdc
TEG Primary Open Circuit Voltage	E_{GPO}	9.7 vdc
TEG Primary Shunt Voltage	V_{GPR}	0.011 vdc
TEG Primary Load Current	I_P	2.85 amps
TEG Bias Power Output	P_{GB}	0.096 watt
TEG Bias Load Voltage	V_{GPL}	0.72 vdc
TEG Bias Open Circuit Voltage	E_{GBO}	1.5 vdc
TEG Bias Shunt Voltage	V_{GBR}	0.0067 vdc
Power Conditioner Back Bias (2.0v min)		3.0 vdc
Note: Pins 1 through 10 will be used for system electrical monitoring.		

The cable connecting plug that mates with the electrical receptacle will be blank and it will have to be machined by NRDL. The electrical and watertight connection to the cable will be the responsibility of NRDL. Marsh and Marine (the plug vendor) should be consulted before the plug is machined.

NRDL has been investigating data acquisition systems but as yet they have made no decision as to what system will be used. Various methods of interconnection between the system pressure vessel and the shore located data collection unit were discussed. NRDL would have preferred direct wires to data collection from the system. However, the long wire length would cause too much power loss to the bias circuit of the power conditioner, resulting in marginal operation. Temperature changes of the water will also cause resistance changes and this will result in data variations. This factor alone would make data evaluation precarious and affect normalization of data. This reasoning also applies to the power conditioner load circuit where the loop resistance of current carrying wires would be constantly changing the readout values.

Another method discussed was that of a combination junction and switching enclosure at the free socket end of the high pressure cable or with the enclosure bolted to the pressure vessel cover. The enclosure would contain high quality relays for the functions of reverse biasing to stop the power conditioner and open its load circuit. This method would require very short loop resistances, thereby producing much more accurate data. One drawback is the possibility of malfunction of switching components necessitating a pull-up of the system. Good components and a redundant circuit should provide long term operation expectancy. All electrical wires in the measurement circuit would be non-current conducting voltage taps, providing accurate measurement to the shore-based data system. It was tentatively agreed that this method would be used.

3M stated that it may be advantageous for NRDL to have individual modules to make up a special system. This is a long lead time item and the order will have to be placed as soon as possible.

A detailed test plan will be written for system testing. NRDL will write the plan but will work closely with 3M. The outline for the test plan which will be started in June will be distributed for review. A detailed implantment procedure will also be prepared by NRDL.

Because of the necessity of careful handling of the system during implantment, it was agreed that a simulated implantment should be done with an accelerometer attached to a dummy weight.

2.6 NAVSHIPS RESEARCH AND DEVELOPMENT 10 - COUPLE MODULES

2.6.1 ASSEMBLY

Assembly of the 10-couple modules has been delayed because of lack of acceptable cold frames from the NAVSHIPS R&D Center. Problems have been encountered in machining follower holes which will meet the concentricity and surface finish requirements.

Procedures for soldering ceramic headers into the cold base were completed. The procedure developed uses 157 flux and solder which gives a good bond between copper, stainless steel and copper.

All subassemblies for the first module have been assembled and are waiting for further assembly when a cold frame becomes available.

The 10-couple module test plan has been revised to incorporate the comments of the AEC.

3.0 TASK II – 20-WATT SYSTEM

No effort was expended on this subtask during this report period.

4.0 EFFORT PLANNED NEXT QUARTER

The following items are planned for the next quarter:

- Start and complete system integration of Systems S10D2 and S10D3.
- Begin system tests of System S10D2 (short-term performance, shock and vibration to specification levels, hydro test to specification level, shipping container thermal test and long-term performance).
- Complete fuel pellet preparation.
- Fabricate remainder of fuel capsule components and ship to Oak Ridge National Laboratory for calorimetry, fueling and welding.
- Complete biological shield isothermal test.
- Remainder of biological shields will be completed by National Lead.
- Complete the evaluation of Insulation System 10D4 dynamic test results.
- Begin assembly on remainder of insulation systems.
- Berylco to complete components for three pressure vessels (two covers, three bodies) and deliver to 3M.
- Complete fabrication of the remainder of the segmented retaining rings.
- Complete assembly of thermoelectric generators A10D8 and A10P1.
- Complete assembly and process of remaining Task I 10-watt power conditioners.

- Complete electrical receptacle and strain relief plug assembly for Systems S10D2 and S10D3.
- A purchase order will be let for fabrication and delivery of four shipping containers.

APPENDIX A
CALCULATION OF COOLING FIN REQUIREMENTS FOR SNAP-21 SYSTEM DURING SHIPMENT

GENERAL

During handling, shipping and storage, the SNAP-21 System must reject the decay heat from its radioisotope fuel to an air environment that can reach temperatures of +130°F.

This appendix presents the calculations used to determine the size and number of fins required to dissipate this heat without overheating the system. The actual solution was a trial-and-error type solution which required several iterations; however, only the final set of calculations is presented.

The method used to determine the fin geometry and quantity was taken from a paper by J. G. Bartas and J. N. Shinn, Predicting the Performance of Free-Convection Air Heat Exchanges, ASME 62-HT-7. Reference to equation numbers in this appendix will be to equations from this reference.

ANALYSIS

The mode of heat transfer between the cooling fins and circulating air is free convection. This requires that the shell and shipping container provide openings for an adequate amount of air flow to cool the system. This air flow is illustrated in Figure 4-1.

Simplifying assumptions were used for some of the parameters used in the analysis; however, they were always made in a manner that would provide some conservation in the analysis.

1. Calculations

a. Data used as a baseline for the cooling fin design:

1) Total amount of heat (~BOL Fuel Loading);

q_T = 225 watts

= 768 BTU/Hr

2) Temperature of air outside the shipping container;

t_a = 130°F

3) Temperature of the cooling fin base;

$t_{F.B.}$ = 160°F

4) Thermal conductivity of the fin material;

k_M = 100 BTU/Hr - °F - ft.

5) Vertical fin height (the length that is parallel to the air flow);

H = 13.0 in. = 1.08 ft.

6) Fin length (the length that is perpendicular to the air flow);

1 = 4.0 in. = 0.333 ft.

b. Dissipation capacity of the unfinned surface of the system:

1) Estimated projected surface area;

$A_{UF.S.} = \pi (d) (H)$

$= \pi (1.25) (1.08) = 4.25 \text{ ft.}^2$

2) Heat transfer coefficient of the unfinned surface for air at standard conditions;

$h_\infty = 0.28 (\Delta t/H)^{1/4}$

$= 0.28 (160-130/1.08)^{1/4}$

$= 0.64 \text{ BTU/Hr - °F - ft.}^2$

3) Amount of heat dissipated;

$$q_{UF.S.} = h_{\infty} A_{UF.S.} \Delta t$$
$$= 0.64\ (4.25)\ (30)$$
$$= 81.5\ \text{BTU/Hr.}$$
$$= 23.9\ \text{watts}$$

The graphs contained in the previously mentioned paper show the fin thickness, spacing and effectiveness as a function of $\ell\ (\Delta t/H)^{1/4}$. So, let

$$r = 1\ (\Delta t/H)^{1/4}$$
$$= 0.333\ (30/1.083)^{1/4}$$
$$= 0.762$$

c. Dissipation capacity of fins when on the system:

1) Determine fin multipler (effectiveness);

(From Figure 17)

$$M = 10.5$$

2) Amount of heat dissipated;

$$q_{F.S.} = M\ q_{UF.S.}$$
$$= 10.5\ (81.5)$$
$$= 856\ \text{BTU/hr}$$
$$= 250\ \text{watts}$$

d. Thickness of the fins; (From Figure 18)

$$\frac{b}{l} = 0.0093$$

$$b = 0.0093\ (0.333) = 0.0031\ \text{ft.} - 0.026\ \text{in.}$$

e. Spacing of the fins; (From Figure 19)

$$S = 0.09$$

$$a = \frac{b}{S} - b$$

$$= \frac{0.0031}{0.09} - 0.0031 = 0.0313 \text{ ft.} - 0.261 \text{ in.}$$

f. Number of fins around the system;

$$N = \frac{\text{System Circumference}}{\text{Length per fin}}$$

$$= \frac{(15)\,\pi}{0.261 + 0.026}$$

$$= 164 \text{ Fins}$$

SUMMARY

Comparison of the results (225 watts vs. 250 watts) indicates the design should be adequate to dissipate the heat from the system. Several items may tend to reduce the safety margin. One is that the air surrounding the shipping container can be at +130°F with the air entering the shell warmer. Another item is that several fins must be omitted to provide space for the lifting equipment or bolts used to join the fin sections together. This would tend to reduce the capacity of the fins. A practical lower limit on the spacing of fins is approximately 0.25 inch which yields a total of 180 fins. This increase, from 164 fins, would reduce the effects of the lowered capacity without greatly increasing the manufacturing problems.

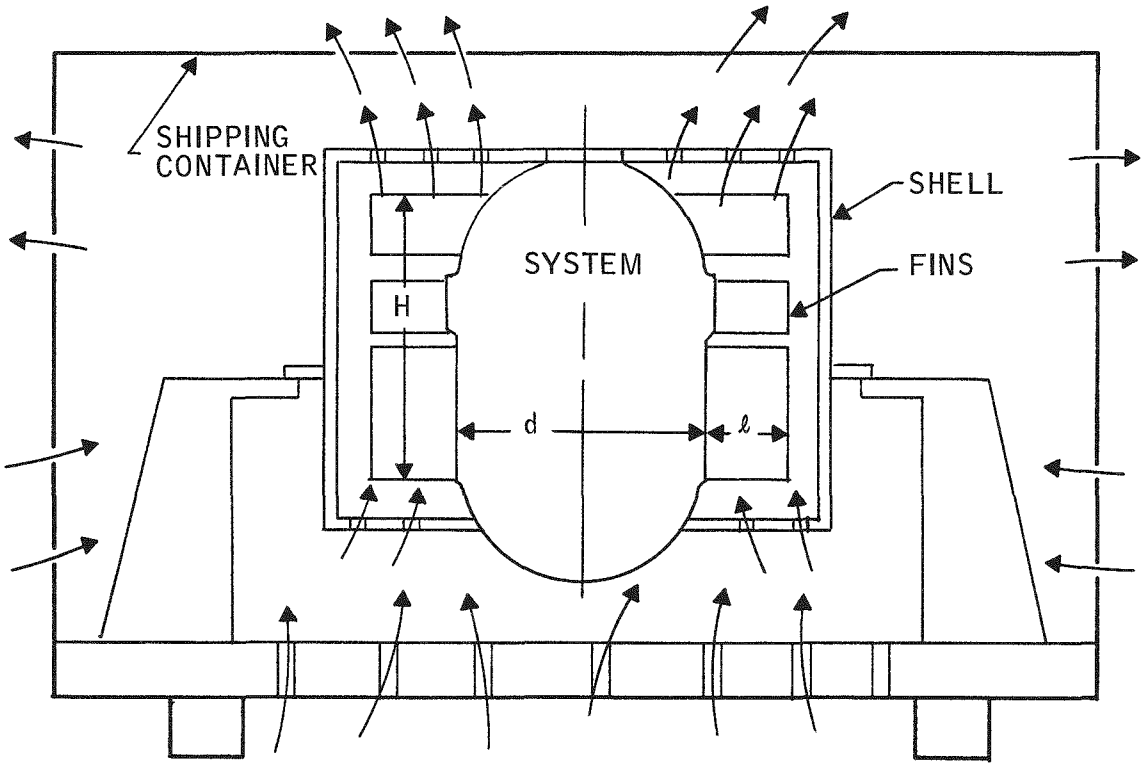

Figure A-1. Air Circulation Within and Through the Shipping Container

APPENDIX B
SHOCK AND VIBRATION TEST REPORT

UNIVERSAL REPORT NO. _____

ORIGINATORS REPORT NO. 6B18-2

REVISION _____

REPORT OF TEST ON

MODEL A HTVIS
S/N 10-D1

TEST PERFORMED BY Ogden Technology Laboratories, Inc.

TEST AUTHORIZED BY LINDE DIVISION, UNION CARBIDE CORP.

CONTRACT NUMBER _____

PURCHASE ORDER NUMBER 825-L-44899

OTL JOB NUMBER 7503

	Date	Signature	
Test Initiated			
Test Completed	1/11/68		
Report Written By	2/2/68	H. Golinger	H.Golinger
Technician			
Test Engineer	2/2/68	H. Golinger	H.Golinger
Supervisor Chief Engr.	2/2/68	A. Helfand	A.Helfand
Supervisor			
Quality Assurance	2/2/68	W Hall	W.Hall
Government Repr. (if applicable)			
Final Release			

TABLE OF CONTENTS

Notices

When Government drawings, specifications or other data are used for any purpose other than in connection with a definitely related Government procurement operation, the United States Government thereby incurs no responsibility nor any obligation whatsoever; and the fact that the Government may have in any way formulated, furnished, or supplied the said drawings, specifications, or other data, is not to be regarded by implication or otherwise as in any manner licensing the holder or any other person or corporation of conveying any rights or permission to manufacture, use, or sell any patented invention that may in any way be related thereto.

ADMINISTRATIVE DATA

TEST REPORT: 6B18-2

TEST CONDUCTED: Vibration, Shock and Shock to Failure Tests

MANUFACTURER: Union Carbide Corporation
Linde Carbide Corporation
P.O. Box 152
Tonawanda, New York

MANUFACTURER'S TYPE OR MODEL NO.:
Model A HTVIS
S/N 10-D1

DRAWING, SPECIFICATION OR EXHIBIT: Development Test Plans-UCC-Linde Div.
Dynamic Vibration Test dated 3/23/67
Dynamic Shock Test dated 3/23/67
Dynamic Shock Test to Failure dated 6/26/67

QUANTITY OF ITEMS TESTED:
One (1) unit

SECURITY CLASSIFICATION OF ITEMS: Unclassified

DATE TEST COMPLETED: 11 January 1968

TEST CONDUCTED BY: Ogden Technology Laboratories, Inc.

DISPOSITION OF SPECIMENS: Returned to Linde Division, Union Carbide Corp.

DATE OF TEST REPORT: 2 February 1968

MANUFACTURER'S PURCHASE ORDER NO.: 825-L-44899

ABSTRACT:
Refer to Para. 4.0 "Test Results"

1.0 TEST EQUIPMENT

a. Leak Detector
Veeco
Model: MS-9
Calibration Interval: Annually
Last: 11/29/67

b. Leak Indicator
Veeco
Model: MS-9 Related
Calibration: None required

c. Sensitivity Calibrator
Veeco
Model:SC-4
Calibration Interval: Annually
Last: September 67

d. Vibration Exciter
Ling Electronics
Model: 275
Calibration: None required

e. Power Amplifier
M. B. Electronics
Model: T-995
Calibration: None required

f. Automatic Vibration Exciter Controller
Bruel & Kjaer
Model: 1015
Calibration Interval: Prior to use
Last: 12/18/67

g. Signal Conditioning Amplifiers (2)
Unholtz-Dickie Corp.
Model: 607-RMG-3
Calibration Interval: Prior to use
Last: 12/18/67

h. Accelerometers (4)
Columbia Research Labs.
Model: 902 S/N's: 133,135,139 and 156
Calibration Interval: 6 months
Last: 9/6/67

i. Oscillograph Recorder
Consolidated Electrodynamics Corp.
Model: 5-124A
Calibration Interval: Prior to use
Last: 12/18/67

j. Multi Meter
Vancos
Model: EMA
Calibration Interval: 6 months
Last: 11/27/67

k. Oscillograph
Midwestern
Model: 621HT
Calibration: Before each use

l. Vibration Exciter
M. B. Electronics
Model: C200
Calibration: None required

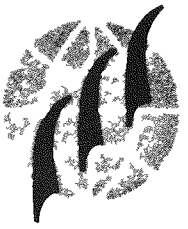

m. Power Amplifier
M. B. Electronics
Model: T999
Calibration: None required

n. Oscilloscope
Tektronix
Model: RM32
Calibration Interval: 6 months
Last: 12/20/67

o. Cathode Follower
Columbia Research Labs.
Model: 4000
Calibration Interval: 6 months
Last: 12/12/67

p. Waveform Synthesizer
Exact
Model: 200 "D"
Calibration: Before each use

q. Scope Camera
Dumont
Model: 5B52
Calibration: None required

r. Bridging Transformer
Hewlett-Packard
Model: 110 A
Calibration: None required

s. Isolation Transformer
Sorenson
Model: MVR250
Calibration: None required

t. Voltage Regulator
Sola
Model: 5005
Calibration: None required

u. Variac
General Radio
Model: 100R
Calibration: None required

v. Shunt (10a)
Weston
Model: 430
Calibration: Annually
Last: 11/27/67

All instrumentation and equipment calibration is conducted in accordance with Specification MIL-Q-9858A as further defined in MIL-C-45662A "Calibration System Requirements" and is traceable to the National Bureau of Standards.

2.0 TEST SEQUENCE

2.1 Leak Testing

2.2 Dynamic Vibration Test

2.3 Dynamic Shock Test

2.4 Dynamic Shock Test to Failure

2.5 Supplemental Vibration Testing

3.0 TEST PROCEDURE

3.1 Leak Detection Procedure

1. The test enclosure was evacuated below 10 u pressure with the leak detector vacuum pump and the leak detector scale zeroed.
2. The standard Veeco leak unit was opened into the system and the value of the standard leak was recorded.
3. The standard leak unit was then valved off from the system and observation of the detector scale returning to zero was noted.
4. The leak detector was then connected to the HTVIS with a copper line valved off at the unit. The line was evacuated to approximately 1×10^{-6} mm. Hg.
5. The line was then leak tested with helium to ensure that no leaks existed between the leak detector and the valve.

6. The unit valve was then opened and the steady state background was recorded.

7. The area to be leak tested was then enclosed in a plastic shroud containing helium at atmospheric pressure.

8. The steady state value of the scale reading was recorded after which the plastic shroud was removed and the leak detector was valved off.

9. The leak rate was calculated as follows:

$$\text{Leak Rate } \frac{\text{std-cm}^3}{\text{sec}} = \frac{\text{Steady state detector scale reading (unit)}}{\text{Standard leak detector scale reading (unit)}} \times \text{Value of standard leak } \left(\frac{\text{std-cm}^3}{\text{sec.}}\right)$$

Note: The background noted in Step 6 (above) was subtracted from the steady state detector scale reading.

3.2 Dynamic Vibration Test

The HTVIS unit was subjected to the vibration testing with the nuclear radiation shield at operating temperature (+1285^{o}F). The heat was supplied by the test heaters, (250 watts, 2 amps, 120 volts max) imbedded in the heater block located at the bottom section of the neck tube. The heater block and the heater was securely located in the neck tube during the entire vibration test.

A schematic of the HTVIS unit and instrumentation setup is presented in Figure 1.

The test unit was positioned as shown in Figure 2. The test load was positioned uniformly on the exciter in order to minimize the effects of unbalanced loads. The vibration environment specified herein was applied to each of the three (3) mutually perpendicular axes of the unit (vertical, horizontal and in a position turned 90^{o} from the horizontal position). The acceleration

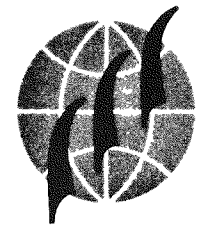

levels along each axis were measured by accelerometers mounted on the unit during each test sequence.

The vibration test schedule was applied to the unit as indicated herein.

TABLE I

Frequency (Hz.)	Amplitude
5 - 8	0.4" d.a.
8 - 26	± 1.3 g
26 - 40.5	0.036" d.a.
40.5 - 50	± 3 g

The cycling rate was logarithmic and such that the frequency range of 5 to 50 Hz and return to 5 Hz. was traversed in 15 minutes.

A helium leak test was performed in accordance with the procedure noted in Paragraph 3.1 (herein) after installation of the unit in the test fixture.

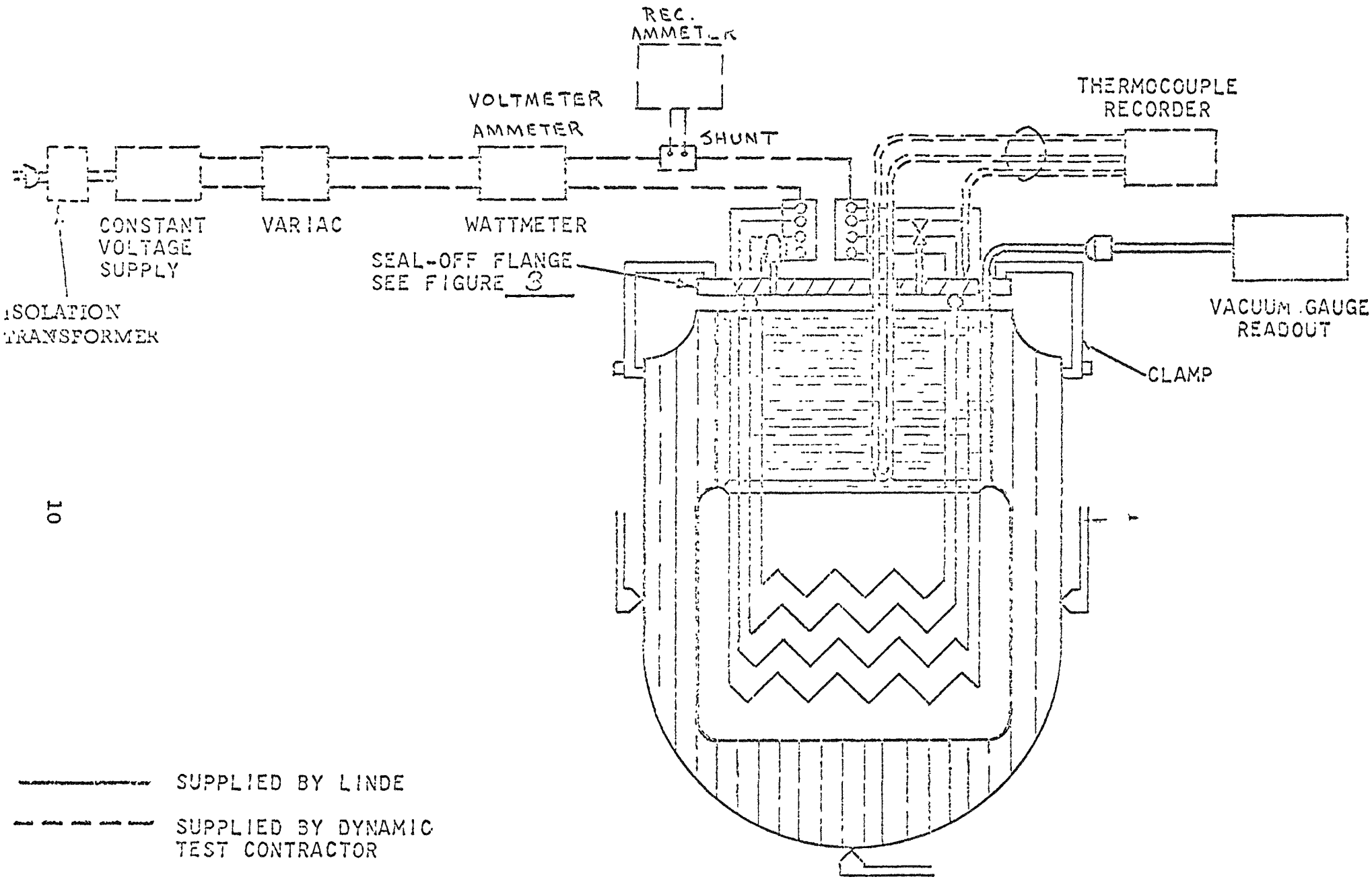

SCHEMATIC OF INSTRUMENTATION FOR DYNAMIC VIBRATION TEST

FIGURE 1.

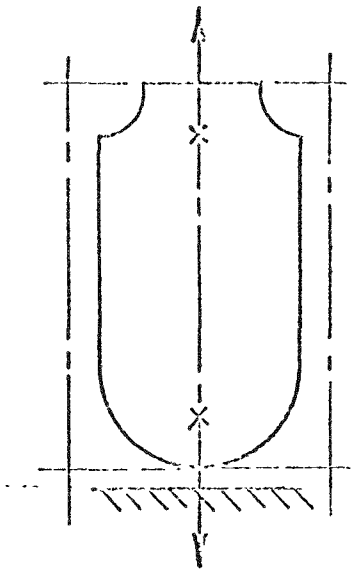

POSITION-A

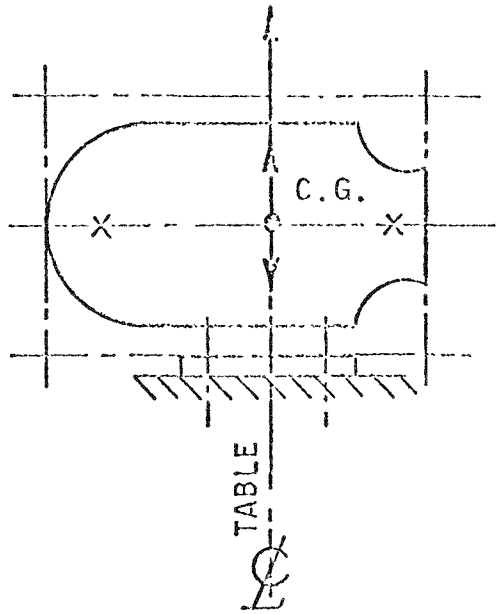

POSITION-B

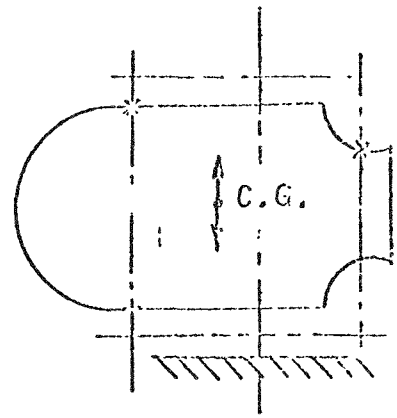

POSITION-C
ROTATED 90°
FROM POSITION B

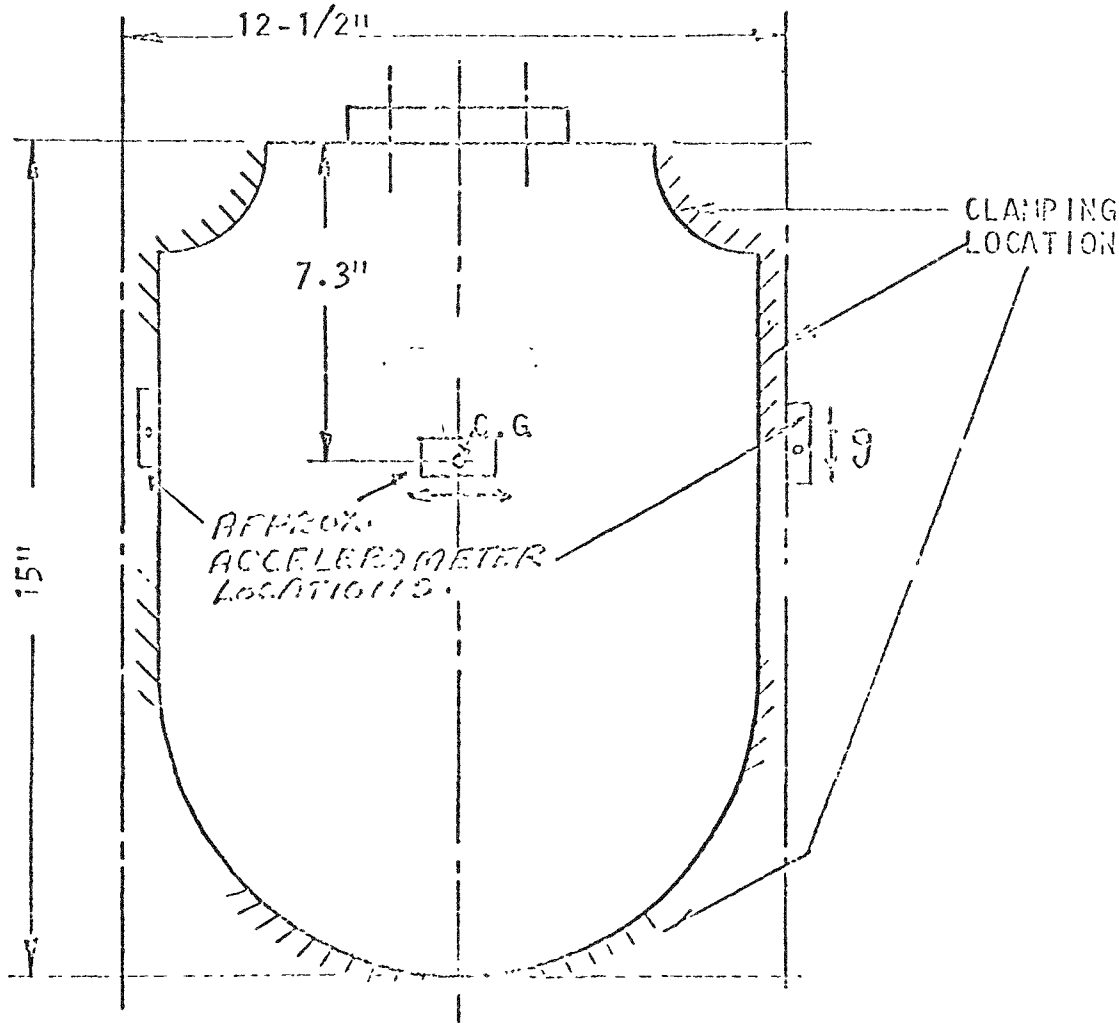

SCHEMATIC POSITION OF VIBRATION
SET UP

FIGURE - 2

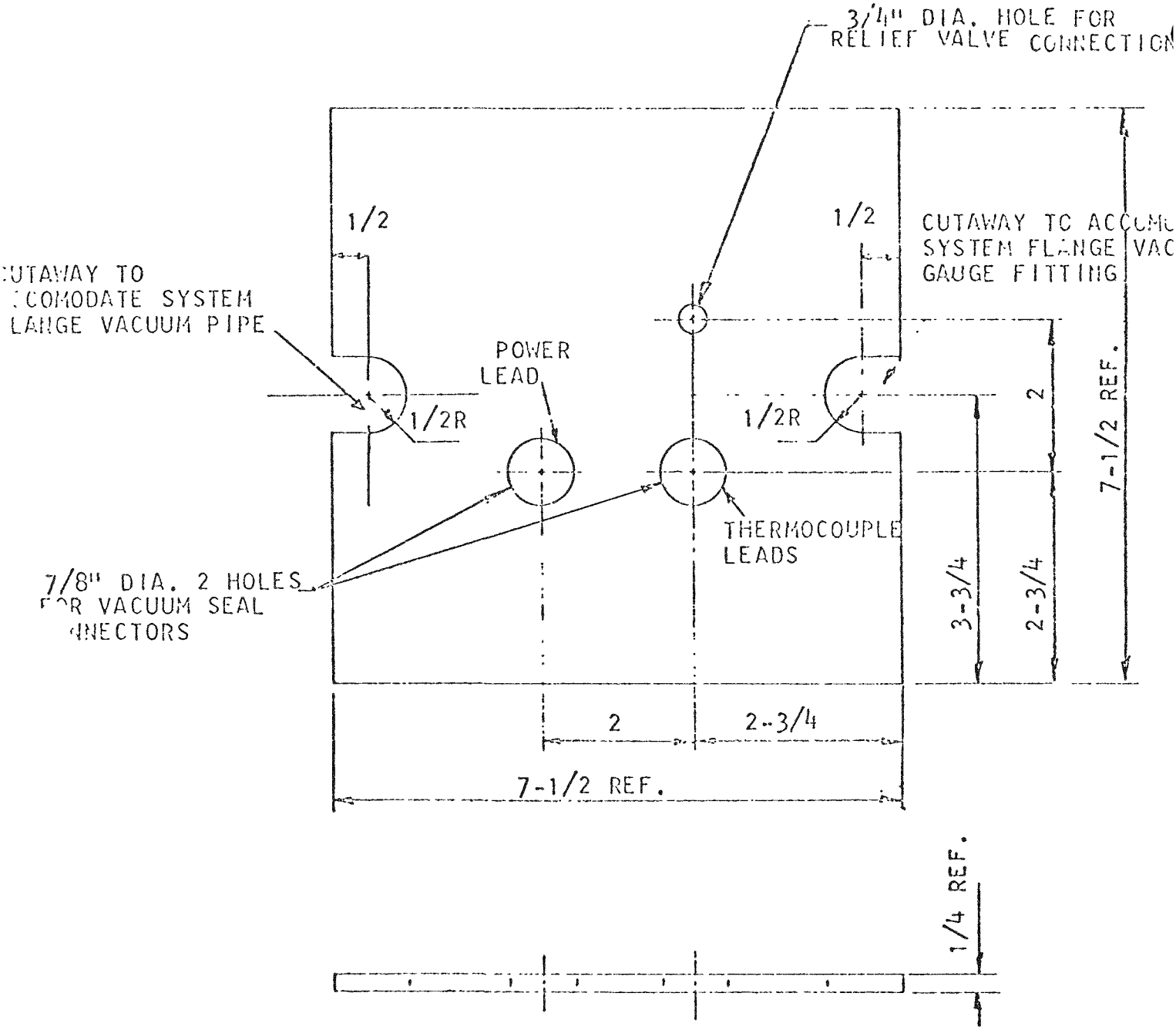

MATERIAL

PLATE, 1/4" THK. TYPE 304 STAINLESS
STEEL, 7-1/2" X 7-1/2"

SCHEMATIC SEAL-OFF FLANGE

FIGURE - 3

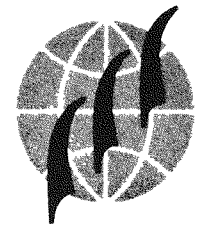

The throat section of the neck tube (see Figure 1) was brought to a steady state temperature of +1285°F. (50 watts input for 24 hours, increased to 70 watts for approximately 70 hours.) During this time, temperatures T_1 through T_7 and the vacuum level were monitored periodically. During vibration testing, the vacuum was continuously monitored as the loss of vacuum was regarded as a barometer of failure.

1. The unit was secured for testing and a low level sinusoidal survey sweep (0.5 g) was performed for one (1) axis of vibration.
2. At the completion of the sweep, Linde personnel recorded temperatures (T_1 through T_7) and vacuum readings every 10 minutes for a period of ½ hour. The power input to the heater was maintained at the original level during the ½ hour observation period.

3. The unit was then subjected to the first 15 minute vibration sweep per Table I.
4. Step 2 was then repeated.
5. The unit was then subjected to the second 15 minute vibration sweep.
6. Step 2 was then repeated.
7. The unit was then subjected to the third 15 minute vibration sweep thereby completing the testing in the first axis.
8. The helium leak test was then performed per paragraph 3.1 and the pressure rise in an argon atmosphere was observed every 30 minutes for a four-hour period.
9. This procedure (Steps 1 through 8) was repeated for the two (2) other test axes.
10. For each axis of testing, the temperature and vacuum of the test unit was recorded in its mounted position and the throat section of the neck tube was brought to a steady state temperature of +1285^{o}F. prior to any vibration testing.

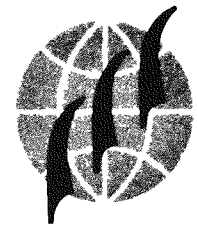

3.3 Dynamic Shock Test

The HTVIS was subjected to shock testing while at operating temperature. The same fixturing concept as utilized for the vibration testing was also employed for the shock testing. The instrumentation was identical to that previously noted and referenced as Figure 1. Failure of the system was determined by a specified change in the vacuum reading of the insulation system. Three (3) shocks in each direction were applied along the three (3) mutually perpendicular axes of the test unit (18 shocks total). The calibration shock pulse was in accordance with Figure 516-1, of MIL-STD-810A (included herein as Figure 4 for reference) with a peak value (A) of 6g and a nominal duration of 6 milliseconds. The instrumentation included the accelerometers located in each of the three (3) axes referenced in Figure 2.

1. A simulated dummy mass was calibrated to produce the specified shock loading.

2. The dummy mass was removed and the test unit was securely mounted to the vibration exciter and subjected to the shock test in both directions along an axis.
3. Vacuum, temperature and power input were then recorded every 30 minutes. The leak test of paragraph 3.1 was performed.
4. The shock pulse was then calibrated for a second axis utilizing the dummy mass.
5. Steps 2 and 3 were repeated.
6. The shock pulse was then calibrated for the third axis utilizing the dummy mass.
7. Steps 2 and 3 were repeated.

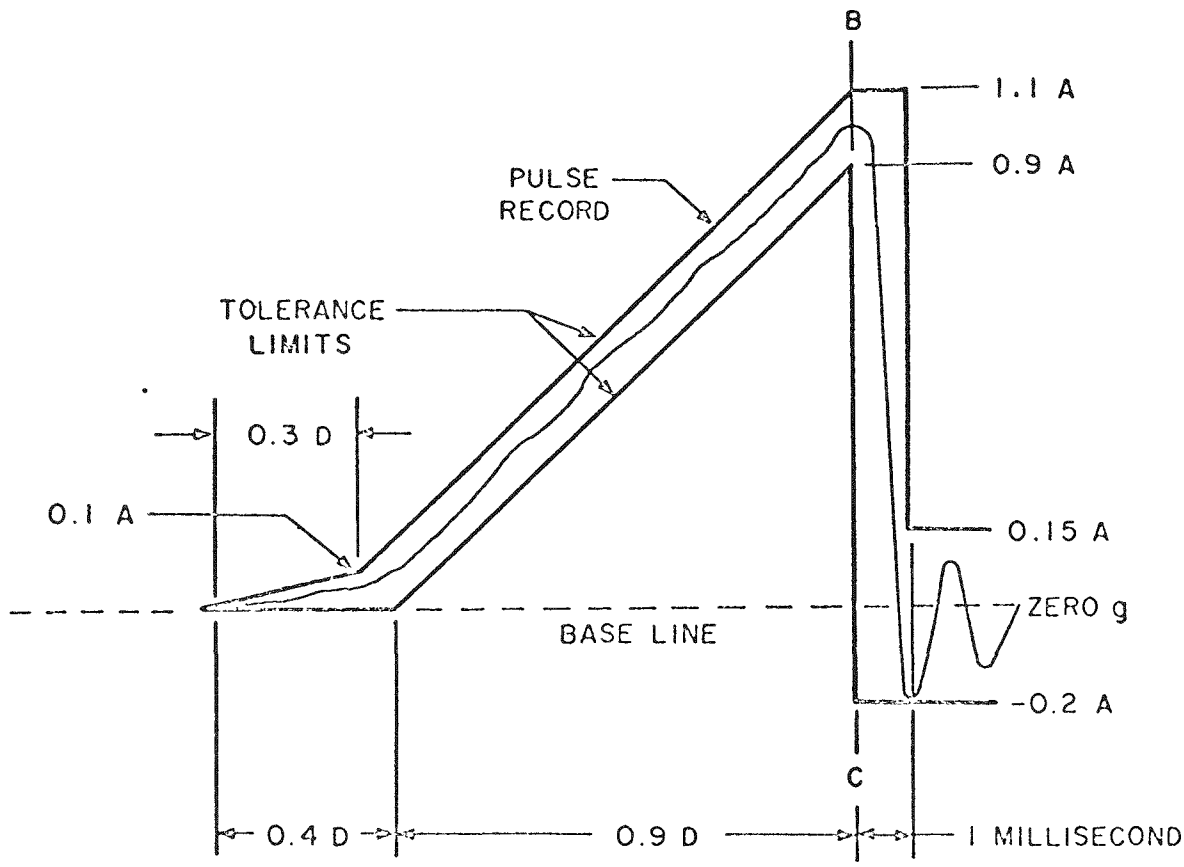

D = NOMINAL DURATION IN MILLISECONDS

A = SPECIFIED PEAK ACCELERATION IN GRAVITIES (g'S)

g = ACCELERATION OF GRAVITY ON EARTH 386 IN./SEC./SEC.

FIGURE 4

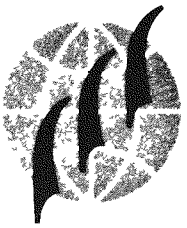

3.4 Dynamic Shock Test to Failure

The dynamic shock test to failure was performed on the HTVIS unit in only one (1) axis chosen by the cognizant Linde representative as the weakest condition of the test unit.

Utilizing the identical fixturing concept as applied in Para. 3.2, the shock test to failure was conducted in accordance with the following schedule:

Test No.	No. of Blows	Peak Value of Shock Level	Nominal Duration
I	6	6 g's	6 m.s.
II	6	7.5 g's	6 m.s.
III	6	9 g's	6 m.s.
IV	6	10.5 g's	6 m.s.
V	6	12.0 g's	6 m.s.

The helium leak test as described in Para. 3.1 was performed at the completion of each of the 5 steps above with the exception of the 10.5g test (Test IV).

3.5 Supplemental Vibration Testing

At the completion of the 12.0 g shock testing, an additional vibration test in the same axis as that utilized for the Shock Test to Failure was performed in the same manner as described in Paragraph 3.2 in accordance with the following table:

TABLE II

Frequency (Hz.)	Amplitude
5 - 8	0.4" d.a.
8 - 21	± 1.3 g
21 - 40	0.055" d.a.
40 - 50	± 4.5 g

At the completion of this sweep, the Linde representative performed the standard vacuum check.

4.0 TEST RESULTS

4.1 Leak Testing

a. The computed leak rate for all leak testing performed is presented in tabulated format in Appendix A - Test Data.

b. See Appendix B - Photographs

4.2 Dynamic Vibration Testing

a. X-Axis Testing

1. 0.5 G Survey - No significant resonances were observed throughout the test frequency range.

2. No damage was observed at the completion of the test.

3. See Appendix A - Test Data for leak test data

4. See Appendix B - Photographs

b. Y-Axis Testing

1. The final location for the control accelerometer was chosen on the side plate near the neck end of the unit after several surveys .

2. 0.5 G Survey - No significant resonances were observed throughout the test frequency range.
3. No damage was observed at the completion of the test.
4. See Appendix A - Test Data for leak test data.
5. See Appendix B - Photographs

c. Z-Axis

1. 0.5 G Survey - No significant resonances were observed throughout the test frequency range.
2. No damage was observed at the completion of the test.
3. See Appendix A - Test Data for leak test data.
4. See Appendix B - Photographs

4.3 Dynamic Shock Testing

a. All data as analyzed from the oscillograph records is presented in tabulated format in Appendix A, Test Data.

b. In many cases, the noise produced as a result of the shock input prevented an accurate analysis of the shock loading on the unit.

c. The leak test data is presented in Appendix A.

d. Appendix C contains the poloroid photographs recorded of the shock pulses.

Note: In some cases, the poloroid photos were unusable. Notations are included with the photographs when this situation occurred.

e. No damage was observed at the completion of this test.

4.4 Dynamic Shock Test to Failure

a. All data as analyzed from the oscillograph records is presented in tabulated format in Appendix A, Test Data.

b. Several records and photographs were retained by the Linde representative witnessing the test. Those items which were taken are so noted in the tabulation of the analyzed data presented in Appendix A.

c. A leak test was not performed following the 10.5 g test level per instructions of the Linde representative.

d. No damage was observed at the completion of this test.

e. The leak test data is presented in Appendix A.

f. The shock test photographs are presented in Appendix D.

4.5 Supplemental Vibration Testing

a. At the completion of this sweep, the test unit failed to meet the vacuum requirement and thus concluded all testing on this unit.

Notes to Test Results

1. All test data as regards thermocouple data, vacuum data, voltage current and wattage data, other than that presented in Appendix A was recorded and retained by the cognizant Linde representative witnessing the test.
2. All oscillograph records have been forwarded under separate cover.

5.0 RECOMMENDATIONS

None. Test results contained herein are submitted for your evaluation.

APPENDIX A

Test Data

DATA SHEETS

Ogden Technology Laboratories, Inc.

Job Number: 7503 | Engineer: Galinger
Test: Dynamic Testing | Unit Part No: H.T.V.1.S
Test Technician: A. Lavigne | Unit Serial No: 10-D1
Date Photo Taken: --- | Date 12-6-67

Date	Time	Voltage (Volts)	Current (Amps)	Power (Watts)
12-6-7	1800	16.0	2.8	50
12-7-7	1600	21.0	3.3	70
12-7-7	2400	21.0	3.3	70
12-8-7	0800	21.0	3.25	70
12-8-7	1530	26.0	3.9	100
12-9-7	0800	26.0	3.8	100
12-9-7	1800	26.0	3.9	100
12-10-7	1100	25.5	3.8	97
12-11-7	0800	25.5	3.8	97
12-11-7	1530	36.5	5.45	200
12-11-7	1730	31.0	4.7	150
12-12-7	0800	27.2	4.05	110
12-13-7	0800	28.0	4.2	118
12-13-7	1700	28.5	4.2	120
12-14-7	0800	28.0	4.2	118
12-15-7	0800	24.5	3.6	90
12-15-7	1700	26.5	3.9	105
12-19-7	0900	19.0	2.7	50
12-19-7	0900	25.7	3.85	100
12-20-7	0820	26.0	3.8	100
12-20-7	1700	26.5	3.87	103

Note: All other data was recorded by the equipment build representative in a personal log/Record Book. The data [illegible]

DATA SHEETS

Ogden Technology Laboratories, Inc.

Job Number: 7503 | Engineer: Golinger
Test: Dynamic Testing | Unit Part No: H.T.V.I.S.
Test Technician: A. Lavigne | Unit Serial No: 10-D1
Date Photo Taken: — | Date 12-7-67

Date	Time	T1	T2	T3	T4	T5	T6	T7
		Temperature Thermocouples						
12-7-7	2400	455	462	78	75	87	77	
12-8-7	0800	570	574	82	75	93	80	
12-8-7	1700	690	695	84	75	95	80	
12-9-7	0800	910	925	88	75	108	88	
12-9-7	1800	1010	1030	93	78	115	94	
12-10-7	1100	1060	1095	95	80	120	98	
12-11-7	0800	1190	1200	98	83	125	105	
12-11-7	1530	1220	1238	92	82	90	108	
12-11-7	1730	1265	1275	95	83	90	108	
12-11-7	2030	1275	1265	95	84	94	108	
12-11-7	2330	1285	1290	95	84	96	108	
12-12-7	0230	1295	1300	95	85	98	110	
12-12-7	0800	1330	1340	98	86	100	115	
12-12-7	2245	1285	1300	105	82	135	110	
12-13-7	0830	1295	1302	115	85	180	115	
12-13-7	1700	1305	1320	102	83	183	112	
12-14-7	0800	1305	1313	108	85	145	115	
12-15-7	0800	1290	1300	110	85	150	115	
12-15-7	1700	1290	1300	110	85	158	113	
12-17-7	0900	1310	1325	105	80	155	110	
12-19-7	0900	1280	1295	115	88	165	115	
12-20-7	0830	1280	1300	104	80	155	116	
12-20-7	1700	1289	1300	107	82	158	118	

T7 (written vertically): Thermocouple [illegible] so No Data

Note: All other data was recorded by the equipment [illegible] representative in a permanent log/record book. The data herein was re-copied into that record.

UAL/ENG/1

OGDEN TECHNOLOGY LABORATORIES, INC. **DATA SHEETS**

United Aerotest Laboratories, Inc.

Job Number: 7508 Engineer: H. Golinger

Test: LEAK TESTING Unit Part No: Model A IITVIS

Test Technician: N. Sexton Unit Serial No: 10-D1

Date Photo Taken: 12-14-67 DATE 12-14-67

Test Condition	A Steady State Reading (div)	B Std. Leak Reading (div)	C Value of Standard Leak (atm cc/sec)	Leak Rate [illegible] atm cc/sec = A/B × C	
Initial	9.02	2.65	2.2×10^-8	12-14-67	7.4668 ×10^-8
Post X Vib	3.05	4.9	2.2×10^-8	12-19-67	1.3694 ×10^-8
Post Y Vib	5.2	5.8	2.2×10^-8	12-20-67	1.9784 ×10^-8
Post Z Vib	7.1	4.2	2.2×10^-8	12-21-67	3.719 ×10^-8
Post Z Shock	6.25	4.8	2.2×10^-8	12-26-67	2.8644 ×10^-8
Post Y Shock	6.1	4.0	2.2×10^-8	12-27-67	3.355 ×10^-8
Post X Shock	6.94	4.3	2.2×10^-8	12-28-67	3.5507 ×10^-8
Post 7½ G	2.38	3.2	2.2×10^-8	1-10-68	1.6363 ×10^-8
Post 9 G	2.3	2.8	2.2×10^-8	1-10-68	1.8071 ×10^-8
Post 12 G	3.06	2.8	2.2×10^-8	1-11-68	2.4043 ×10^-8

Note: Background has been subtracted from the value of A

[illegible signature]

QUAL/ENG/1

Test Data Analyzed from
Oscillograph Records

(may not coincide with Poloroids)

Shock Test to Failure

		Pulse #	Input	Unit X	Unit Y	Unit Z
7½ g	(-)	1	8	-	8	-
		2	7.5	-	7.5	-
		3	Taken by Linde representative			
	(+)	4	7.0	-	7.0	-
		5	7.0	-	7.0	-
		6	7.0	-	7.0	-
9 g	(+)	1	taken by Linde representative			
		2	9.0	-	9.0	-
		3	9.0	-	9.0	-
	(-)	4	9.0	-	9.3	-
		5	9.2	-	9.2	-
		6	9.0	-	8.4	-
10½ g	(-)	1	taken by Linde representative			
		2	taken by Linde representative			
		3	11.0	-	10.7	-
	(+)	4	10.0	-	10.0	-
		5	10.0	-	10.2	-
		6	10.2	-	10.5	-
12 g	(+)	1	12.0	-	12.0	-
		2	11.2	-	11.0	-
		3	11.0	-	11.0	-
	(-)	4	taken by Linde representative			
		5	12.0	-	12.5	-
		6	11.8	-	11.6	-

Dynamic Shock Test

		Pulse #	Input	Unit X	Unit Y	Unit Z
Z Axis	(+Z)	1	5.5	-	-	- *
		2	6.25	-	-	- *
		3	6.25	-	-	- *
	(-Z)	1	6.25	-	-	- *
		2	6.25	-	-	5.5
		3	6.25	-	-	5.4

* The noise developed during and as the result of the shock allows only an approximation of the g-level.

Y Axis	(+Y)	1	6.3	-	3.0	-
		2	6.0	-	3.1	-
		3	6.0	-	3.1	-
	(-Y)	1	6.6	-	5.4	-
		2	6.8	-	6.0	-
		3	6.8	-	5.8	-
X Axis	(-)	1	6.5	-	-	- *
		2	6.5	-	-	- *
		3	6.7	-	-	- *
	(+)	4	7.0	-	-	- *
		5	6.8	-	-	- *
		6	7.0	-	-	- *

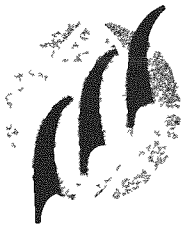

APPENDIX B

Photographs

LEAK DETECTION EQUIPMENT AND SETUP

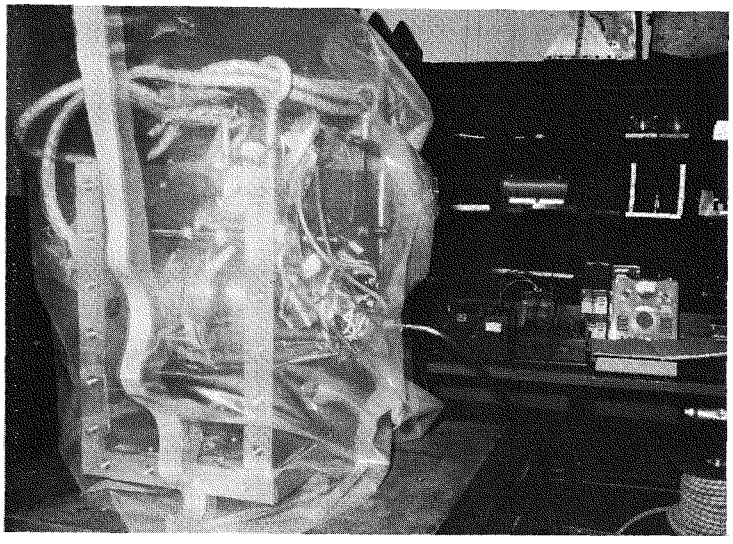

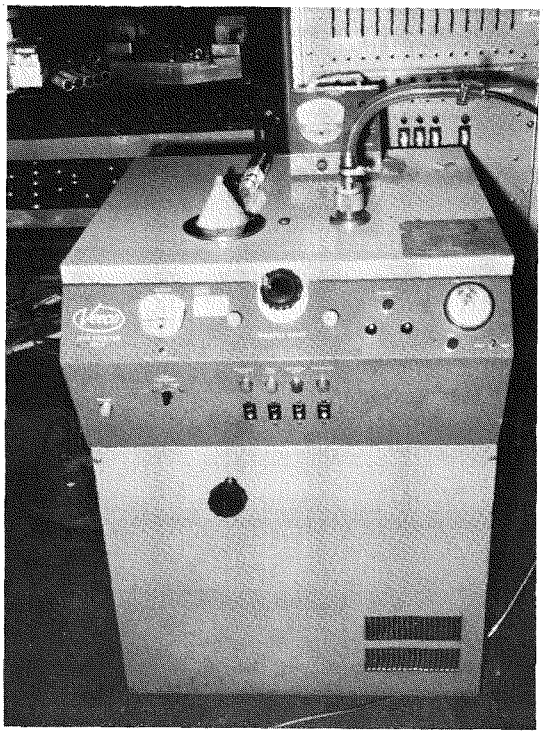

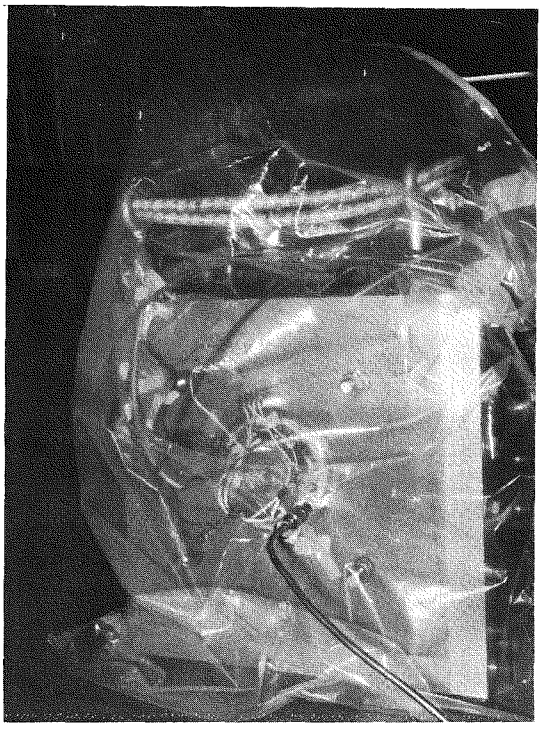

X Axis Vibration Test

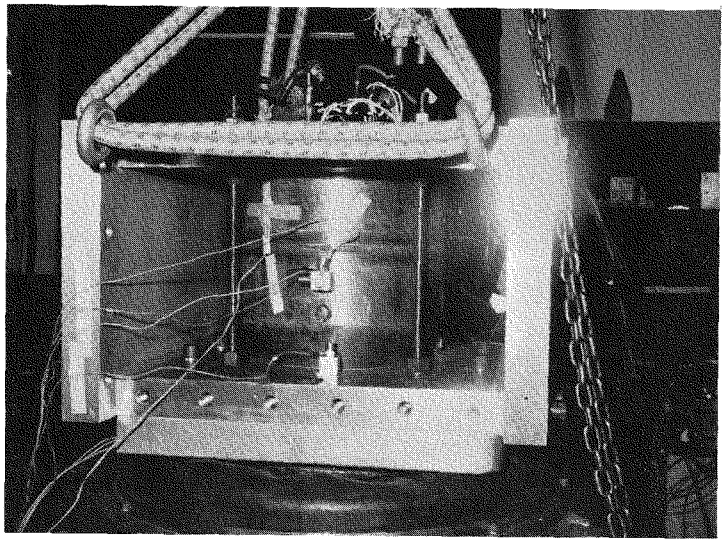

Y Axis Vibration Test

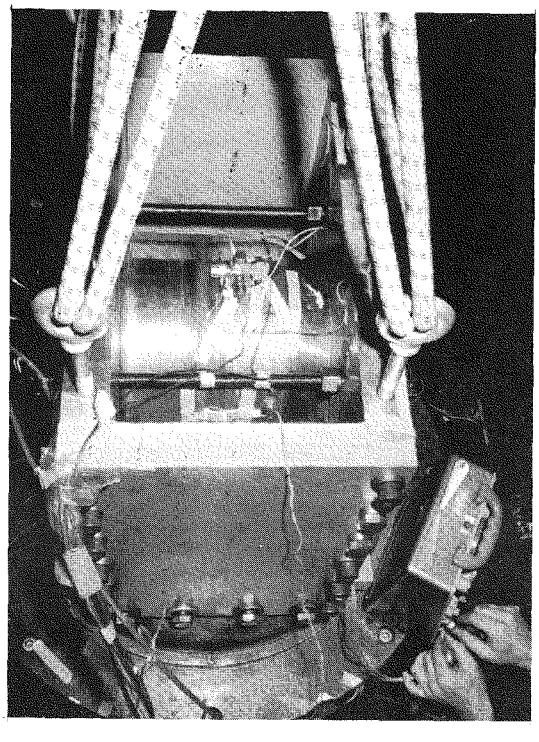

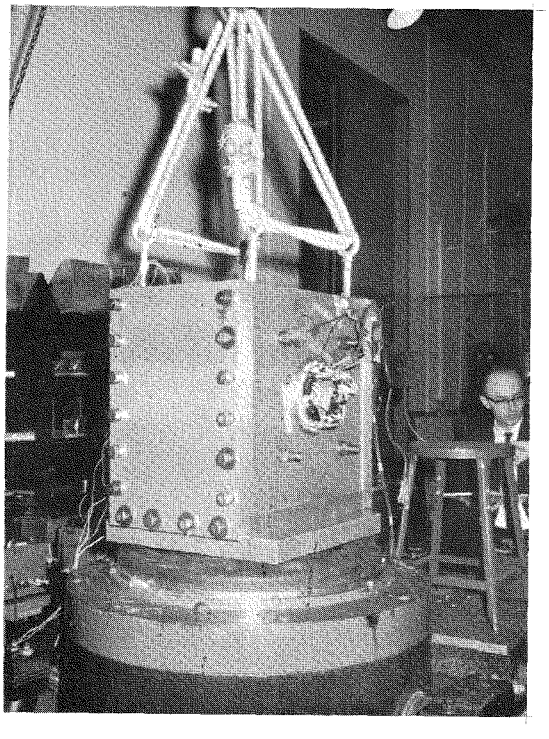

Z Axis Vibration Test

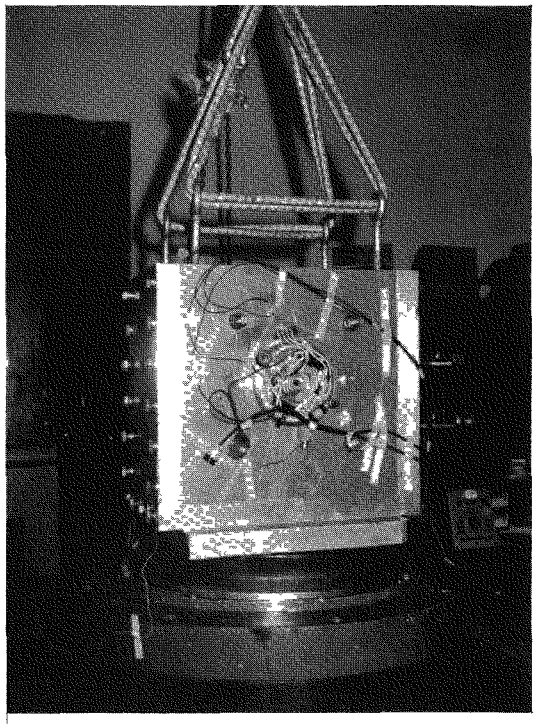

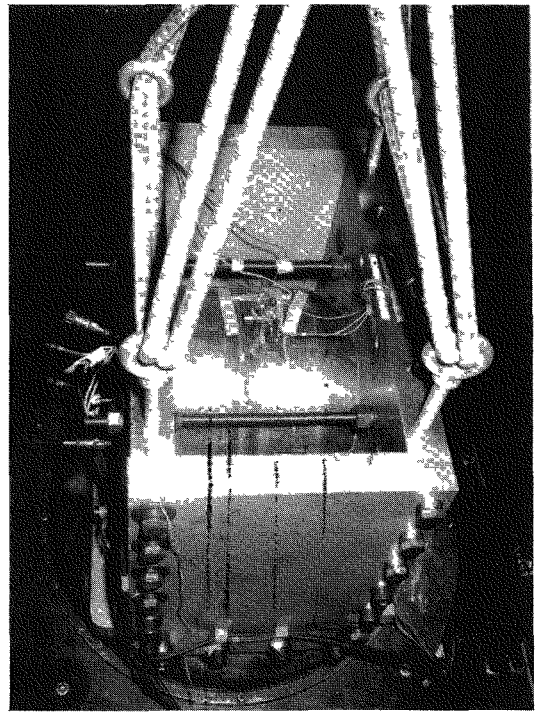

SHOCK TEST SET-UP
TYPICAL

(Z Axis)

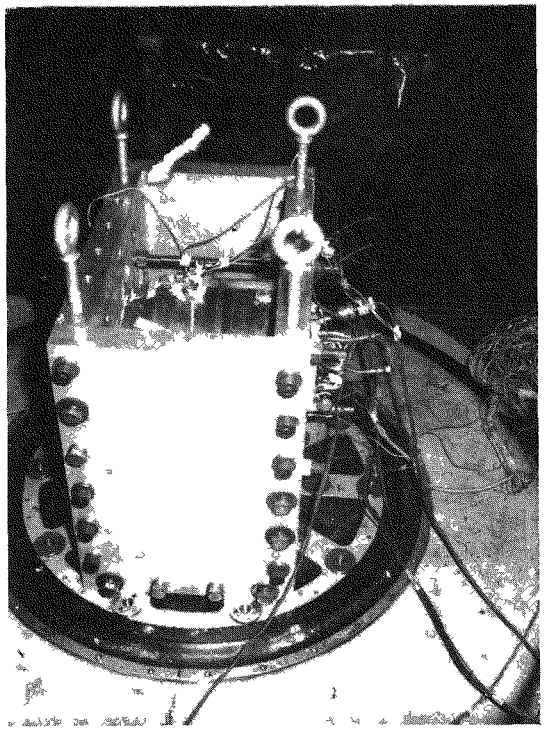

APPENDIX C

Dynamic Shock Testing

DYNAMIC SHOCK TEST

Calibration Pulses

Calibration

Vertical: 2G/cm
Horizontal: 2 ms/cm

X Axis

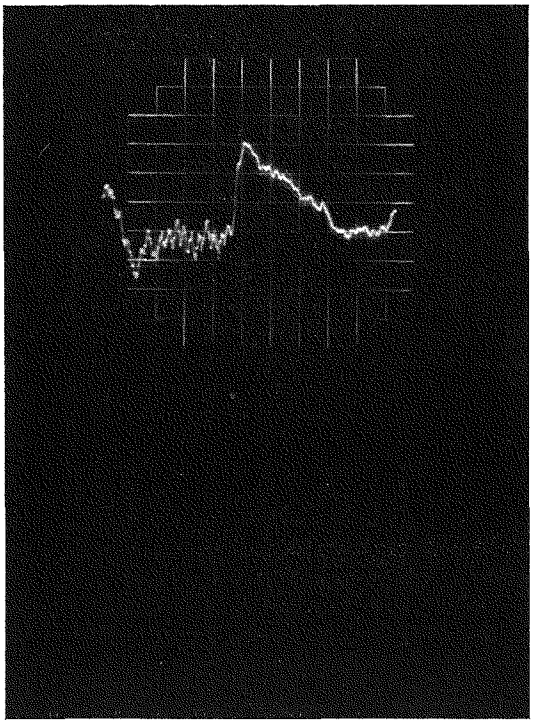

Y Axis

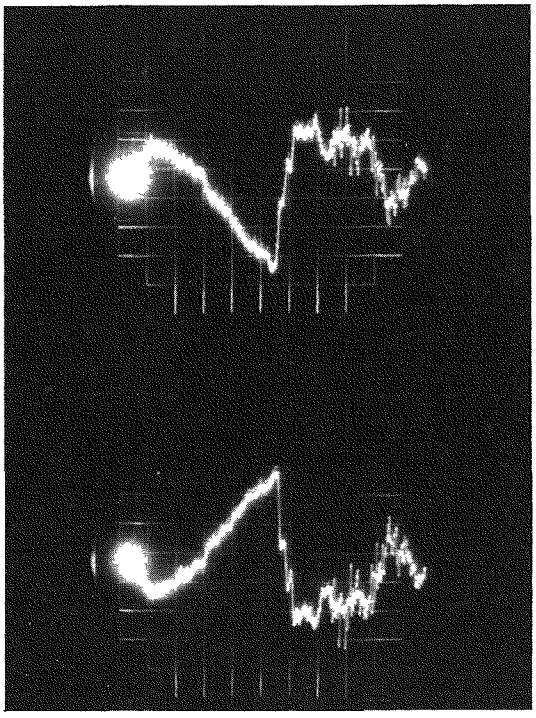

Z Axis

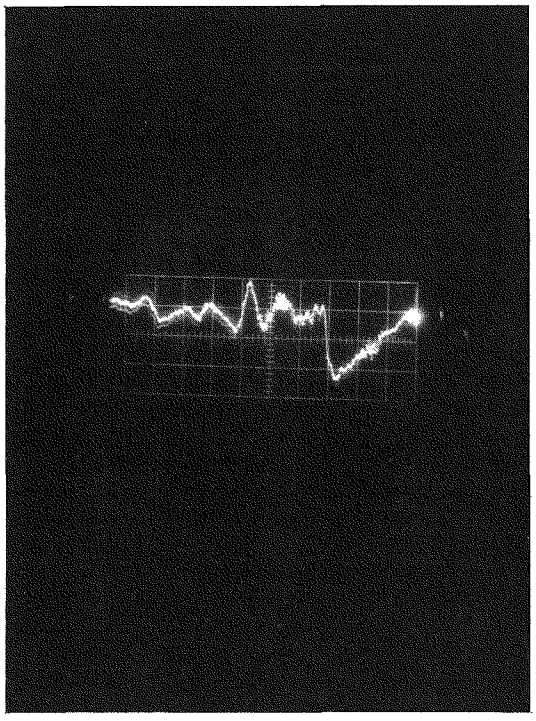

DYNAMIC SHOCK TEST

+ X and - X Axis

Note: No photographs obtained for Blows 1 and 4

No. 2 (+)

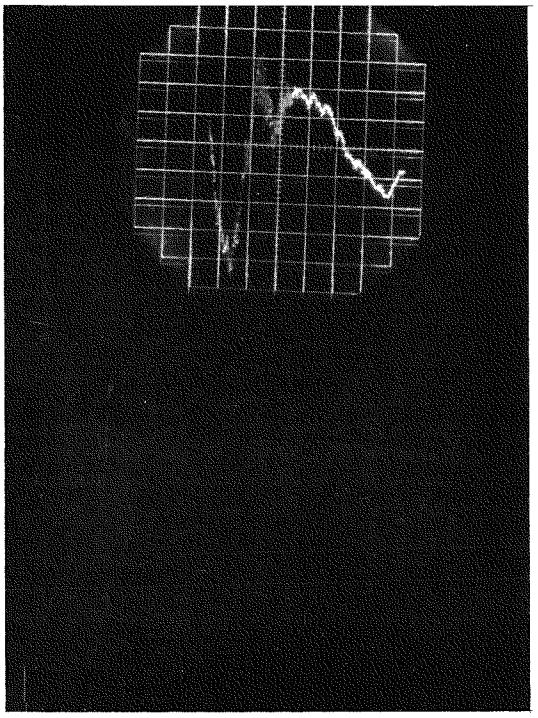

No.3 (+)

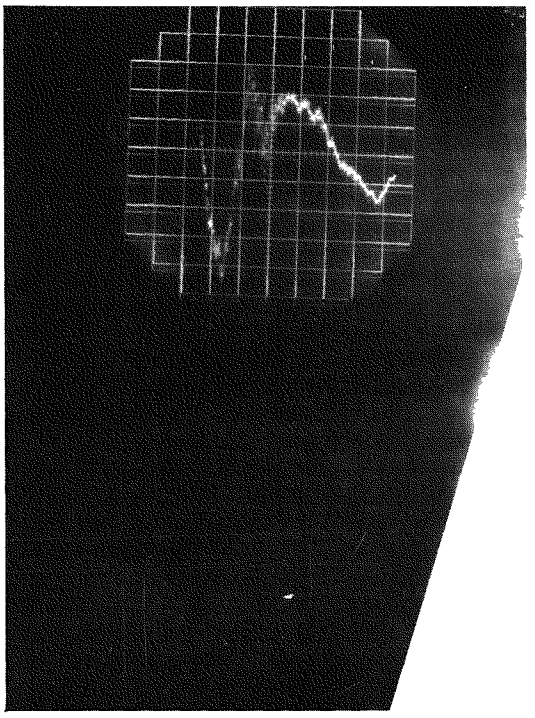

No. 5 (-)

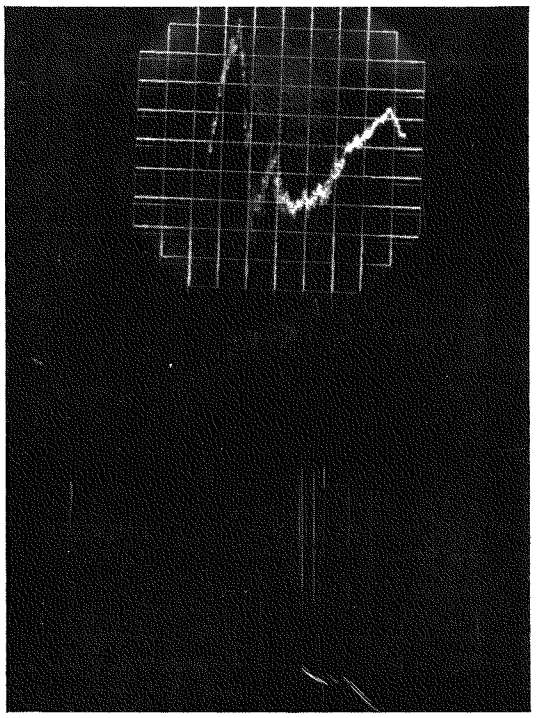

No. 6 (-)

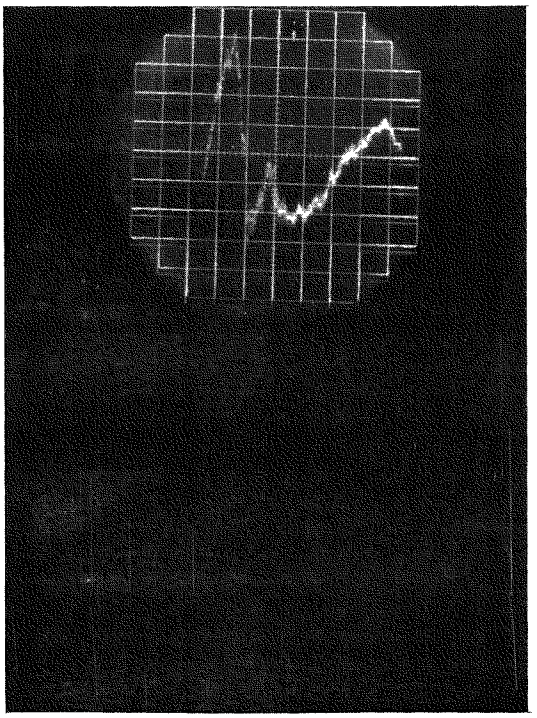

DYNAMIC SHOCK TEST

Y Axis

Note: Photographs for Blows 2 & 3 of -Y Axis were not obtained.

+Y Axis
Blow 1

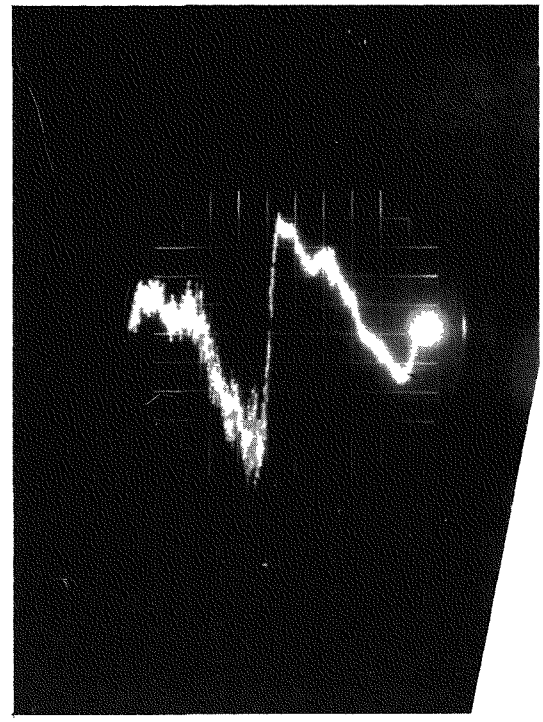

+Y Axis Blows 2 & 3

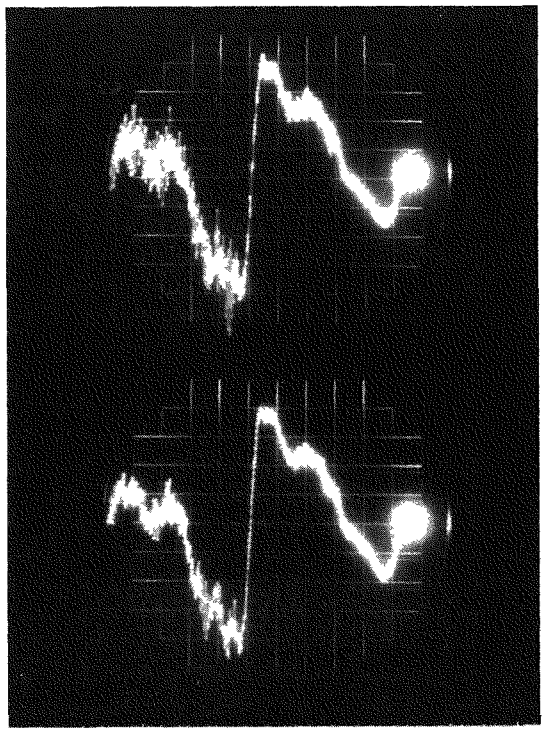

-Y Axis Blow 1

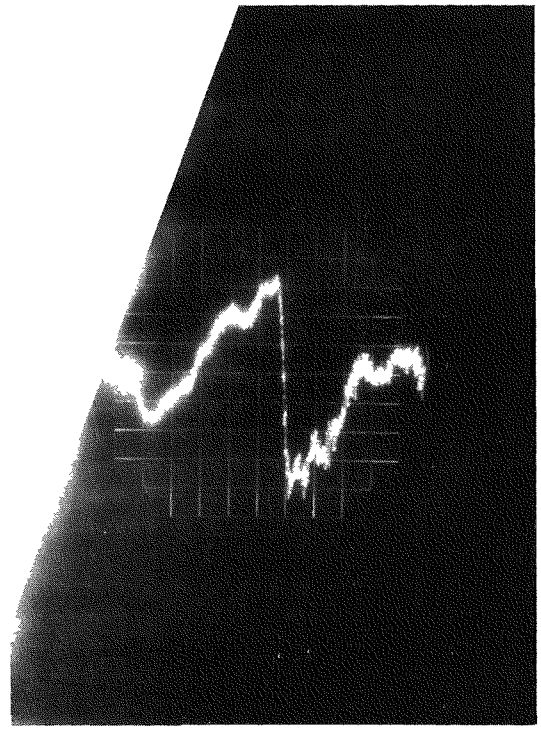

DYNAMIC SHOCK TEST

+Z Axis

3 blows

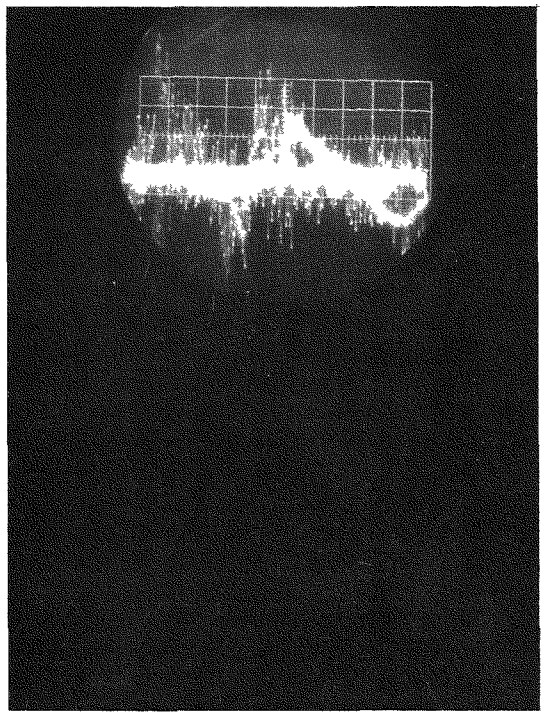

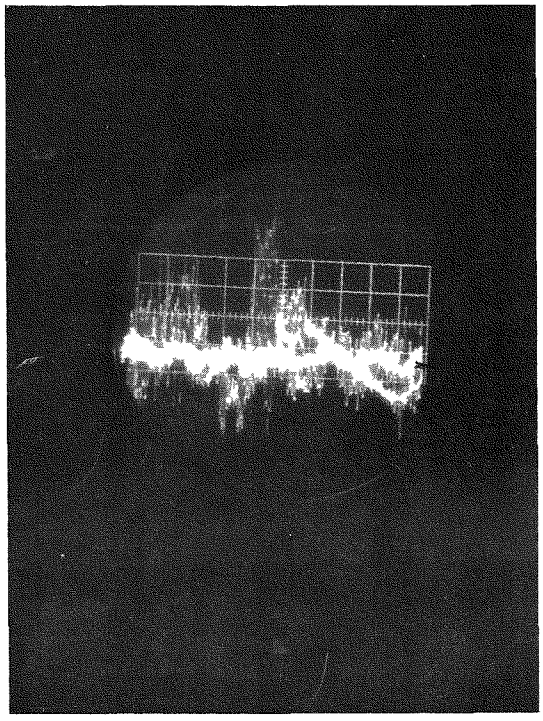

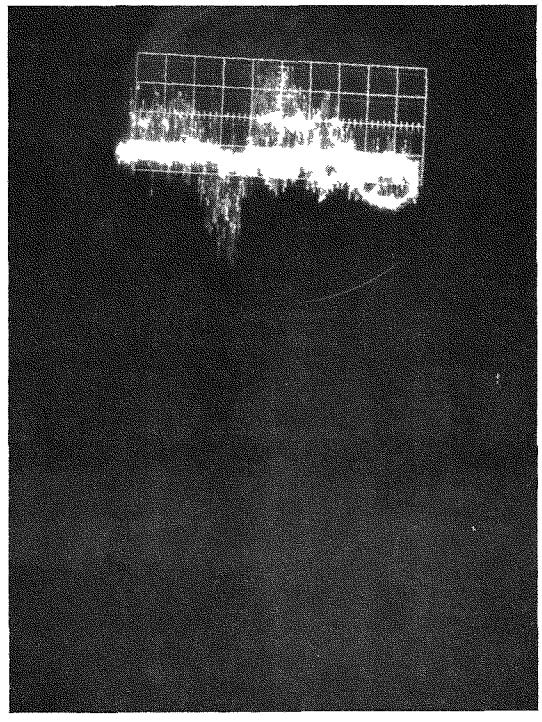

DYNAMIC SHOCK TEST

-Z Axis

3 Blows
with Polarity Reversed
to indicate Positive

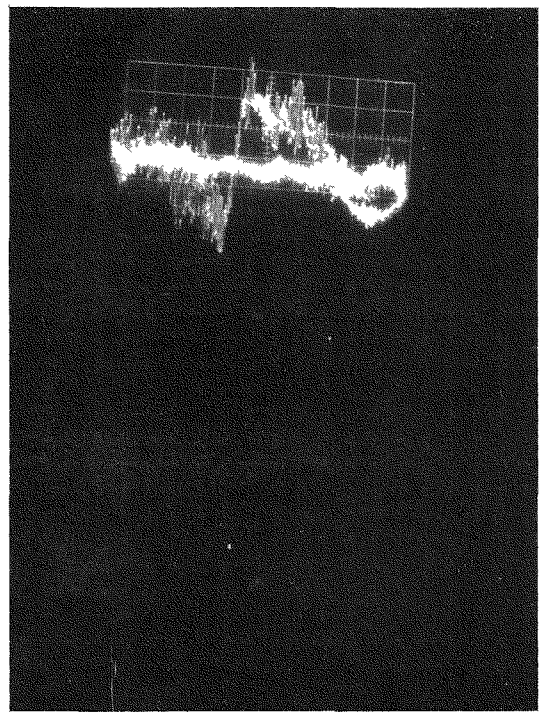

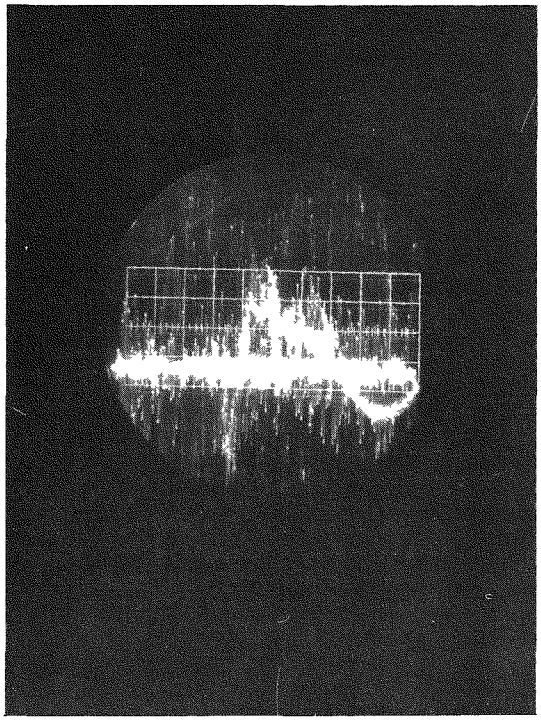

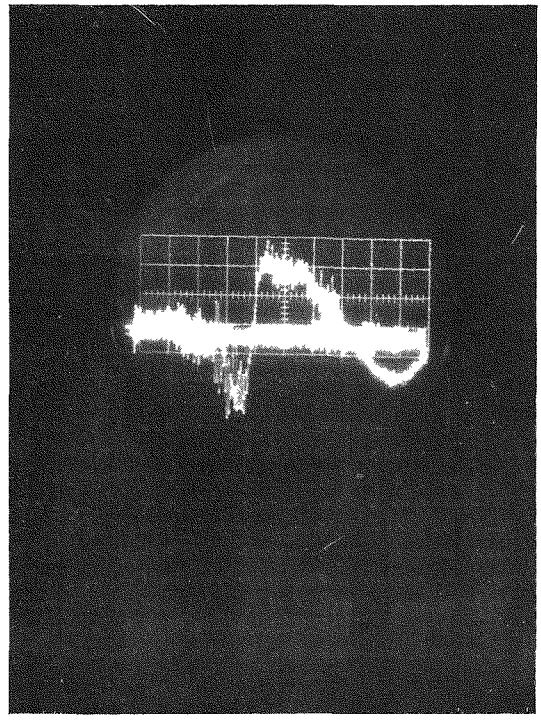

APPENDIX D

Shock Test to Failure

Calibration: Horizontal: 2 ms/cm
Vertical: 10g/cm

SHOCK TEST TO FAILURE 7.5G Level

Note: Pulse No. 6 taken by Linde Representative

Pulse No.1

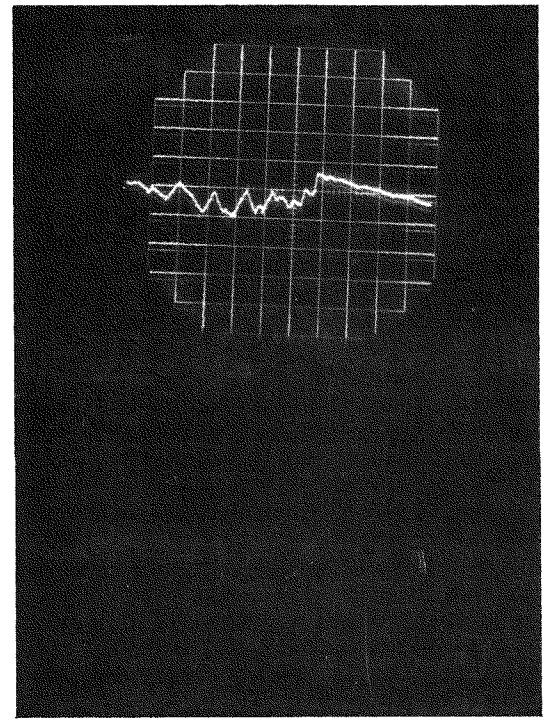

Pulse #2

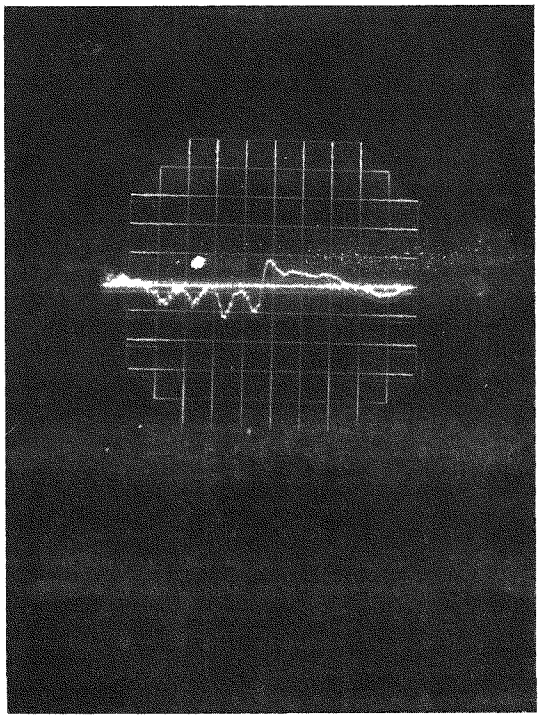

Pulse #3

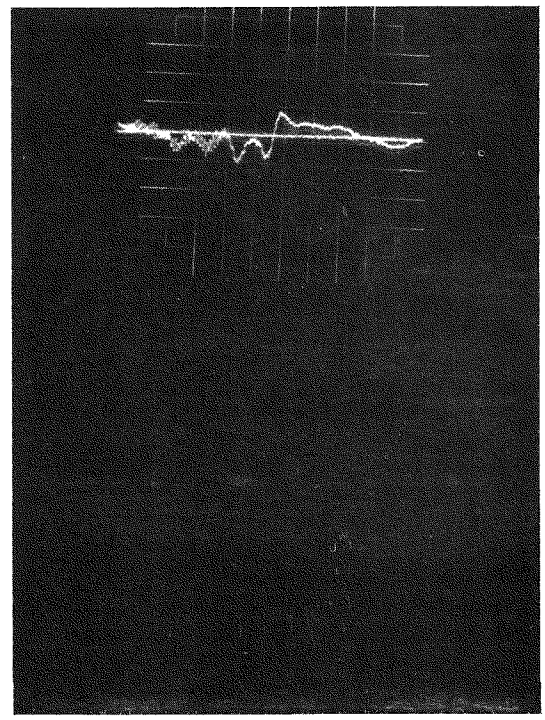

7.5 G Level

Pulse No.4

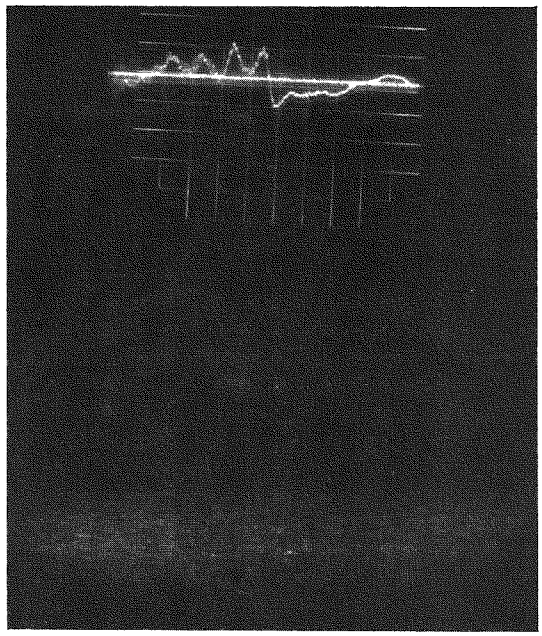

Pulse No.5

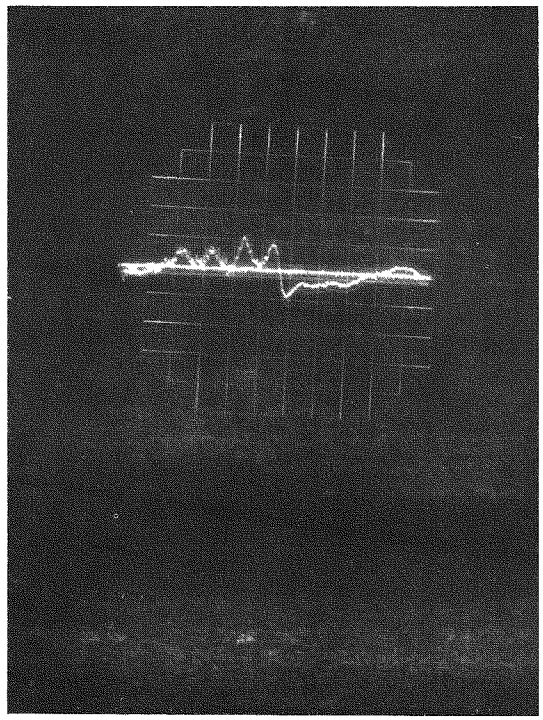

SHOCK TEST TO FAILURE 9.0 G Level

Note: Pulse No. 4 taken by Linde Representative

Pulse No. 1

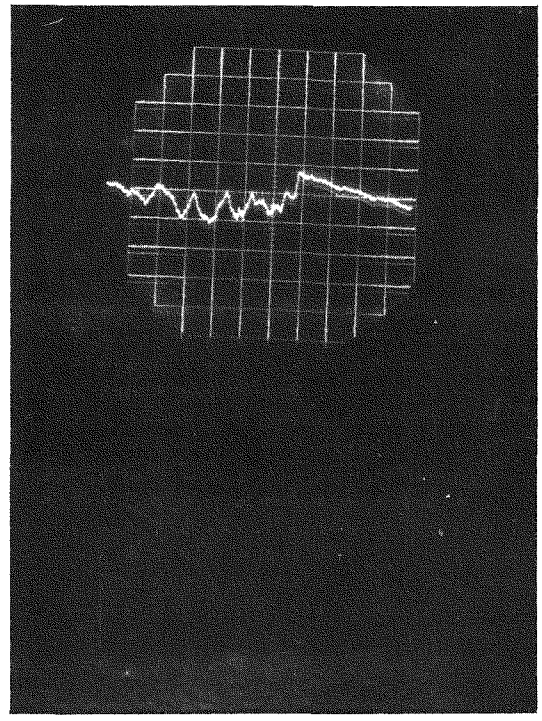

Pulse No.2

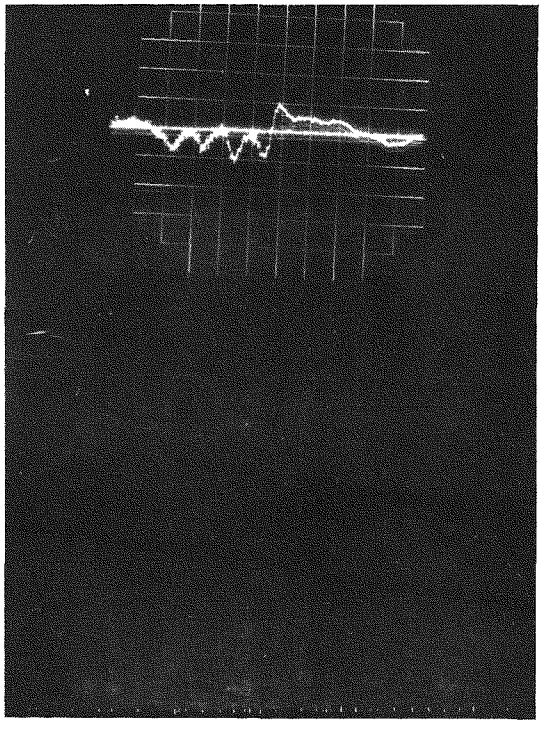

Pulse No.3

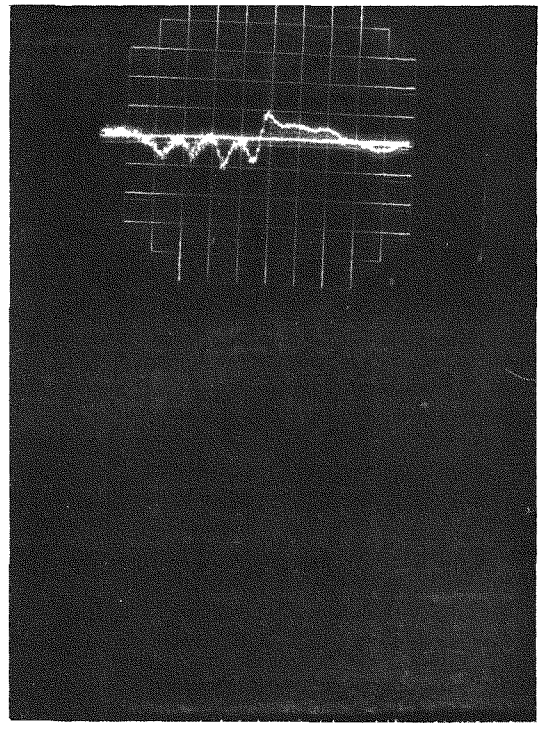

9.0 G Level (continued)

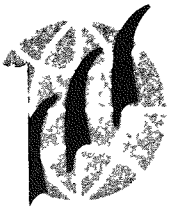

Pulse No. 5

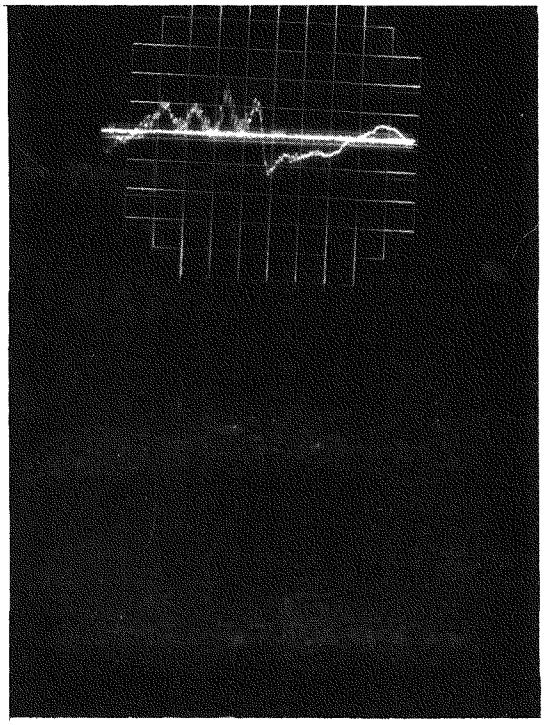

Pulse No. 6

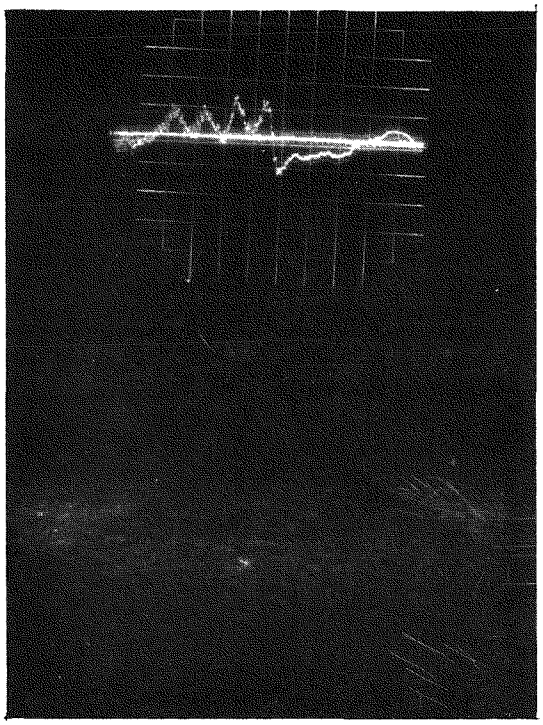

SHOCK TEST TO FAILURE 10.5 G Level

Note: Pulse No. 3 taken by Linde Representative

Pulse No. 1

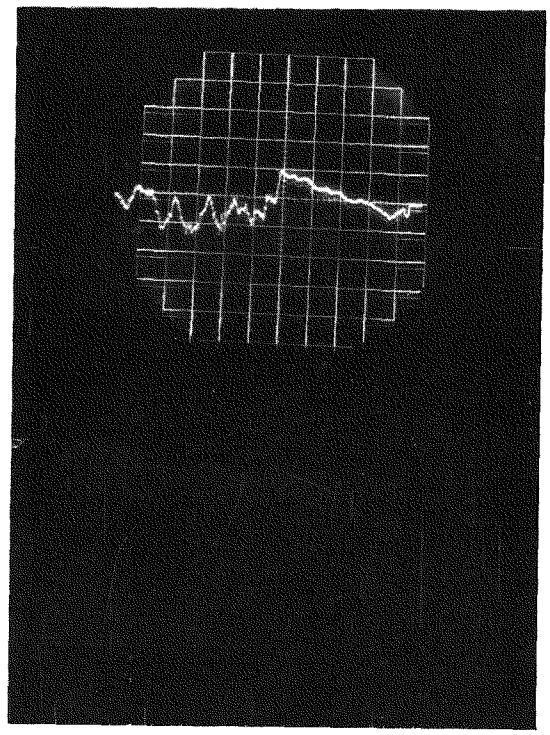

Pulse No.2

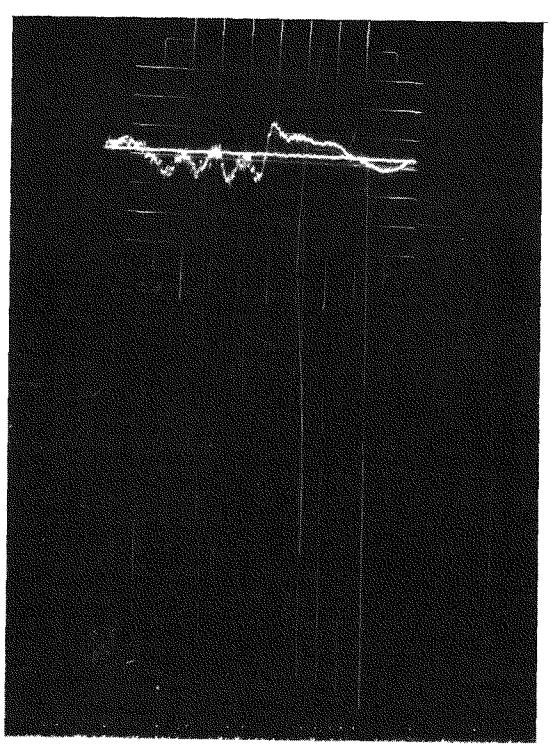

Pulse No. 4

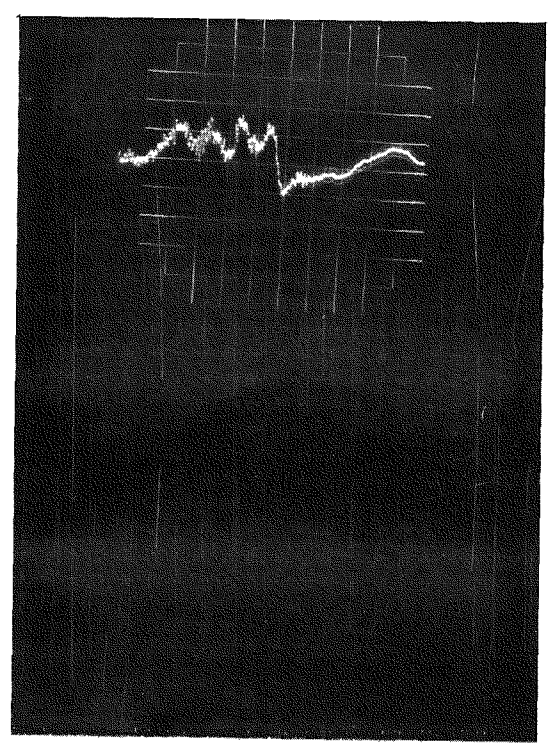

10.5 G Level (continued)

Pulse No.5

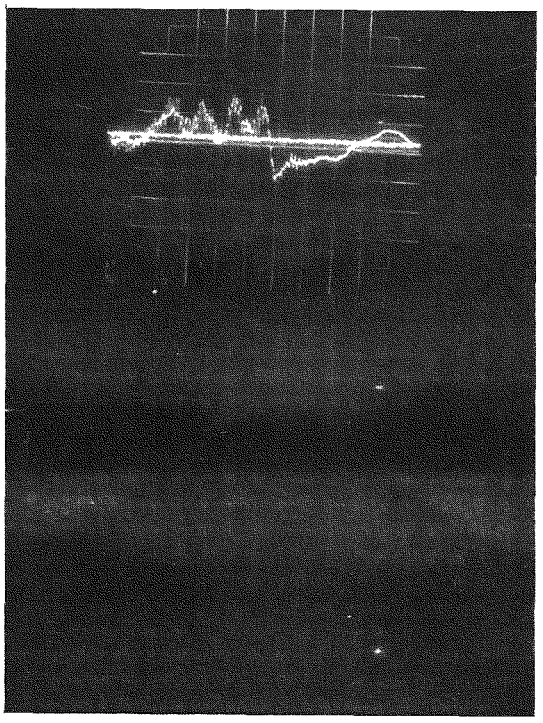

Pulse No.6

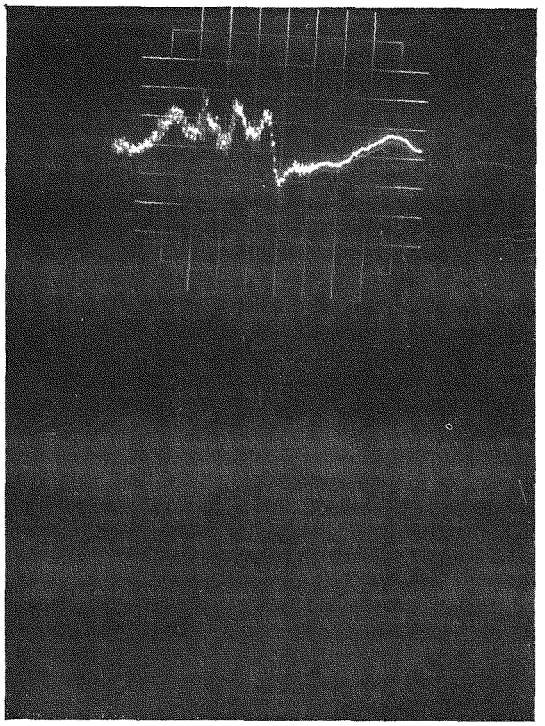

SHOCK TEST TO FAILURE 12 G Level

Note: Pulse No. 4 taken by Linde Representative

Pulse No.1

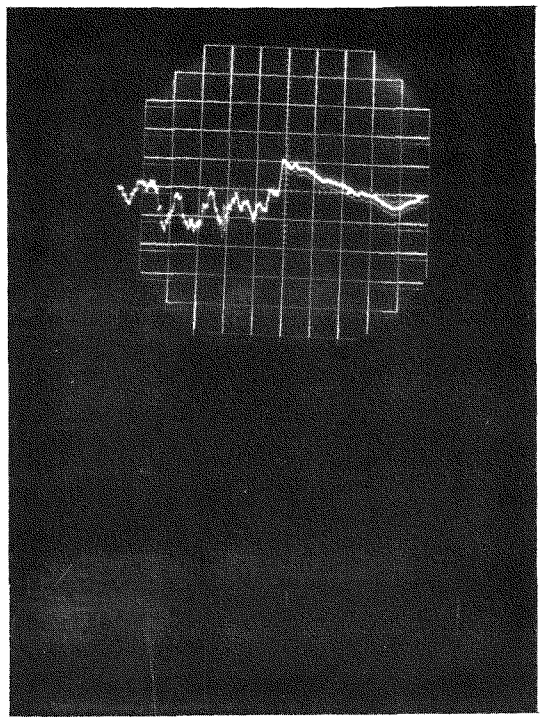

Pulse No. 2

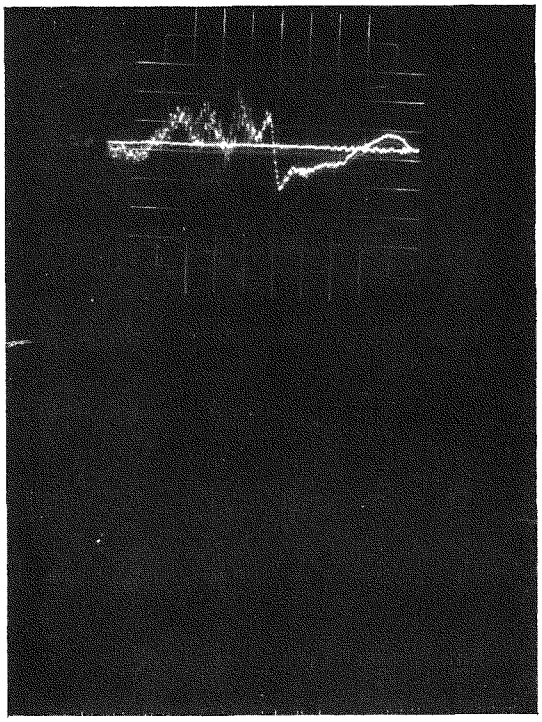

Pulse No. 3

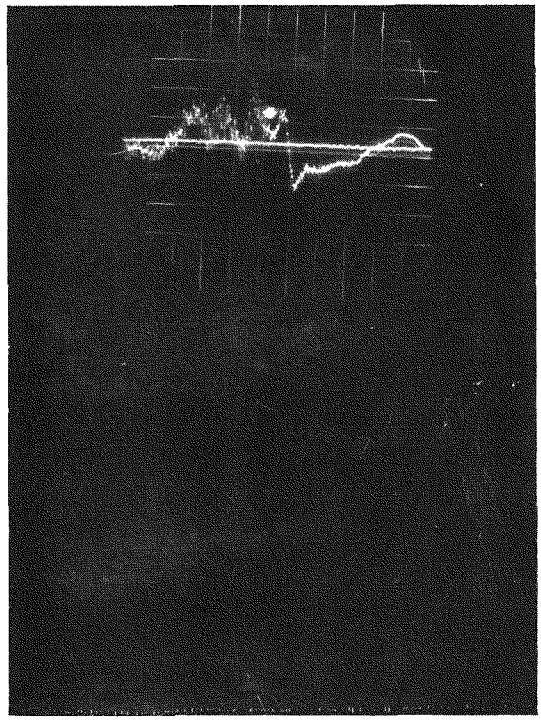

12.0 G Level (continued)

Pulse No. 5

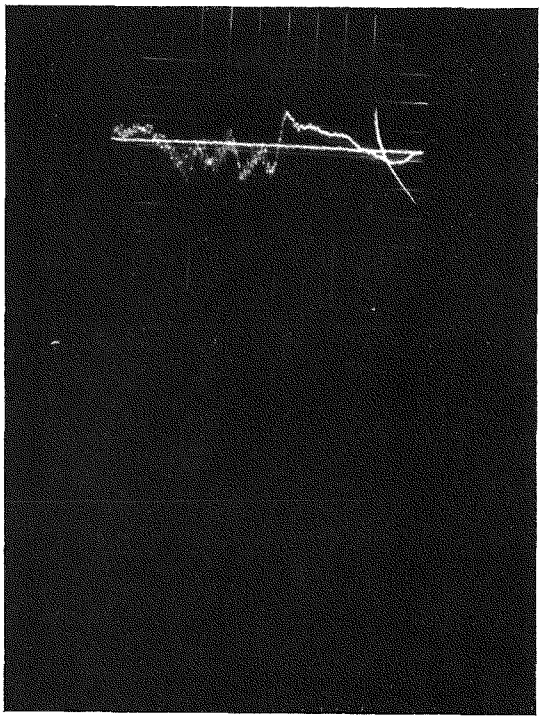

Pulse No. 6

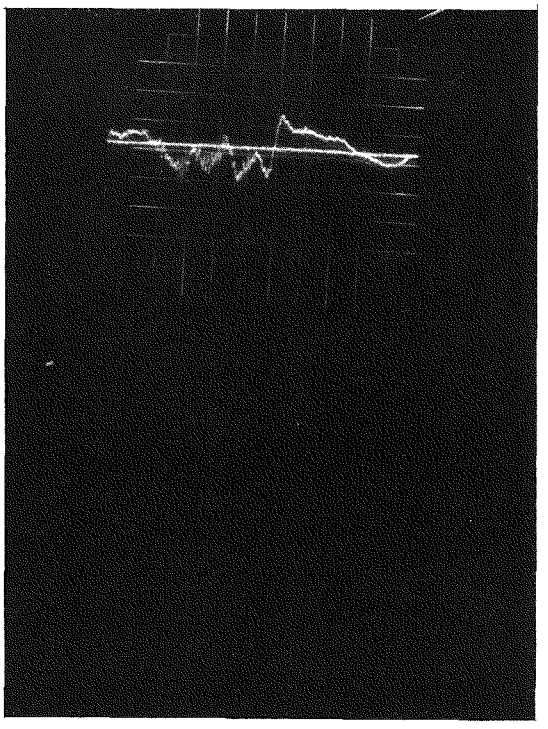

APPENDIX C

SHOCK AND VIBRATION TEST REPORT– ADDENDUM

OGDEN TECHNOLOGY LABORATORIES, INC.
Subsidiary of OGDEN CORPORATION

LINDE DIVISION
P.O.BOX 152
TONAWANDA, NEW YORK

ADDEMDUM I of Test Report #6B18-2

3M - HTVIS S/N 10-D3

Prepared by

Ogden Technology Laboratories,Inc.
Deer Park, Long Island, New York

8 MARCH 1968

OTL Job Number 7503
Linde P.O. 825-L-44899

FORMERLY: UNITED AEROTEST LABORATORIES INC.

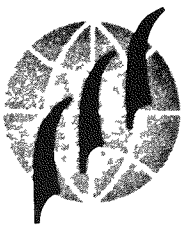

1.0 TEST EQUIPMENT

a. Vibration Exciter
M. B. Electronics
Model: C200
Calibration: None required

b. Power Amplifier
M. B. Electronics
Model: T999
Calibration: None required

c. Automatic Vibration Exciter Controller
Bruel & Kjaer
Model: 1019
Calibration: Prior to use
Last: 2/20/68

d. Signal Amplifier
Unholtz-Dickie Corp.
Model: 607-RMG-3A
Calibration: Prior to use
Last: 2/20/68

e. Accelerometer (4)
Columbia Research Labs.
Model: 902
Calibration Interval: 6 months
Last: 9/6/67

f. Oscillograph Recorder
Consolidated Electrodynamics Corp.
Model: 5-119
Calibration: Prior to use
Last: 2/20/68

g. Oscilloscope
Tektronics
Model: RM32
Calibration Interval: 6 months
Last: 12/20/67

h. Waveform Synthesizer
Exact Electronics
Model: 200 "g"
Calibration: Before each use

i. Scope Camera
A.B. Dumont
Model: 5B52
Calibration: None required

j. Isolation Transformer
Sorenson
Model: MUR 250
Calibration: None required

k. Voltage Regulator
Sola
Model: 5005
Calibration: None required

l. Variac
General Radio
Model: 100R
Calibration: None required

All instrumentation and equipment calibration is conducted in accordance with Specification MIL-Q-9858A as further defined in MIL-C-45662A "Calibration System Requirements" and is traceable to the National Bureau of Standards.

2.0 TEST SEQUENCE

2.1 Vibration Test

2.2 Shock Test

3.0 TEST PROCEDURE

3.1 Vibration Test

This test procedure is identical to Paragraph 3.2 of OTL Test Report 6B18-2 except that the Helium Leak tests were not performed.

3.2 Shock Test

This test procedure is identical to Paragraph 3.3 of OTL Test Report 6B18-2 except that the Helium Leak tests were not performed.

TEST SETUP PHOTOGRAPHS

VIBRATION AND SHOCK TEST SETUP

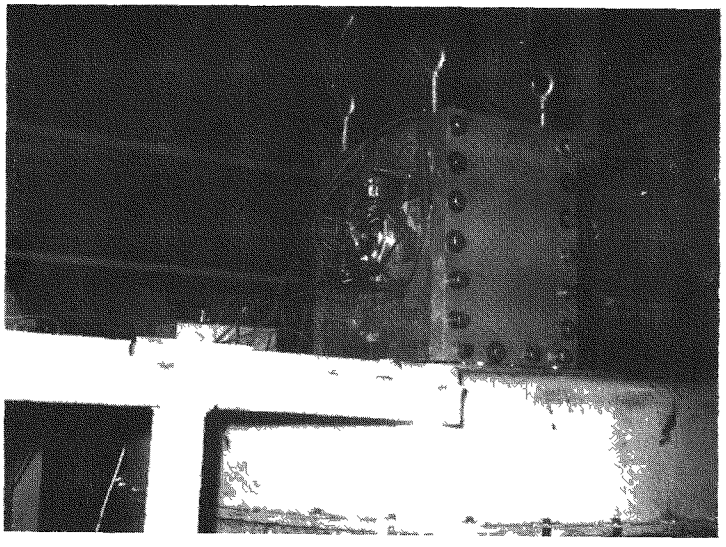

Y AXIS

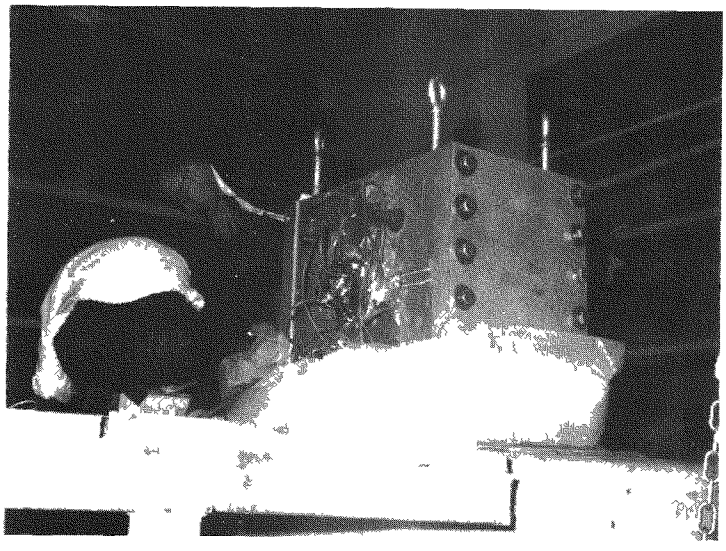

Z AXIS

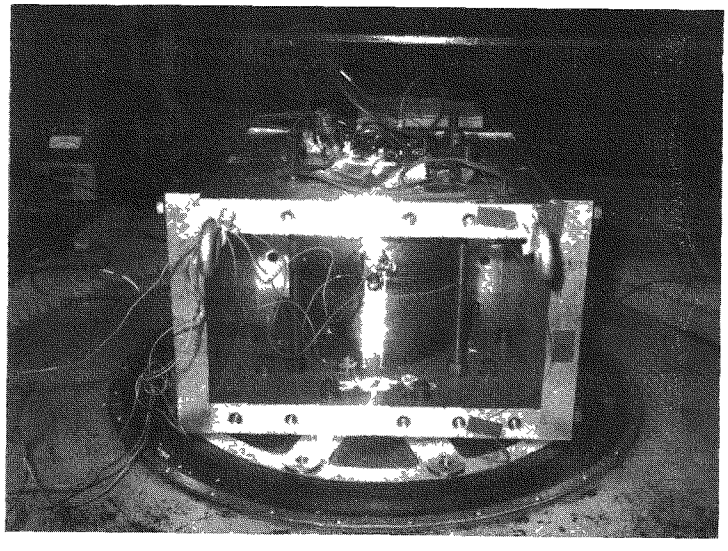

X AXIS

SHOCK PULSE PHOTOGRAPHS

CALIBRATION PULSE WITH DUMMY LOAD

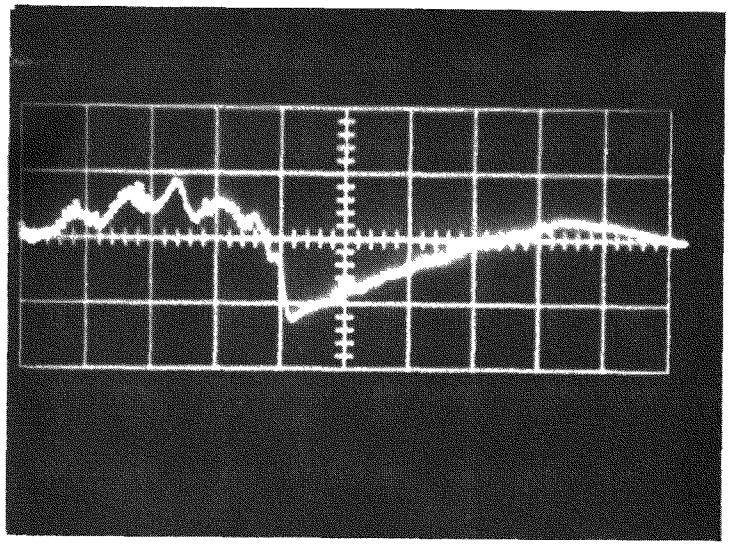

- Direction

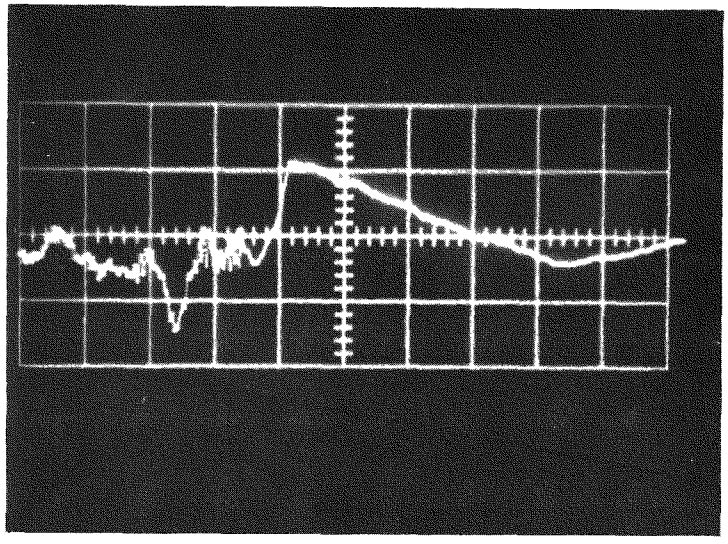

+ Direction

Calibration: Horizontal 2 ms/cm
Vertical 5g/cm

X AXIS (+) DIRECTION

PULSE #1

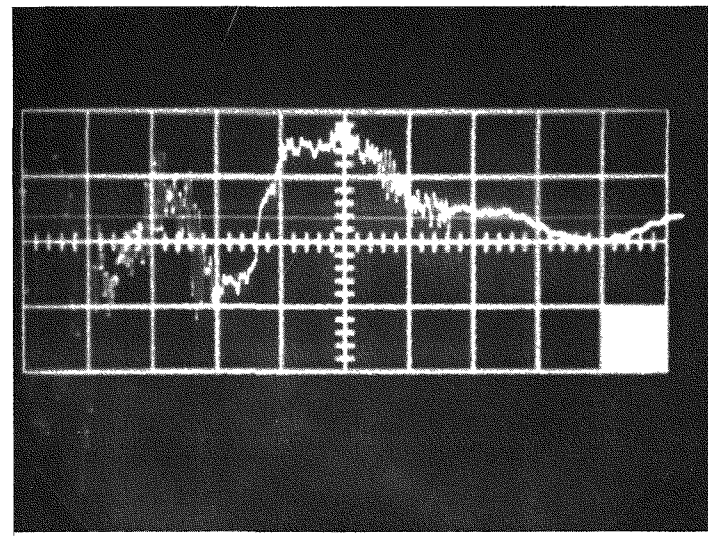

PULSE #2

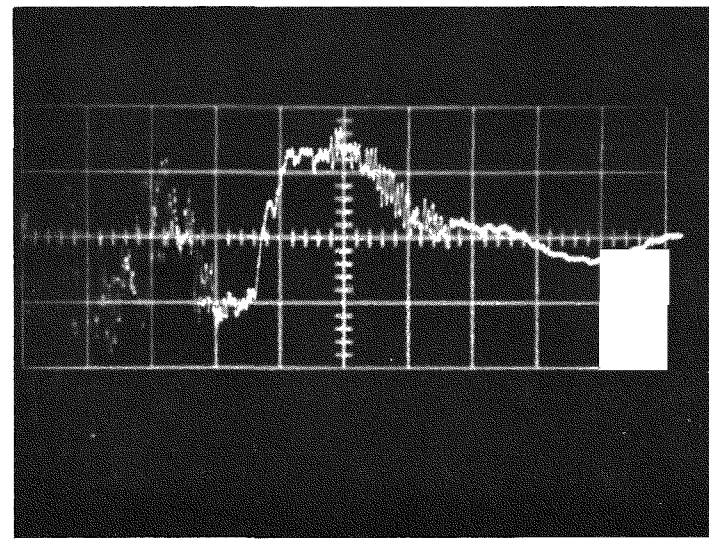

PULSE #3

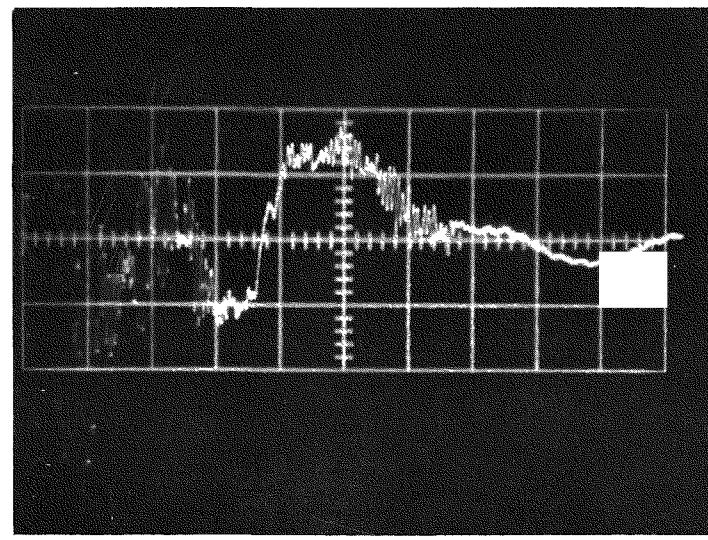

Calibration:
Horizontal: 2 ms/cm
Vertical: 5 g/cm

X AXIS (-) DIRECTION

PULSE #1

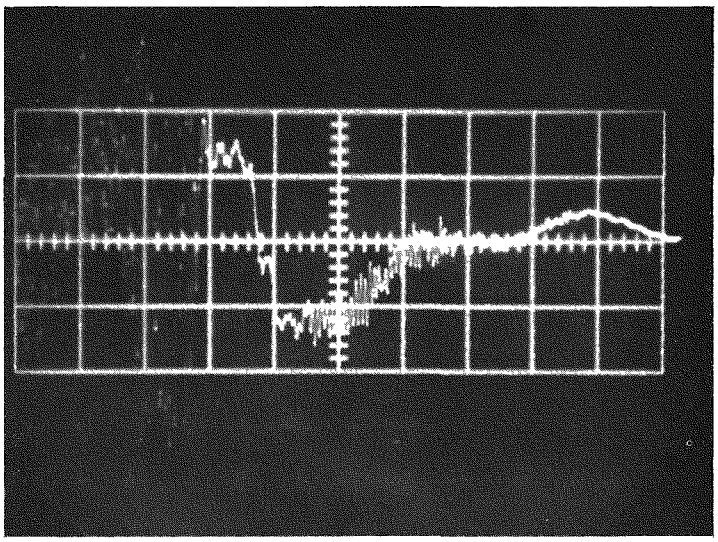

PULSE #2

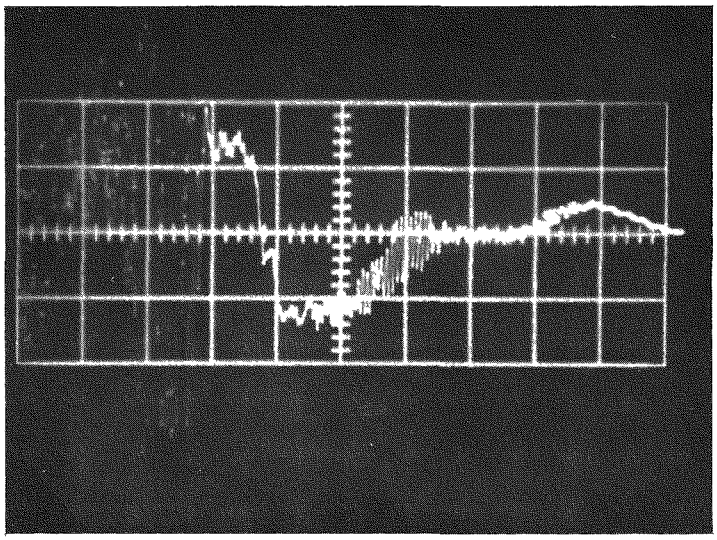

PULSE #3

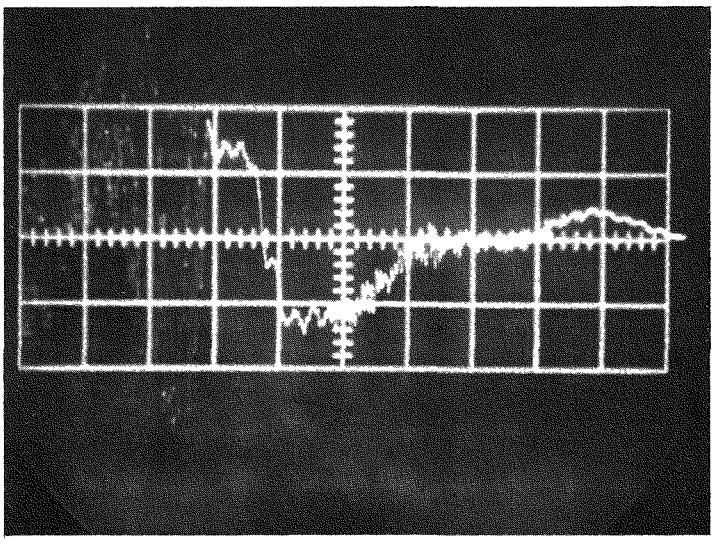

Calibration:

Horizontal: 2 ms/cm

Vertical: 5 g/cm

Z AXIS (-) DIRECTION

PULSE #1

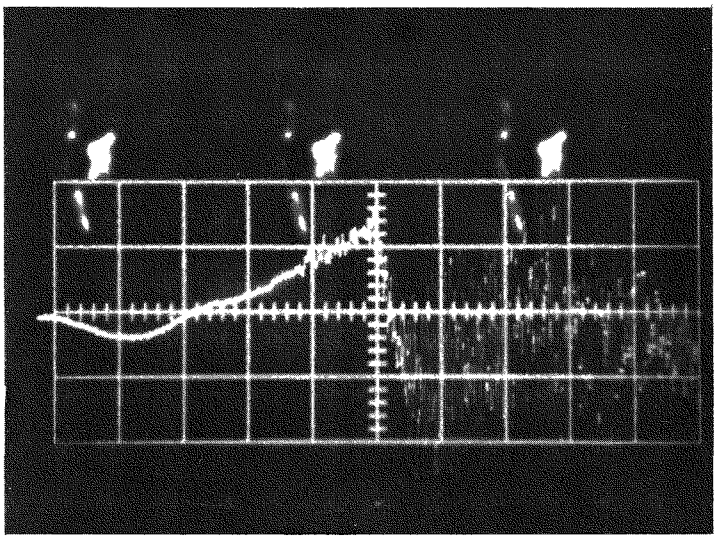

PULSE #2

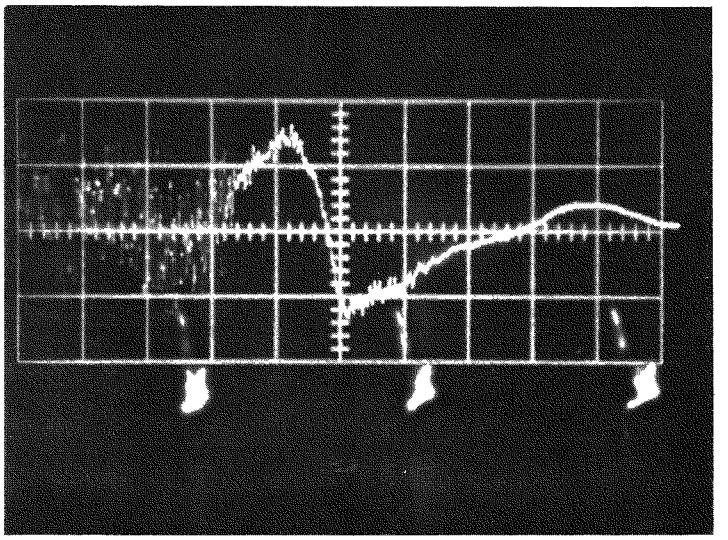

PULSE #3

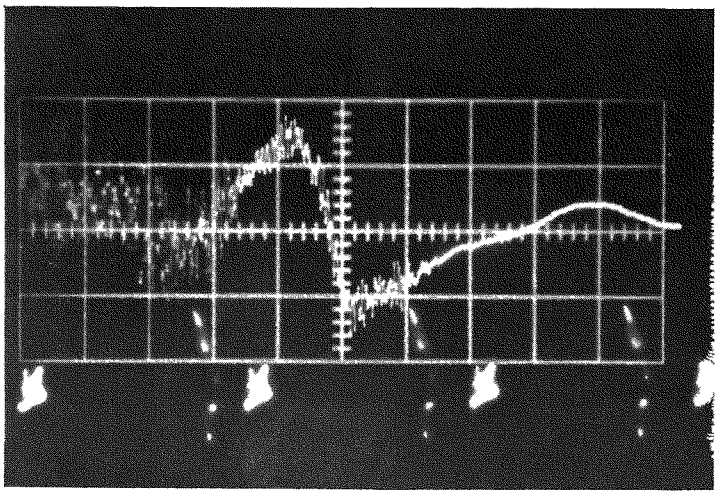

Calibration:
Horizontal: 2 ms/cm
Vertical: 5 g/cm

Z AXIS (+) DIRECTION

PULSE #2

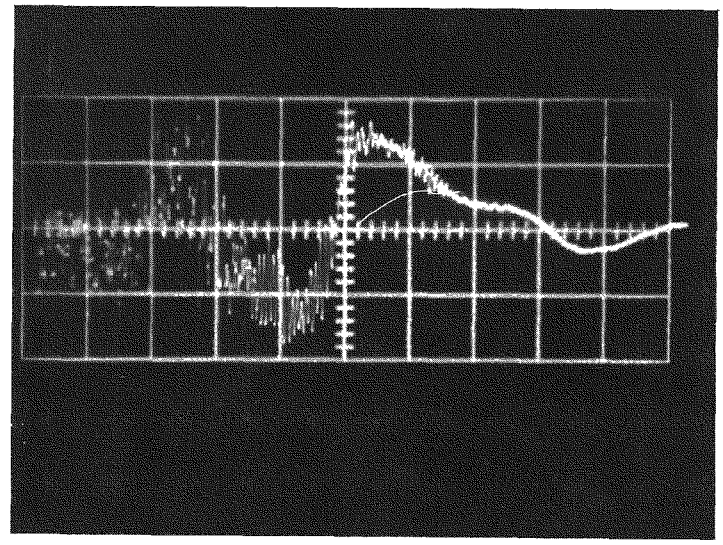

PULSE #3

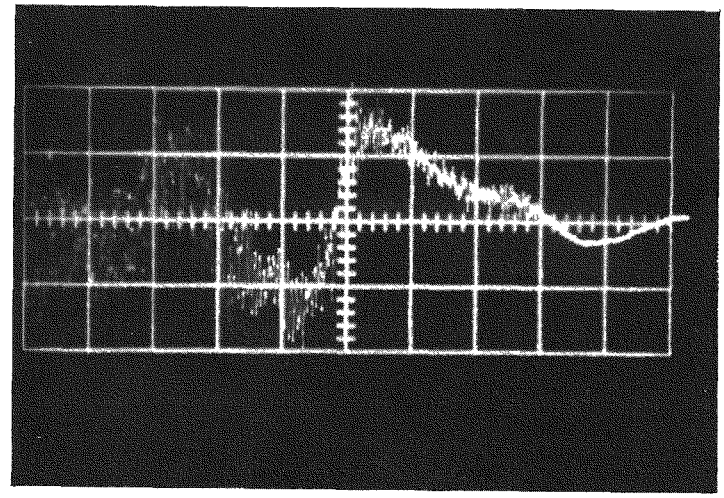

Calibration:

Horizontal: 2 ms/cm
Vertical: 5 g/cm

Y AXIS (+) DIRECTION

PULSE #1

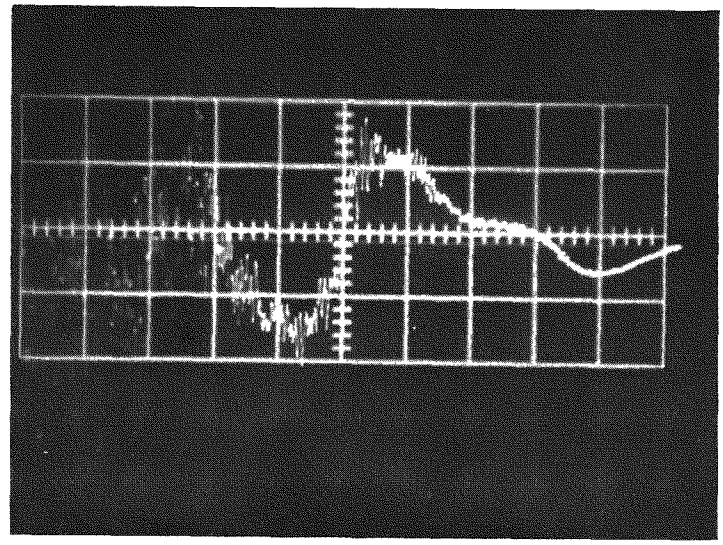

PULSE #2

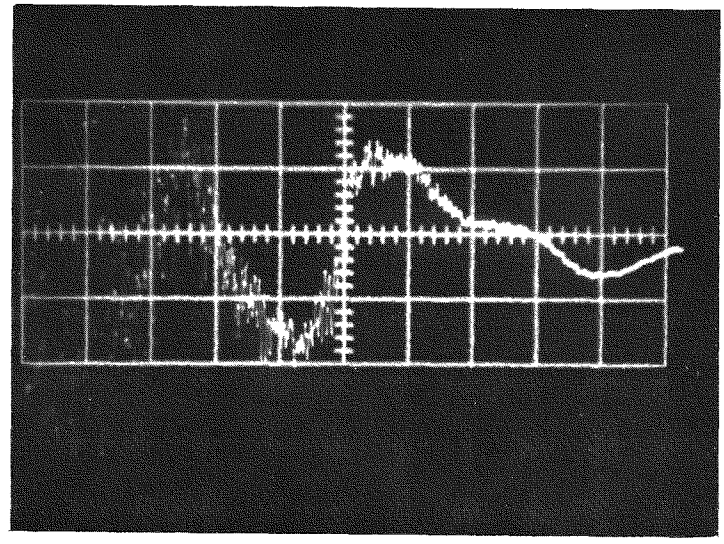

PULSE #3

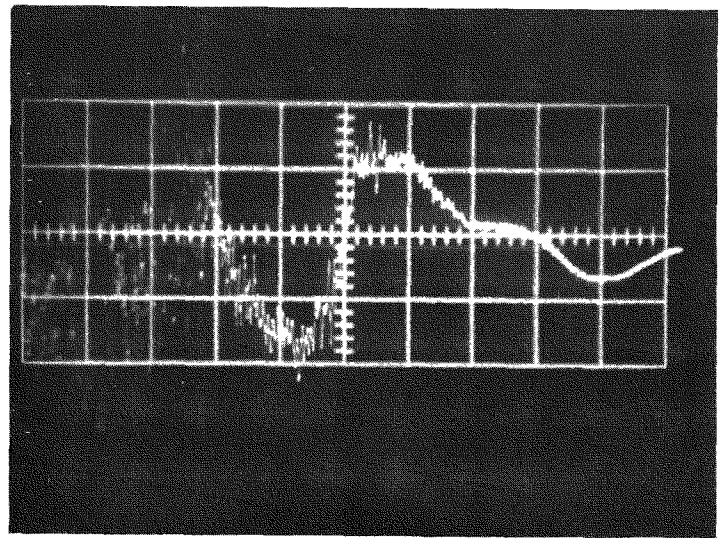

Calibration:
Horizontal: 2 ms/cm
5 g/cm

Y AXIS (-) DIRECTION

PULSE #1

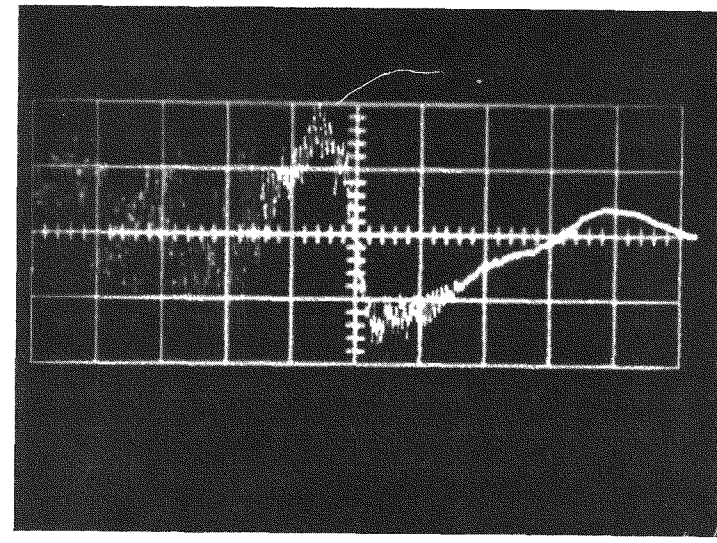

PULSE #2

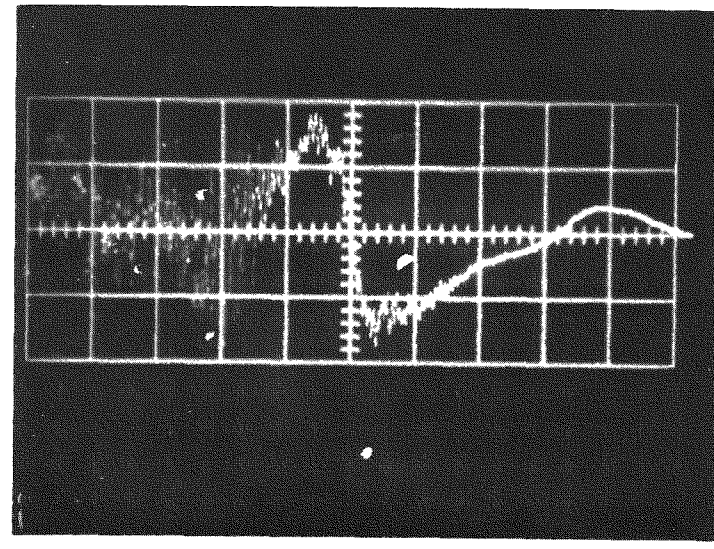

PULSE #3

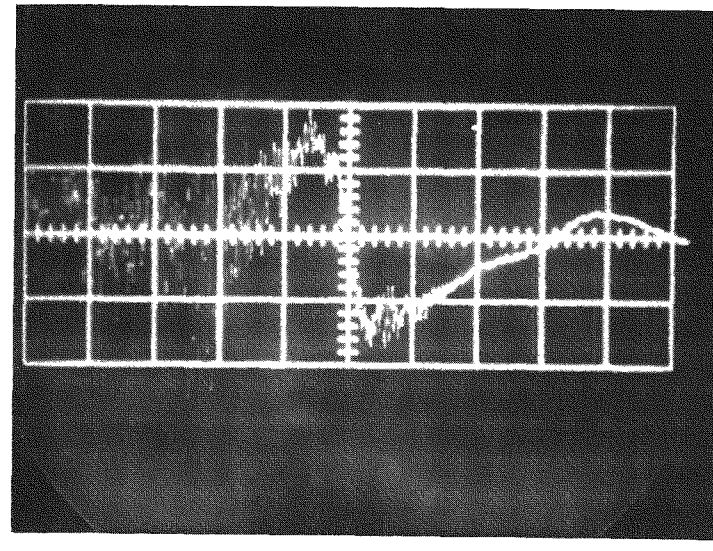

Calibration:
Horizontal: 2 ms/cm
Vertical: 5 g/cm

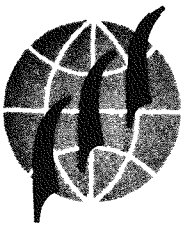

TEST LOG SHEETS

OGDEN TECHNOLOGY LABORATORIES, INC. **DATA SHEETS**

United Aerotest Laboratories, Inc.

Job Number: 2505 Engineer:

Test: Vib Unit Part No: 3M-1HTV15

Test Technician: [illegible] Unit Serial No: 10D3

Date Photo Taken:

DATE 2-20-68.

Y-Y AXIS

2050- Start 1 G survey. Stopped at 8 cps. Stopped at 10 cps. Shaker rattled [illegible].

2141- Continue 1 G survey.

2145- Complete " " to 60 cps.

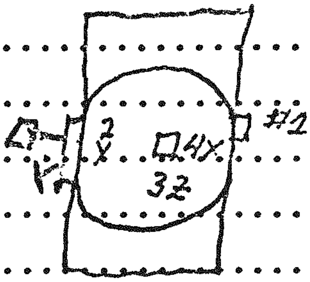

2152. Start test sweep.

2157- Stopped #2 Accel. Reading more than 3.36 at 39 cps.

2203- Ran a high speed Record 36-39 cps.

2217. Ran camera Record 36 - 42 cps.

22[illegible] [illegible] To [illegible] of [illegible] Ran 36-43 cps at [illegible].

2245- Continue sweep 43-50 cps. CUSTOMER DECIDED To STOP TESTING. UNIT RESPONSE CURVE [illegible] 45 G's.

2/21/68

[illegible]48 to 701 - PERFORMED 1 G SURVEY 8-50 cps Y-AXIS

[illegible]3 to 705 - " SPEC. LEVEL FROM 35 TO 50 Y-AXIS

complete " " " " "

1717- Start [illegible] sweep of first sweep

1807- Start second sweep.

1822- Complete " "

UAL/ENG/1

United Aerotest Laboratories, Inc.

Job Number: 7015 Engineer:

Test: VIB Unit Part No: 3M-HTVIS

Test Technician: [illegible] Unit Serial No: 1023

Date Photo Taken: DATE 2-21-68

1900: Start 3rd Loop X-AXIS

1915: Complete " " "

2202: Start 4th Loop Z AXIS

2215: Complete " " "

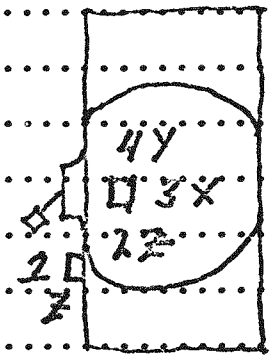

2210: Start 1st Loop Z AXIS

2225: Complete " " "

2310: Start 2nd Loop Z-AXIS

2325: Complete " " "

2/22/68

0845 - CUSTOMER ARRIVED

0900 - STARTED 3RD SWEEP Z-AXIS

0915 - COMPLETED " " "

Z-AXIS COMPLETED !!

0920 TO 1000 } PERFORMED LEAKAGE CHECK ON UNIT.

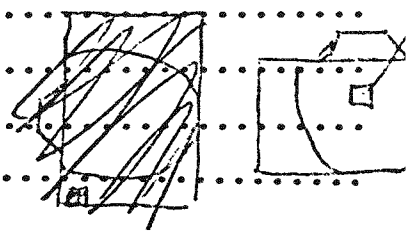

1010 TO 1055 - SWITCHED TO X-X-AXIS

DATA SHEETS

EN TECHNOLOGY LABORATORIES IN
nited Aerotest Laboratories, Inc.

ob Number: 7058 Engineer: "H"

est: VIBRATION Unit Part No: 3M-HTVIS

est Technician: V. J. McGRI Unit Serial No: 10-D3

ate Photo Taken:

DATE 2/22/68

X-AXIS

6 TO - PERFORMED LO SWEEP X-AXIS
58

058 - STARTED 1ST SWEEP X-AXIS SPEC LEVELS

113 - COMPLETED " " " " "

120 TO 1150 } LEAK CHECK

1158 - STARTED 2ND SWEEP X-AXIS

1205 - STOPPED AT COMPLETION OF UP SWEEP MONITOR ACCELS. FELL OFF @ APPROX 30 CPS.

1207 - STARTED DOWN SWEEP 2ND SWEEP X-AXIS (ACCEL RECOVER SO)

1215 - COMPLETED " " " "

220 TO 255 } LEAK CHECK

1256 - STARTED 3RD SWEEP X-AXIS

1311 - COMPLETED " " "

X-X-AXIS COMPLETED!

315 TO 1345 } LEAK CHECK!

AL/ENG/1

DATA SHEETS

Ogden Technology Laboratories, Inc.

Job Number: 7503 Engineer: "H"

Test: ½ SHOCK Unit Part No: 3M-HTV-1S

Test Technician: V.U./AHL Unit Serial No: 10-D3

Date Photo Taken: Date 3/23/68

0830 TO 1330 - CALIBRATED SHOCK PULSES WITH LEAD WGT.

1330 - MOUNTED UNIT IN X-AXIS

1355 TO 1425 PERFORMED SHOCK TEST X-AXIS

1430 TO 1500 LEAK CHECK!

1505 TO 1550 CHANGE TO Z-AXIS

1600 TO 1620 PERFORMED SHOCK TEST Z-AXIS (LOST PHOTO ON PULSE # 1 Z-AXIS (+))

1630 TO 1700 LEAK CHECK

1705 TO 1745 Change to "Y" Axis

1800 TO 1825 PERFORMED SHOCK TEST "Y" AXIS

1830 TO 1900 LEAK CHECK

UAL/ENG/1

APPENDIX D
SYSTEM S10D1A ASSEMBLY

Components and test station equipment were trucked to ORNL. Manufacturing personnel performed a preliminary assembly to check dimensional fit. It was determined that alteration of the segmented retaining ring was necessary because it was approximately 1/8-inch too thick. This prevented proper compression by the pressure vessel cover and further resulted in an excessive radiation gap between the emitter plate and the hot frame of the generator. The entire top surface of the ring was machined down 0.150 inch. This provided the correct pressure vessel mating interface and the proper radiation gap. The thermal transfer surfaces were coated with heat transfer grease and the retaining ring placed in the lower assembly which consists of the pressure vessel body and the insulation system.

This assembly was then transferred to the hot cell area for fueling (Figure D1) The fueling operation proceeded smoothly and was accomplished within two hours. However, rather than start at mid-day, completion of the assembly was deferred until the next day. To prevent heat up of the system, a cooling block was attached to the emitter plate. At the start of assembly the plate temperature was about 190°F. After coating the mating surfaces with heat transfer grease, the generator was bolted in place and the Min-K insulation was packed in. This took about three hours. After an electrical checkout of the system the pressure vessel cover was lowered into place. When bolting the cover in place, it was found that the bolt hole threads in the pressure vessel were either tapered or not of full depth and that it was necessary to place from 5 to 8 washers under the bolt heads to draw the pressure vessel halves together.

Unfortunately, the pressure vessel holding ring prevented visual observation of the pressure vessel mating joint during tightening. A vinyl hose had to be used as a shim to raise the interface for viewing. The next ring will be designed to overcome this deficiency by moving the chamfered support shoulder to the upper part of the ring. This ring will also have an easy release clamp to facilitate removal.

The assembled system was checked out both before and after the pressure vessel cover was bolted down; however, after about 16 hours of operation an internal short was discovered in the system. The cover was removed and the short located.

a) Lower Assembly Ready for Fueling

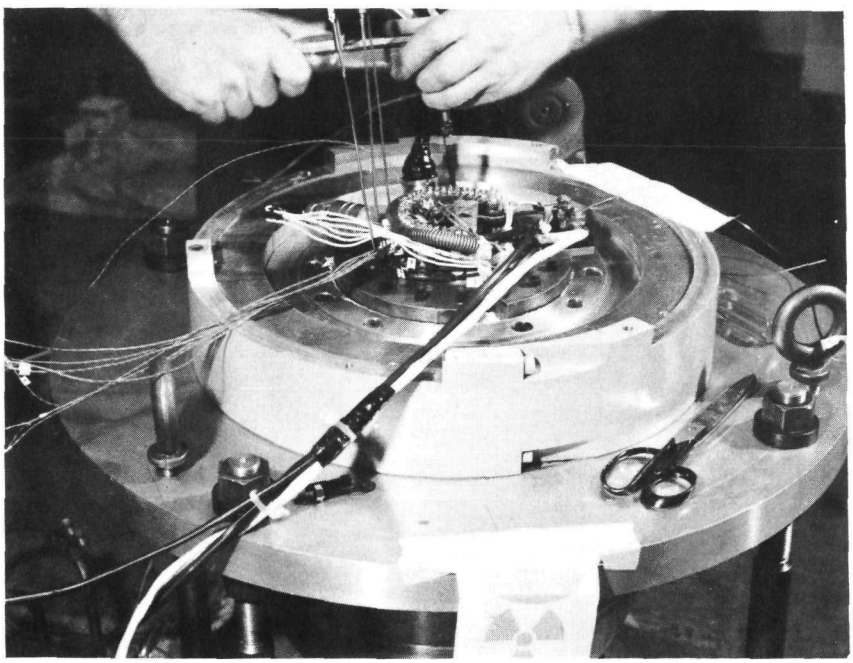

b) Fueled System Showing Thermoelectric Generator in Place

Figure D1. Steps in Fueling and Assembly, System S10D1A

c) System With Wiring Complete

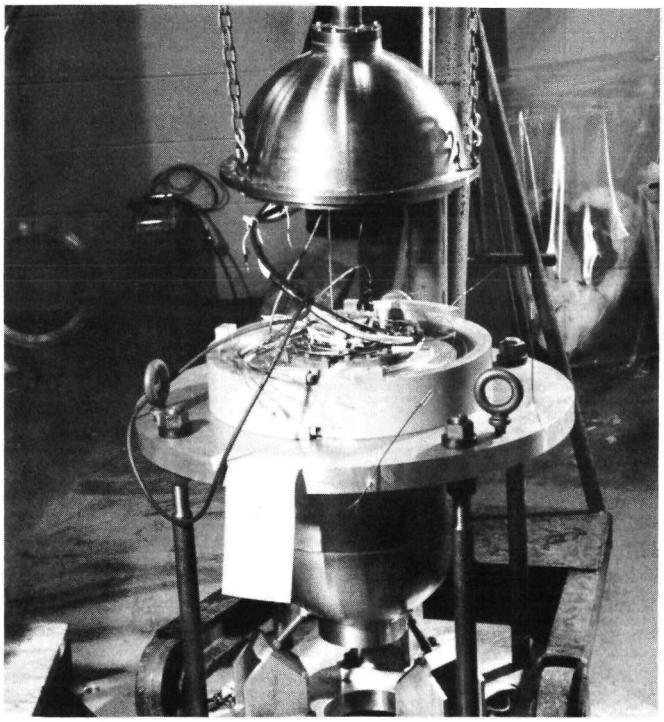

d) Lowering Pressure Vessel Cover Completing System Integration

Figure D1. Steps in Fueling and Assembly, System S10D1A (Continued)

It was caused by a protuberance of the power conditioner pressing down on the generator terminal block. This was corrected and the system was put back on test.

All of the test instrumentation was check by ORNL upon arrival and found to be in calibration. ORNL personnel were instructed by 3M test people on proper data taking procedures. They will provide daily parameters and submit complete data forms weekly. Still photography and movie coverage was provided for part of the assembly and fueling operations. Film will be made available to 3M after editing by ORNL. System performance and operating characterics are given in Table 1.

Table 1. S10D1A System Performance

Temperatures (Ave)	°F
Water	29
Cold Frame	83
Cold Cap	99
Hot Button	830
Hot Frame (Internal)	873
Fuel Loading	186.8 watts (Th)
TEG Power	10.89 watts
Power Conditioner Efficiency	88.3%
System Efficiency	5.15%